

The Pennsylvania State University

The Graduate School

**PLANTS, PRECIPITATION, AND PEOPLE IN DHOFAR, OMAN: DRYLAND
ECOSYSTEM RESILIENCE IN A CHANGING WORLD**

A Dissertation in

Geosciences

by

Kaitlyn Eileen Horisk

© 2024 Kaitlyn Eileen Horisk

Submitted in Partial Fulfillment
of the Requirements
for the Degree of

Doctor of Philosophy

May 2024

The dissertation of Kaitlyn E. Horisk was reviewed and approved by the following:

Sarah J. Ivory
Wilson Faculty Fellow in the College of Earth and Mineral Sciences
Department of Geosciences
Dissertation Advisor
Chair of Committee

Katherine H. Freeman
Evan Pugh University Professor
Department of Geosciences

Erin DiMaggio
Associate Research Professor
Department of Geosciences

Rebecca Bleige Bird
Professor
Department of Anthropology

Joy McCorriston
Joan N. Huber Faculty Fellow
Department of Anthropology
The Ohio State University
Special Member

Donald Fisher
Professor
Department of Geosciences
Chair of the Graduate Program

ABSTRACT

Dryland ecosystems cover nearly half of the world's land surface and are home to nearly a third of the human population. These ecosystems are areas which receive less than 400mm of precipitation per year and thus are more sensitive to changes in rainfall. These qualities make drylands, and the people who rely on them, especially at risk under projected climate change conditions. While modern observational data is too brief to assess long-term effects of climate on vegetation, the paleoecological record provides a vast natural laboratory to investigate these dynamics. Rock hyrax (*Procapra capensis*) middens are preserved in these arid regions where traditional archives, such as lake cores, are unavailable. Additionally, the archaeological record allows us to infer past foodways and changes in human mobility across the landscape. Using these two sets of information in tandem can help us better understand the role of humans in shaping plant communities. Dhofar, Oman, provides a unique setting for this kind of study: this region is a highly biodiverse, dryland ecosystem with a long history of pastoralism, which is still practiced today. Southern Arabia was subject to decreasing rainfall across the Holocene, making this time frame ideal for investigating how changes in precipitation and people impacted plant communities. Here, we present a pollen record and geochemical information from leaf wax *n*-alkanes from rock hyrax middens collected in Dhofar, as well as results from agent-based modelling experiments. These results suggest resilience of dryland vegetation communities to large-scale state shifts under increasing aridity, as well as to high grazing and browsing pressures from domesticated herds. However, despite indications from the pollen records of changes in plant communities, the geochemical data suggest that ecosystems have had modern arid affinities for the last 4000 years. This implies threats to species-specific resources in Dhofar with increasing future aridity which could initiate more catastrophic change.

“We are showered every day with gifts, but they are not meant for us to keep. Their life is in their movement, the inhale and the exhale of our shared breath. Our work and our joy is to pass along the gift and to trust that what we put out into the universe will always come back.”

– Robin Wall Kimmerer, Braiding Sweetgrass

TABLE OF CONTENTS

LIST OF FIGURES	vii
LIST OF TABLES	ix
ACKNOWLEDGEMENTS	x
Chapter 1 Introduction	1
Climate vegetation dynamics in arid regions	3
Human-environment interactions in a pastoralist framework	5
Study setting.....	8
Rock hyrax middens as a paleoenvironmental archive	10
Regional paleoecology.....	12
Reconstructing pastoralist activity from the archaeological record	15
Summary of Chapter 2: In the dens of dassies: Vegetation dynamics in Dhofar, Oman from the late Holocene to present inferred from rock hyrax middens.....	19
Summary of Chapter 3: The only thing certain in grad school is death and (leaf) waxes: Late Holocene hydrologic variability and ecosystem structure	19
Summary of Chapter 4: Modelling movement: Climate change, human activity, and vegetation response	20
 Chapter 2 In the dens of dassies: Vegetation dynamics in Dhofar, Oman from the late Holocene to present inferred from rock hyrax middens	 22
Abstract.....	22
Introduction.....	23
Modern setting	27
Hyrax middens as paleoenvironmental archives.....	30
Methods	33
Palynological analysis	36
Radiocarbon dating and stable isotopes	38
Results.....	41
Modern pollen	41
Fossil pollen zones	43
Fossil midden Detrended Correspondence Analysis (DCA).....	45
Fossil midden stable isotopes	46
Discussion	48
Hyrax midden pollen and modern vegetation	48
Fossil pollen interpretation.....	49
Monsoon dynamics and aridity	54
Human-environment interactions.....	57

Conclusion	59
Chapter 3 The only thing certain in grad school is death and (leaf) waxes: Late Holocene hydrologic variability and ecosystem structure.....	61
Abstract.....	61
Introduction.....	62
Background	64
Modern environment.....	64
Leaf wax <i>n</i> -alkanes.....	66
Methods	69
Rock hyrax middens.....	69
Modern herbarium plant specimens	71
Results.....	72
Modern herbarium plant specimens	72
Rock hyrax middens.....	74
Discussion	76
Interpreting plant community change through <i>n</i> -alkane distributions.....	76
Applications of leaf wax isotopes for rock hyrax middens	77
Paleohydrology and vegetation change in the late Holocene.....	78
Conclusion	83
Chapter 4 Modelling movement on the Dhofar landscape: Climate change, human activity, and vegetation response	85
Abstract.....	85
Introduction.....	86
Background	88
Biodiverse plant communities in Dhofar.....	88
Climate and vegetation dynamics	89
Pastoralism through the Holocene.....	90
Agent-based modelling	91
Methods	92
Results.....	95
Discussion	99
Conclusion	102
Chapter 5 Conclusion.....	103
References Cited	106
Appendix A Hyrax midden pollen count data	136
Appendix B Hyrax midden sampling and processing methods	179

LIST OF FIGURES

- Figure 1-1: Map of Dhofar with ecological zones, which are defined by elevation and vegetation composition. Generated using Google Earth. 10
- Figure 2-1: Map of Dhofar depicting the four ecological zones. The midden sampling locations are shown by the boxes. Inset shows the geopolitical boundaries of Oman on the Arabian Peninsula. 29
- Figure 2-2: Pictures of representative rock hyrax middens. 33
- Figure 2-3: Pollen diagram of modern hyrax middens and two camel dung samples, in order from North to South. The middens are grouped by their ecological zone (East Nejd, West Nejd, Distal Plateau, Escarpment, Coastal plain). The two escarpment samples are camel dung specimens. Submodern hyrax middens are included with their median calibrated ages. Pollen abundances are on the x-axis. The green shade indicates tree pollen habits, grey indeterminate habits, and yellow are herbaceous pollen habits. The CONISS dendrogram is plotted on the right. 42
- Figure 2-4: Detrended Correspondence Analysis (DCA) of all modern samples (right) and including submodern samples (left). Samples are color coded by their ecological zone. 42
- Figure 2-5: Pollen diagram of selected taxa from East Nejd fossil middens. Abundances are plotted on the x-axis and age in calibrated years BP on the y-axis. The four modern samples are plotted individually. The green shade indicates tree pollen habits, grey indeterminate habits, and yellow taxa with herbaceous pollen habits. Pollen zones determined via CONISS cluster analysis are represented by the column on the right. Replace this with figure caption below figure. 45
- Figure 2-6: Detrended Correspondence Analysis (DCA) of fossil middens. Samples are coded by their quantitatively determined pollen zone. 46
- Figure 2-7: Panel A plots the $\delta^{15}\text{N}$ values of the middens by age in calibrated years BP. Panel B plots average speleothem $\delta^{18}\text{O}$ against midden N. Panel C is a plot of the bulk $\delta^{13}\text{C}$ values by midden age in calibrated years BP. Panel D shows a boxplot of midden $\delta^{13}\text{C}$ values by age bin. 47
- Figure 2-8: A. Archaeological periods of monument building and settlement, along with the earliest evidence for the introduction of domesticated camels in Dhofar (2000 yrs BP) and elsewhere in Arabia (3000 yrs BP). B. Mesic Taxa relative abundances (%): *Ficus*, *Boswellia sacra*, *Boscia/Cadaba*, *Maytenus* C. Nejd Associations relative abundances (%): *Amaranthaceae*, *Salvadora persica*, *Senegalia* I, *Senegalia* III, *Commiphora* D. Grazing Indicators relative abundances (%): *Dodonaea viscosa*-type, *Cornulaca/Aerva*, *Cassia*-type, *Heliotropium* E. Gray bars showing *Sporormiella* relative abundance (%) and black line indicating microcharcoal concentrations (particles/g) F. Speleothem $\delta^{18}\text{O}$ from Fleitmann et al. (2007). 53

- Figure 3-1: Map of the Dhofar region indicating the four ecological zones. Black squares are modern samples, white circles represent fossil samples. The stars denote the weather stations in Salalah and Thumrait.66
- Figure 3-2: Proportions of the C27, C29, and C31+ C33 *n*-alkanes in plant herbarium specimens. The C27 and C29 compounds are generally associated with trees, and the C31+ C33 with herbs and grasses. From left to right are the Trees: *Terminalia dhofarica*, *Salvadora persica*, *Boscia arabica*, *Ziziphus spina-christii*; Shrub: *Cadaba heterotracha*; Herbs: *Cleome*, *Cenchrus ciliaria*, *Euphorbia granulata*, *Heliotropium fartakense*, *Cleome brachycarpa*.73
- Figure 3-3: Ternary plots showing the proportions of the C27, C29, and C31+C33 *n*-alkanes in plant herbarium specimens. The left panel is color-coded by plant habit (tree, herb, or shrub) and the right panel is color-coded based on ecological affinity in the region (more mesic or xeric).74
- Figure 3-4: From top to bottom: CONISS cluster analysis of the relative abundances of the pollen in each sample; the relative abundances of Tree, Herb, and Indeterminate pollen habits; proportions of *n*-alkane homologues in each sample.75
- Figure 3-5: Top panel: δD_{wax} (blue) and $\delta^{13}C_{wax}$ data (green) plotted against midden sample age (cal yrs BP). Bottom panel: $\delta^{18}O$ data replotted from the Qunf cave speleothem record of Fleitmann et al. 2007. Blue bars represent periods where local and regional records indicate it is relatively wetter, compared to yellow bar which is a time frame that is generally accepted to be the driest time.82
- Figure 3-6: δD_{wax} data with applied ϵ value based on average of the C3 and C4 plant ϵ values described in the literature. Purple bar represents range of isotopic values from modern Nejd groundwater and the blue from modern monsoon rainfall and runoff, as presented by Strauch et al. (2014) and Friesen et al. (2018).83
- Figure 4-1: Map of Dhofar with ecological zones and locations of Salalah and Thumrait weather stations.88
- Figure 4-2: Rainfall experiment results: average vegetation fractions with increasing rainfall by vegetation zone.97
- Figure 4-3: Figure illustrating the growth in the average tree fraction on the escarpment with increasing khareef season length (weeks).97
- Figure 4-4: Left column: Khareef Extent experiment run without herds; Right column: Khareef Extent experiment run with a constant of 2500 cattle herds. From top to bottom are the Nejd, Escarpment, and Coast vegetation zones. The vertical axes represent the average vegetation proportion and the horizontal axes are khareef extent in kilometers.98

LIST OF TABLES

Table 2-1: The four ecological zones of Dhofar and their dominant vegetation taxa.....	30
Table 2-2: Modern midden sampling locations, AMS radiocarbon dates, calibrated ages, and bulk stable isotope information.. ..	35
Table 2-3: Fossil midden sampling locations, AMS radiocarbon dates, calibrated ages, and bulk stable isotope information.	36
Table 3-1: <i>N</i> -alkane chain lengths for herbarium plant samples.....	73
Table 3-2: <i>N</i> -alkane chain length concentrations and stable isotope results for the hyrax midden samples.....	75
Table 4-1: Table describing each of the model experiments.	95

ACKNOWLEDGEMENTS

Thank you to my family for your unending love and support, especially my sister Kayla, Mom, Dad, my stepmom Erica, my stepdad Shane, my stepsisters Haley and Sydney, Me-me, Pa-pa, Nana, Abuelo, Uncle Joey, and Uncle Evan. You inspired my love of the natural world, were my biggest fans, and helped me become who I am today. We have shared laughter and tears, and you have surrounded me with so much joy and warmth. From walks in the woods, cooking my favorite meals, trips to the thrift store, and watching spooky shows, my life is so full because of you. I love each and every one of you with my entire heart. And thank you to my friends both near and far for being there through the ups and downs, the good times and the bad: Alyssa Eveland, Emma Hartke, Leah Klaila, Kayla Irizarry, and Darryl Angel. From being random roommates to discovering we are related, navigating ResLife, renaissance faires, road trips, craft nights, coffee dates, and more, I could not have done this without you all. Lastly, thank you to my furry friends, Mitzy, Igoe, and little Lemon Meringue, who make life brighter and remind me to stop and smell the roses.

To my advisor, Sarah, thank you for being an incredible mentor. You guided me through from the beginning of this journey, where I took this project and ran with it, and saw this thing through to the end. You supported and fostered my creativity, helped me pursue my non-traditional aspirations, and made space for vulnerability. Thank you for sharing coffee and conversation about life on the beaches of Oman, supporting my never-ending quest to find the desert melon pollen, and always advocating for me. It has been my honor and privilege to be one of your first students and to have worked with you these five years. What an incredible ride! I am sure there is much more to come for us as a team.

Thank you to my committee of brilliant women and incredible scientists. Your guidance and advice have been invaluable. Joy McCorrison, your enthusiasm for this work and your

unwavering support kept me smiling through it all. Thank you as well to the entire ASOM team. Despite many folks moving on in their careers, you have all continued to support this work. Daniel Peart and Mark Moritz, your input and assistance was vital to shaping the modelling project. I am grateful to have been a part of such a wonderful team.

I would like to thank colleagues with the Oman Ministry of Heritage and Tourism, specifically Ali Al-Kathiri and Ali Al-Mahri, as well as the Oman Botanic Garden. Ali Al-Kathiri, thank you for sharing your wisdom and for your abundant kindness and generosity. Additionally, I would like to acknowledge Dr. Annette Patzelt and Dr. Darach Lupton for their assistance in the field. I would also like to thank Dr. Julianne Snider with the EMS Museum & Art Gallery and Dr. Kim Lau for their support with professional development. A big thank you to Heike Betz and Allie Baczynski for your indispensable help and support with all things' chemistry. Similarly, special thanks to Shaver's Creek Environmental Center, Rufous, and the team at Centre Wildlife Care, it was an honor to work with you all.

This work was funded by NSF CNH 1617185, the Elsevier Organic Geochemistry Research Award, and the Marilyn Fogel Fund of the Earth and Environmental Systems Institute (EESI) at Penn State University. I would like to honor the life and legacy of Dr. Marilyn Fogel and offer my gratitude for this award to her and her family. Other funding sources include the Teaching Assistant Award, Richard Standish Good Graduate Scholarship, Michael Loudin Family Graduate Scholarship, RJ Cuffey Fund for Paleontology, Richard R. Parizek Graduate Fellowship, and the Krynine Award through the Department of Geosciences at Penn State University. My sincere thanks to the Geosciences Department and the alumni, former faculty, and their families for their endowments, which enable students to conduct their research and share it with the broader scientific community. The findings and conclusions do not necessarily reflect the view of the funding agency.

Chapter 1

Introduction

Dryland ecosystems are defined by limited water availability (mean annual precipitation <400mm/yr), and these comprise 41% of the Earth's terrestrial surface (D'Odorico and Bhattachan, 2013; Maestre, 2016; Stavi et al., 2022). Over 1/3 of the human population relies on dryland ecosystems for food and water resources (Maestre et al., 2016). These ecosystems are especially sensitive – small decreases in precipitation or increases in domestic animal browsing can lead to degradation of the vegetation (Asner et al., 2004; Maestre et al., 2016; Ivory et al., 2021). Climate Model Intercomparison Project 6 (CMIP6) models predict up to a 3.3°C increase in temperature before the end of this century (Almazroui, 2012; Majdi et al., 2022). This will cause higher evapotranspiration ultimately leading to a net moisture deficit, even with the predicted small increases in precipitation (Maestre et al., 2012; Ault et al., 2016; Almazroui, 2012; Majdi et al., 2022). However, mechanisms behind changes in vegetation in these regions are poorly understood.

Degradation of the vegetation due to anthropogenic climate change conditions could have a devastating impact on water and food security in these regions (Stavi et al., 2022; Ivory et al., 2021). Drylands support approximately half of the world's livestock and represent over 40% of cultivated lands (Stavi et al., 2022). Predicted changes in temperature and precipitation will lead to increased drought and flooding events, which will impact crop yields that provide food for both people and livestock (Stavi et al., 2022). With growing populations, there has been an emphasis on “water trade”, wherein countries with more reliable access to freshwater produce more food resources that can then be imported by countries with less freshwater for food production

(D'Odorico and Bhattachan, 2013). However, with this unsustainable depletion of freshwater resources and increasing aridity and drought conditions, it is predicted that populations in these drylands will be less resilient (D'Odorico and Bhattachan, 2013). Moreover, the vast majority of drylands are located in developing countries, with populations that are spread-out and lack infrastructure that would assist in distributing aid during times of crisis (Maestre et al., 2012). These factors underscore the importance of assessing how climate mechanisms force vegetation changes as we look towards an uncertain future.

Humans are themselves unprecedented agents of landscape change (Dietl et al., 2014). While anthropogenic climate change continues to accelerate, other human activities such as animal grazing will likely cause drastic changes in ecosystems (IPCC, 2022; Maestre et al., 2016, Dahinden et al., 2017). Domesticated animal grazing and browsing is the predominant land-use strategy in dryland ecosystems, and increased stocking rates threaten overexploitation of the vegetation (Asner et al., 2004; Maestre et al., 2016). Approximately 20% of drylands are already in a degraded state, and it is essential to understand how this important lifeway affects long-term ecosystem change (Maestre et al., 2012). Some studies indicate that managed grazing can affect vegetation biomass as well as species composition, with the overall encroachment of woody taxa (Asner et al., 2004; Maestre et al., 2016; Ball and Tzanopoulos, 2020). Browsing animals, as opposed to grazers, are preferential to woody or herbaceous materials rather than grasses and can reduce woody taxa (Shipley, 1999; Ball and Tzanopoulos, 2020). Hence, the types of domesticated livestock which are the most dominant can have different impacts on the vegetation. Moreover, the complex ways in which human activity and climate change interact and may amplify these impacts on the vegetation are not yet well constrained. Modern data is too brief to assess natural variability and ecosystem dynamics (Dietl et al., 2014). There is a need for longer term records to investigate these processes.

Climate-vegetation dynamics in arid regions

The world's drylands are highly susceptible to interactions between the land and the atmosphere (Nicholson, 2015). These interactions are mitigated by factors such as temperature, rainfall, surface albedo, soil moisture, and vegetation, among others (D'Odorico and Bhattachan, 2014; Nicholson, 2015). However, observing these processes can be confounded by the potentially longer timescale of vegetation response to environmental perturbations (Williams and Albertson, 2006). Modern data in addition to paleoecological data can be utilized to build long-term records of changes in climate and vegetation to interpret these processes, in addition to modeling techniques (Williams and Albertson, 2006; D'Odorico and Bhattachan, 2014; Nicholson, 2015). This helps build a better understanding of risk to these sensitive ecosystems under modern climate change conditions.

Rainfall in dryland ecosystems is generally highly seasonal as well as spatially patchy, but critically tied to vegetation cover and productivity (Williams and Albertson, 2006; Nicholson, 2018). Despite the intermittent rainfall in drylands, ecohydrological box models suggest the vegetation is best adapted to this seasonality as opposed to more constant rainfall (Baudena et al., 2007). Changes in rainfall frequency in addition to the amount of rainfall may consequently cause drastic changes in dryland plant communities (Baudena et al., 2007; Maestre et al., 2016). Generally, rainfall enters the soil through two pathways: throughfall, or directly onto the ground, and stemflow, where rain lands on a plant and trickles down the trunk or stem (Friesen et al., 2018; Magliano et al., 2022). Stemflow combined with throughfall represents the net precipitation that can be utilized by vegetation and has not been evaporated (Friesen et al., 2018; Magliano et al., 2022). Vegetation type is a feedback in this system, wherein the throughfall and stemflow can differ based on whether vegetation cover is dominated by trees, shrubs, or herbaceous plants (Hildebrandt et al., 2007; Friesen et al., 2018; Magliano et al., 2022). In drylands, there is a

higher amount of stemflow as compared to throughfall (Wang et al., 2010; Magliano et al., 2022). Both precipitation and vegetation dynamically interact in drylands to maintain a productive ecosystem (Williams and Albertson, 2006; Baudena et al., 2007; Nicholson, 2011; Friesen et al., 2018; Magliano et al., 2022).

Soil moisture in drylands exerts a direct control on vegetation transpiration and production and is thus of critical importance to dryland ecosystems (Baudena et al., 2007). While global climate models predict overall increasing rainfall, surface water availability is expected to decrease by as much as 51%, posing an imminent threat to dryland productivity (Zhou et al., 2021). Soil moisture is affected by rainfall, as well as groundwater, surface runoff, and biological processes (Baudena et al., 2007). Vegetation promotes infiltration of precipitation into the soil, but sparser vegetation cover in dryland ecosystem inhibits this increase in soil moisture, and more run-off occurs (Nicholson, 2011). Higher stemflow in drylands partially mitigates this, increasing net precipitation into the soil (Wang et al., 2010; Magliano et al., 2022). Soil moisture is also impacted by water table height, which is typically low in dryland environments (Baudena et al., 2007; Nicholson, 2011). While modern vegetation in drylands is adapted to these conditions, intensifying droughts and an overall reduction in soil moisture may cause catastrophic ecological changes to the world's drylands (Baudena et al., 2007; IPCC, 2022; Hoover et al., 2021; Zhou et al., 2021).

Dryland ecosystems are especially threatened by the process of desertification – the degradation of land due to both climate processes and human activity in arid regions (Reynolds et al., 2007; Ravi et al., 2010). This results in the land becoming bare and inhospitable to life (Albalawi and Kumar, 2013). Abiotic processes which can lead to desertification include increasing aridity and erosion of soils (Albalawi and Kumar, 2013). Predicted changes in surface water availability and increasing drought frequency and intensity can initiate desertification in arid places (Albalawi and Kumar, 2013; Baudena et al., 2007; Zhou et al., 2021). However,

humans play a role in this system, exacerbating these climatic processes through reducing vegetation cover and other land surface disturbances (Albalawi and Kumar, 2013). Therefore, both abiotic and biotic processes should be considered as possible factors in a regime shift towards desertification in different regions (Asner et al., 2004; Peters et al., 2015; Maestre et al., 2016).

Human-environment interactions in a pastoralist framework

It is imperative to understand how both changes in climate and human activity dynamically influence vegetation, as one may accelerate the other. In drylands, nomadic pastoralism is a common subsistence strategy and has demonstrated impacts on local vegetation (Asner et al., 2004; Maestre et al., 2016; Ball and Tzanopoulos, 2020). Nomadic pastoralism is a lifeway in which groups of people primarily depend on domesticated livestock and are highly mobile rather than settled in one location for protracted amounts of time (Dyson-Hudson and Dyson-Hudson, 1980). Early 20th century ecologists contributed to the development of theoretical frameworks of the interplay between pastoralists and the environment, which were then built upon by scientists within the field of anthropology (Clements, 1916; Hardin, 1968; Binford, 1990; Warren, 1995; Odling-Smee et al., 2013). However, this process was heavily influenced by the implicit biases of colonialists who viewed pastoralism as ritual practice rather than founded in ecological knowledge (Warren, 1995). Over the last few decades, there has been an increased understanding of the complex interactions between pastoralism and the landscape, and the emergence of new paradigms in which pastoralism is a complex and adaptive way of life in drylands (Warren, 1995; Walker and Janssen, 2002; Odling-Smee, 2013; McCorrison et al., 2018).

Historically, there has been a lack of understanding regarding how pastoralist practices affect vegetation, and past theoretical frameworks from ecology often focused on the exploitation and depletion of habitat resources (Hardin, 1968; Warren, 1995). Frederic Clements 1916 work, “Plant Succession”, framed pastoralist strategies as a constant balancing act between the opposing goals of increasing animal crops and maintaining stability at some threshold (Clements, 1916; Warren, 1995). Garrett Hardin’s “tragedy of the commons” outlined how resources are inevitably depleted with increasing population, and how an individual herder would only try to maximize their own gain to the detriment of the whole social group (Hardin, 1968). These concepts led to the development of a model for an environments’ “carrying capacity.” One key assumption of this model was that degradation occurs after a fixed point, when in fact it is a continuous process, and moreover affected by natural variability. Therefore, selection of a sustainability threshold is arbitrary, clearly expressed by the fact that pastoralists could maintain herds beyond this manufactured point (Warren, 1995).

These early ecological theories contributed to the development of anthropological frameworks of pastoralism. While the “tragedy of the commons” and Clements model were recognized to be oversimplified, these anthropological works still understood habitat choice as a function of exploitability (Binford, 1990; Warren, 1995). Lewis Binford showed that with increasing temperatures, environmental resources increased, and consequently hunter-gatherer groups became more mobile (Binford, 1990). Likewise, these groups became less dependent on plant resources with increasing latitude, while hunting or fishing subsistence strategies became predominant (Binford, 1990). This work was useful in highlighting that mobility is dependent upon ecological context and cannot be analyzed under universal assumptions of adaptiveness. However, there remains the underlying assumption that human subsistence strategies are purely a depletion of natural resources, which then constrains mobility. This conceptual framework asserts that humans will track hunted prey or reliable patches of food on the landscape, congregating and

settling when these are more limited and there is a forced “tethering” to resources (Binford, 1990). This neglects human impacts on the environment and ecosystem response.

Human Behavioral Ecology (HBE) is the study of human behavior within individual ecological contexts, and how the environment shapes decision-making and thus fitness (Cronk, 1991; Nettle et al., 2013). One product of HBE is the Ideal Free Distribution (IFD) model, which represents human habitat choice in terms of ranked quality. IFD states that people will first populate the habitat with the most resources. As population increases in this area, resources will be depleted and eventually the next best area will become equal to the first in terms of habitat quality. People will then begin to move into new patches successively as resources are used (Fretwell and Lucas, 1969; Cressman and Křivan, 2006; Bliege Bird et al., 2020). This model can be applied to mobility patterns across landscapes. IFD assumes habitat quality decreases as population increases due to limited resources, and competition for these resources (Bliege Bird et al., 2020). While this often holds, in some cases a higher population density can introduce positive feedbacks, called Allee Effects. Allee Effects can take the form of social cooperation and defense of resources (Bliege Bird et al., 2020). Allee effects introduced by pastoralism can include nutrient input to the soil via manure and anthropogenic burning which can convert woodlands to more open grasslands ideal for grazing (Brierley et al., 2018; Vuorio et al., 2014). These positive feedbacks support the idea that pastoralism can in fact be sustainable and adaptive in these ecological contexts.

Niche Construction Theory (NCT) is another model used to understand human interactions with the environment. This theory derives from the field of ecology and refers to the ways in which organisms can modify their evolutionary niches (Odling-Smee et al., 2013; Laland et al., 2016). This is an active process in which the organisms are their own agents, making modifications to their environment rather than passively responding to the environment (Laland et al., 2016). Simple examples of this would be an owl building a nest or a chipmunk digging a

burrow. This process creates selective pressures and can thus cause evolutionary change (Odling-Smee et al., 2013; Laland et al., 2016). Because organisms are creating novel selective pressures, these in-turn affect future generations as well as other organisms within the environment, and this is known as ecological inheritance (Odling-Smee and Laland, 2011; Odling-Smee et al., 2013). NCT can be applied to humans, who have been observed to modify their surroundings for thousands of years: making shelters, domesticating animals, and developing agriculture to adapt to many different landscapes (Laland and O'Brien, 2010).

In pastoralist systems, one example of ecological inheritance would be the conversion of woodlands to grasslands through managed grazing and controlled burning (McCorrison et al., 2018). However, humans are also able to teach and learn, and this social transmission during the process of niche construction results in cultural inheritance (Odling-Smee and Laland, 2011). In this example, teaching new generations the use of fire in creating new pasture would be the cultural inheritance of this niche construction (McCorrison et al., 2018). The ecological and cultural inheritance from the practice of pastoralism can make this system adaptive in different environments, rather than simply degradational, negating older theoretical frameworks such as succession or the “tragedy of the commons” (Clements, 1916; Hardin, 1968; Warren, 1995; McCorrison et al., 2018). NCT highlights the importance of considering humans as a part of complex environmental systems.

Study setting

The Dhofar region of Oman lies in the subtropics and has a semiarid to hyperarid climate. Mean annual temperatures in Dhofar are around 25.7°C. Coastal regions affected by the Indian monsoon receive 200-600 mm of precipitation per year, 70-80% of which falls during the monsoon season, or khareef, that occurs from June-September (Fleitmann et al., 2007; Miller and

Morris, 1988). Further inland conditions are hyperarid, and these desert regions receive as little as 30 mm of precipitation annually. Dhofar is also home to highly biodiverse plant communities (Ghazanfar, 1998; Miller and Morris, 1988). Consequently, the vegetation in Dhofar is particularly at risk under projected climate change conditions of increasing temperatures and decreasing rainfall, which could be extremely damaging to food and water resources (Almazroui, 2012).

The vegetation in Dhofar is characterized by four ecological zones (Figure 1-1). The coastal plain of Dhofar is a low elevation band that stretches from the coast of the Arabian Sea to the foothills of the Dhofar Mountains (Miller and Morris, 1988). The vegetation in this zone is extremely sparse due to overgrazing by domesticated animals as well as urbanization (Miller and Morris, 1988). The escarpment ecological zone in the mountains hosts a seasonal cloud forest (Miller and Morris, 1988; Patzelt, 2015). This ecosystem relies on fog brought in by the Indian Monsoon, and trees such as *Terminalia dhofarica* are specially adapted to intercept this fog moisture and increase net precipitation (Hildebrandt et al., 2007). The plateau zone is mainly grassland with isolated trees (Miller and Morris, 1988; Buffington and McCorrison, 2018). Beyond the plateau is the Nejd, a desert that is home to isolated trees and shrubs. This zone is significantly more arid than those closer to the coast, because it is past the reach of monsoon precipitation (Al-Mashaikhi, 2012).

Human landscape use also poses a unique threat to this landscape. Urban development and other infrastructure have stripped native vegetation. Moreover, recent studies have revealed that overgrazing by domesticated animals is stunting regeneration of native forests (Ball and Tzanopoulos, 2020; Galletti et al., 2016). These changes have only been observed over the last few decades as stocking rates have exponentially increased with rapid economic growth (Almazroui, 2012; Ball and Tzanopoulos, 2020; Galletti et al., 2016). Nomadic pastoralism has been continually practiced in Dhofar for at least the last seven thousand years and remains

culturally and economically important (Ball and Tzanopoulos, 2020; McCorriston et al., 2018). Archaeological and paleoecological data can be used in tandem to understand how climate and human activity influence vegetation, and perhaps lend insight into the development of sustainable practices.

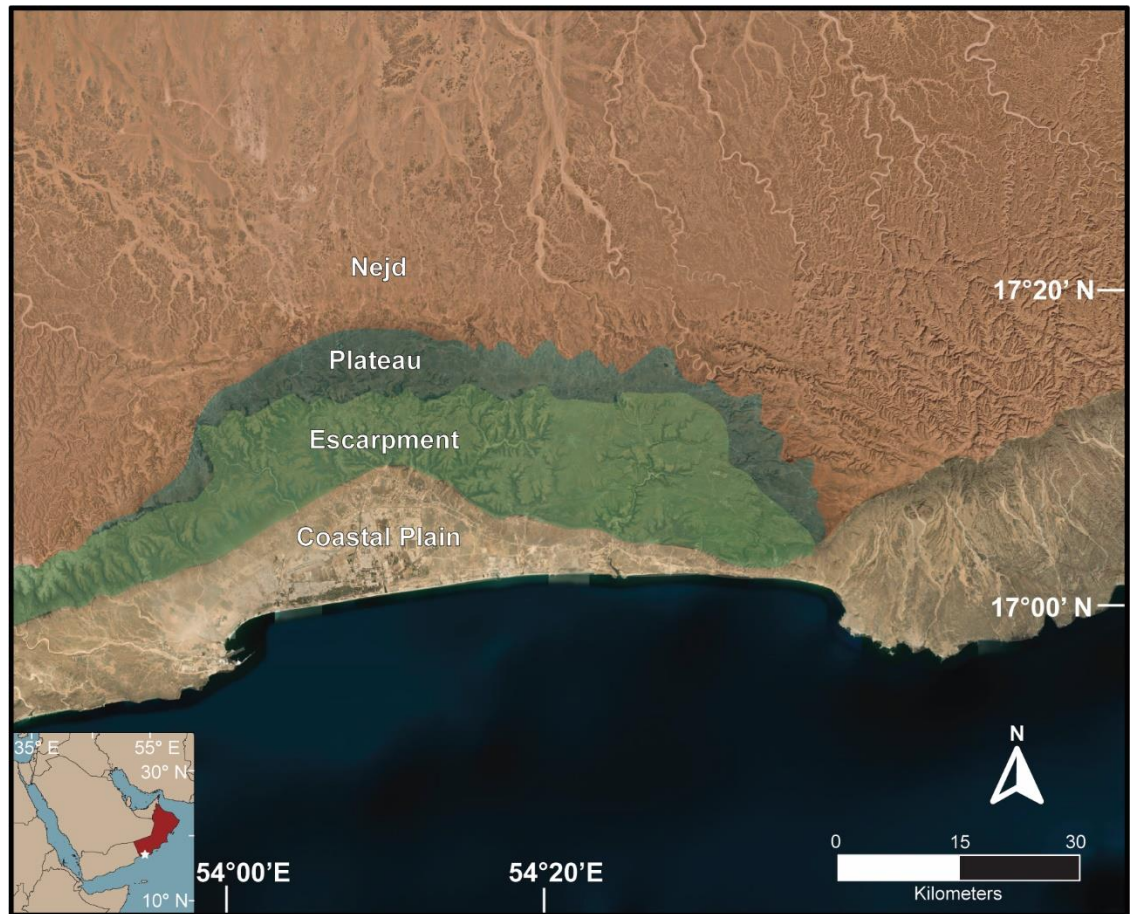


Figure 1-1: Map of Dhofar with ecological zones, which are defined by elevation and vegetation composition. Generated using Google Earth.

Rock hyrax middens as a paleoenvironmental archive

The development of long term paleoecological records in arid regions is complicated by the lack of traditional archives, such as lake cores. Rock hyrax (*Procavia capensis*) middens serve

as well-established paleoecological archives in arid ecosystems, preserving pollen, macrofossils, and isotopic information effectively for thousands of years (Chase et al., 2012, Carr et al., 2010; Ivory et al., 2021). These charismatic animals use communal latrines that are separate from their dens, which form layered deposits of hyraceum, a crystallized urinary product, and fecal pellets (Chase et al., 2012). Sufficiently thick middens can be subsampled to create high resolution time series, while thin accumulations can provide “snapshots” in time (Chase et al., 2012; Ivory et al., 2021). Paleoenvironmental indicators are brought to the middens on the feet or fur of hyraxes, pass through their digestive systems, and are blown in via aeolian deposition (Chase et al., 2012). Thus, these middens are a powerful archive for reconstructing past climate-vegetation dynamics in places where other long-term records cannot be developed.

Pollen within rock hyrax middens represent a local signal of vegetation (Scott and Cooremans, 1992; Chase et al., 2012). Comparison of modern middens to local vegetation descriptions and pollen traps demonstrate that they represent a local spatially averaged signal, as opposed to a dietary signal (Scott and Cooremans, 1992; Chase et al., 2012). The amount of pollen from specific taxa deposited within the middens is affected by pollen dispersal methods, with wind-dispersed pollen taxa being more abundant with respect to insect-dispersed.

In addition to pollen, there are several geochemical indicators that can be used to understand paleoenvironmental conditions. Bulk $\delta^{15}\text{N}$ and $\delta^{13}\text{C}$ isotopes measured on fecal pellets within the middens represent local moisture conditions and the predominant vegetation type, respectively (Carr et al., 2010; Chase et al., 2012). Nitrogen in the soil is taken up by plants and into foliar tissue. When hyraxes eat the leaves, the isotopic composition of the plant foliar nitrogen is preserved within the feces. Stable carbon isotopes reflect the predominant photosynthetic pathway of the vegetation consumed (Chase et al., 2012; Ehleringer et al., 1997). More negative $\delta^{13}\text{C}$ values (-30 to -20‰) are associated with C3 vegetation, while less negative values (-9 to -16‰) are associated with C4 plants (Rao et al., 2017).

Another geochemical indicator within the middens are leaf wax *n*-alkanes. *N*-alkanes are long chain hydrocarbons that are a component of plant leaf waxes (Eglinton and Hamilton, 1967; Killips and Killips, 2013). The isotopes of both carbon and hydrogen within these compounds preserve a record of past vegetation and rainfall, respectively (Bush and McInerney, 2015; Eglinton and Eglinton, 2008). $\delta^{13}\text{C}_{\text{wax}}$ provides another record of changes in C3 ($\delta^{13}\text{C}_{\text{wax}} = -36\text{‰}$) versus C4 ($\delta^{13}\text{C}_{\text{wax}} = -21.5\text{‰}$) vegetation (Carr et al., 2010; Ehleringer et al., 1997). The $\delta\text{D}_{\text{wax}}$ signal records the ratio of deuterium to hydrogen of the leaf water at biosynthesis, which is related to environmental water and thus meteoric rainwater (Chikaraishi and Naraoka, 2007; Sachse et al., 2012; Tipple et al., 2013). Less negative values of $\delta\text{D}_{\text{wax}}$ indicate more arid conditions, making the $\delta\text{D}_{\text{wax}}$ and $\delta^{13}\text{C}_{\text{wax}}$ records from *n*-alkanes complementary paleoenvironmental signals (Sachse et al., 2012; Rao et al., 2017). These compounds have been shown to preserve in rock hyrax middens over geologic timescales in South Africa, and thus can be used to strengthen paleoecological studies in southern Arabia (Carr et al., 2010; Chase et al., 2012).

Rock hyrax middens host multiple well-studied paleoenvironmental indicators which can be leveraged to develop long term records of environmental change (Carr et al., 2010; Chase et al., 2012; Ivory et al., 2021; Scott and Cooremans, 1992). Their preservation of these indicators in arid environments make them especially powerful as an archive: these regions are most sensitive to changes in climate and human land use, but there is an absence of other archives to conduct these studies (Asner et al., 2004; Chase et al., 2012; Maestre et al., 2016; Ivory et al., 2021). Middens collected in the Dhofar Nejd will be used to develop a record of vegetation change over a period of increasing aridity in the late Holocene, where there is currently little paleoecological information.

Regional paleoecology

The paleoecological record can be used as a natural experiment to investigate ecological interactions, such as climate change, changes in vegetation, fire regimes, and human land use (Dietl et al., 2014; Bottjer, 2016). One period that provides an interesting case study for vegetation response to increasing aridity is the end of the Holocene Humid Period (~6-5 ka). This transition was characterized by a substantial decrease in precipitation and the development of modern hyperarid conditions and monsoon dynamics in southern Arabia (Fleitmann et al., 2004; Fleitmann et al., 2007; Cremaschi et al., 2015; Lézine et al., 2017). Although this period has been well studied in places like North Africa, specifically the transition from the “Green Sahara” and desertification, there are only a few regional precipitation records from Southern Arabia, namely speleothem oxygen isotopes (Fleitmann et al., 2004; Fleitmann et al., 2007; Kröpelin et al., 2008). Likewise, there are few paleoecological records demonstrating the effect these climatic changes had on vegetation communities. Herein lies an opportunity to investigate changes in plant communities and better constrain climate-vegetation dynamics in an arid environment.

The Holocene Humid Period (~9-6 ka) was a time of increased rainfall in Southern Arabia and northern Africa, the termination of which resulted in more arid conditions (Morrill et al., 2003; Renssen et al., 2003; Fleitmann et al., 2007). During this period, the Intertropical Convergence Zone (ITCZ) was at its northernmost position, and this combined with higher northern hemisphere insolation created a stronger Indian Monsoon system and thus increased precipitation (Gasse and Van Campo, 1994; Morrill et al., 2003; Renssen et al., 2003; Fleitmann et al., 2007). Evidence for wetter conditions in the early Holocene comes from lake records in northern Africa, which demonstrate increased sediment flux from rivers and higher clays indicating higher weathering from ~6-5ka (Gasse, 2000). Pluvial conditions existed in the Rub’ al-Khali desert in southern Arabia, and these paleolakes dried out by 7-6ka (McClure, 1976;

Lézine et al., 2007; Lézine et al., 1998). In Oman, depleted speleothem $\delta^{18}\text{O}$ values from Hoti and Qunf caves in northern Oman and Dhofar, respectively, also suggest higher precipitation from ~10-7ka (Burns et al., 1998; Fleitmann et al., 2004; Fleitmann et al., 2007). The growth of calcareous flowstones in these same caves is additional evidence for higher precipitation, and these yield similar $\delta^{18}\text{O}$ values to the speleothems (Fleitmann et al., 2007; Cremaschi et al., 2015). Increased sediment flux into estuaries in Dhofar ~2.7-2.4 ka and ~1.7-1.5 ka reflects increased runoff from wadi drainage systems and therefore higher rainfall even into the late Holocene (Hoorn and Cremaschi, 2004).

There is debate surrounding the characterization of the termination of the Holocene Humid Period, namely whether there was an abrupt or gradual decline in precipitation (Morrill et al., 2003; Kröpelin et al., 2008; Fleitmann et al., 2007; Lézine et al., 2017). Compiled paleoclimatic records across Asia and some from East Africa suggest an abrupt transition to more arid conditions ~5 ka (Morrill et al., 2003). Transient climate simulations and pollen records from mangrove pollen records off the coast of Dhofar indicate a stepwise decline in rainfall, with abrupt decreases in precipitation at ~5 ka and ~2.7 ka (Lézine et al., 2017). By contrast, reconstructed paleohydrological conditions based on organic matter deposition and freshwater phytoplankton at Lake Yoa do not provide evidence for an abrupt transition (Kröpelin et al., 2008). Moreover, the speleothem records from southern Arabia suggest the end of this wetter period was characterized by a gradual decline in precipitation, caused by a southward migration of the Intertropical Convergence Zone (ITCZ; Fleitmann et al., 2007). All these records agree, however, that semiarid conditions prevailed by the mid Holocene and raise questions regarding the response of local, biodiverse plant communities (Morrill et al., 2003; Kröpelin et al., 2008; Fleitmann et al., 2007; Lézine et al., 2017).

Some paleoecological studies from this time frame have been conducted in southern Arabia to reconstruct vegetation dynamics over this interval of changing climate. A Holocene lake record of pollen and phytoliths from Emirate of Ras al-Khaimah demonstrate the replacement of *Acacia* and *Prosopis* woodland and savannah grassland with sparser, C4-dominated vegetation associated with increased aridity in the mid-Holocene (Parker et al., 2006). In Yemen, pollen records from the paleolake at al-Hawa suggest an arid environment with few trees (Lézine et al., 2007; Lézine et al., 1998). Pollen analysis from hyrax middens in Wadi Sana, Yemen, provide later records that demonstrate a semi-arid woodland with tropical trees such as *Terminalia* between ~5-4.7 ka (Ivory et al., 2021). Mangrove pollen records also demonstrate a community dominated by tropical taxa from ~6-4.5 ka on the coast of Dhofar (Lézine et al., 2002). Pollen from the estuary sediment cores in Dhofar illustrate changes in coastal vegetation in the mid to late Holocene, which show an increase in more saline, drought tolerant taxa (e.g., *Amaranthaceae*) (Hoorn and Cremaschi, 2004). There is a lack of records from the inland desert of Dhofar, and thus no insight into how changing precipitation affected vegetation conditions in this region. Dessication of paleolake records from Yemen limit vegetation reconstructions in the region after ~7 ka (Lézine et al., 2007). Vegetation records from Dhofar developed from mangrove sites and estuarine sediment cores are relegated to the coast and do not preserve evidence of desert plant communities over this period (Lézine et al., 2002, Hoorn and Cremaschi, 2004).

Hyrax middens from the interior desert of Yemen demonstrate their effectiveness as a paleoecological archive (Ivory et al., 2022). While existing paleoenvironmental records are fragmentary both spatially and temporally, hyrax middens can also be found in the inland desert of Dhofar. Herein lies the opportunity to investigate the outstanding questions surrounding vegetation response to increasing aridity, using the case study of the termination of the Holocene Humid Period.

Reconstructing pastoralist activity from the archaeological record

Archaeological remains can be used to interpret human subsistence strategies and mobility in the past. These artifacts can include constructed settlements or monuments, animal remains, agricultural features, and tools. Domesticated animal herding as a subsistence strategy is considered the beginning of the Neolithic period in Arabia, and faunal remains from cattle appear as early as ~7ka (Drechsler, 2007; Grigson, 1989; Martin et al., 2009). Previous studies have linked archaeological evidence with paleoecological information to infer wetter intervals during the late Pleistocene/early Holocene aided the dispersal of these Neolithic communities (Dinies et al., 2015; Drechsler, 2007; Hilbert et al., 2015b; Martin et al., 2009; Parker and Rose, 2008; Zarins, 2013). Domesticated animal herding in Arabia was practiced without any evidence for plant cultivation, and nomadic pastoralism persisted in southern Arabia through the Holocene (Martin et al., 2009; McCorrison et al., 2018). In Dhofar, nomadic pastoralism continues to be a culturally and economically important subsistence strategy (Ball and Tzanopoulos, 2020).

Archaeological evidence suggests that in the earlier part of the Holocene (~12-8 ka), pastoral groups in Dhofar were highly mobile and grazing their animals far inland in the Nejd during a more humid climate (Cremaschi et al., 2015; McCorrison et al., 2018). There is a lack of permanent settlement structures, rather sites documenting ephemeral use, such as rock shelters with scattered lithic technologies (Cremaschi et al., 2015; Hilbert et al., 2015a; McCorrison et al., 2018; Zarins, 2013). In the mid- to late Holocene (~8-4 ka), the climate began to dry as the Indian Monsoon gradually weakened (Cremaschi et al., 2015; Fleitmann et al., 2007). During this period, pastoralists constructed monuments that marked their passage throughout the desert, and these stoneworks are much of the archaeological evidence that has stood the test of time (Harrower et al., 2014; McCorrison et al., 2014; McCorrison et al., 2018). From ~7-6 ka, low, circular platforms built with limestone cobbles were constructed overlooking wadi drainage

systems (McCorriston et al., 2014). Evidence for visitation of these monuments by mobile groups is provided by the remains of hearths, but their purpose can only be inferred from similar structures in Yemen (McCorriston et al., 2011; McCorriston et al., 2014). The faunal remains of dozens of cattle suggest these were gathering points for feasts (McCorriston et al., 2011; McCorriston et al., 2014).

Later in the mid-Holocene (~5-4 ka), many monuments were built that were funerary in nature. One type, named High Circular Tombs or HCTs, were mound-shaped tombs erected on high promontories (McCorriston et al., 2014). HCTs were constructed with limestone slabs and had inner chambers with corbelled roofs (Harrower et al., 2014; McCorriston et al., 2014). Often these sites were revisited by pastoralists, as indicated by faunal remains placed above tombs after interment of the deceased (McCorriston et al., 2014). Other tombs built at this time, called Wall Tombs, were more rectangular in design and have been found across Southern Arabia (McCorriston et al., 2011; McCorriston et al., 2014; Steimer, 2022). The unity between the architectural styles of these funerary structures in southern Arabia point to a cultural connection across this geographical area (Steimer, 2022).

In the late Holocene or the Iron Age of Dhofar (~3 ka - 1.3 ka), a common but enigmatic type of stone monument began to dot the prehistoric southern Arabian landscape (Garba, 2019; Harrower et al., 2014; Newton and Zarins, 2010; McCorriston et al., 2014; McCorriston et al., 2018). These monuments, called Triliths, consisted of three flat stones placed vertically form a pyramid shape (Garba, 2019; McCorriston et al., 2014; Harrower et al., 2014). Several of these pyramids were oriented in a line across a low cobblestone platform (Garba, 2019; McCorriston et al., 2014; Harrower et al., 2014). While these were built across southern Arabia, in Dhofar they are notably found solely in the Nejd (Newton and Zarins, 2010). Several theories exist as to the purpose of triliths: they may be affiliated with the frankincense trade, due to their location in the preferred habitat of frankincense (*Boswellia sacra*) trees in the Nejd nearest the mountains

(Miller and Morris, 1988; Newton and Zarins, 2010). The coastal port city of Sumharam was an epicenter of this frankincense trade and existed contemporaneously with the construction of triliths (Avanzini, 2008; Harrower et al., 2014; McCorrison et al., 2014; Zarins, 2009). However, the inhabitants of Sumharam were likely an independent cultural group from the indigenous mobile pastoralists of Dhofar, as suggested by the lack of evidence for the trade of material goods between them (Avanzini, 2008; Buffington and McCorrison, 2018; Newton and Zarins, 2010; McCorrison et al., 2014; Zarins, 2009). An alternate theory postulates that they were then erected to signal territoriality and ownership of environmental resources (McCorrison et al., 2014; McCorrison et al., 2018; Zarins, 2009).

Pastoralists also constructed more permanent settlements on the plateau during the Iron Age, from ~2-1 ka (McCorrison et al., 2020; Newton and Zarins, 2010). These were in stark contrast to the ephemeral Nejd sites and indicate a change in mobility during this time (McCorrison et al., 2018; McCorrison et al., 2020). These sites include megalithic structures that would have required cooperative labor to erect and include evidence of occupation and reoccupation over several generations (McCorrison et al., 2020). In addition to domestic features, such as hearths, there are stone structures that are interpreted as pens for domesticated animals (McCorrison et al., 2020). Through paleoclimatic and paleoecological data, it is inferred that this was an especially dry period, and the Nejd may have lacked necessary biomass for cattle grazing (Fleitmann et al., 2007; McCorrison et al., 2014; McCorrison and Harrower, 2020). Hence, the pastoralists congregated near sources of water (McCorrison et al., 2018; McCorrison et al., 2020). Lack of evidence for agriculture demonstrates the continuance of subsistence pastoralism, or the reliance solely on domesticated animals and some wild game (McCorrison et al., 2020). Dhofar is unique in that this practice persisted for thousands of years, despite near neighbors adopting agriculture (McCorrison et al., 2018).

Chapter 2: In the dens of dassies: vegetation dynamics in Dhofar, Oman from the late Holocene to present inferred from rock hyrax middens

There is a lack of long-term records of vegetation change in southern Arabia, especially Dhofar, documenting the response of plant communities increasing aridity over the late Holocene. The records that do exist mainly document changes in coastal vegetation, thus there is a scarcity of information regarding the biodiverse, inland communities in the Nejd desert (Lézine et al., 2002; Hoorn and Cremaschi, 2004). Rock hyrax middens collected in the Nejd of Dhofar provide a unique opportunity to investigate climate-vegetation dynamics in this region. Pollen preserved in the middens provide a record of vegetation change after the onset of decreasing precipitation in this region to the present day. Pollen is diagnostic of plant taxa, and therefore can be used to identify what vegetation was present on the landscape and in what relative proportions based on abundance calculations. The development of a paleocological record from the middens addresses these questions: *(1) How did vegetation communities change during increasing aridity over the late Holocene in the Dhofar Nejd? (2) How did pastoralist activity over this time frame affect vegetation?*

Chapter 3: The only thing certain in grad school is death and (leaf) waxes: late Holocene hydrologic variability and ecosystem structure

Changes in rainfall can have a significant impact on vegetation in arid places (Maestre et al., 2016). Geochemical proxies are effective tools to reconstruct changes in precipitation in deeper time and better constrain this relationship. Regional paleoprecipitation records in Dhofar based on speleothem $\delta^{18}\text{O}$ indicate a decrease in precipitation and monsoon strength in the Late Holocene (Fleitmann et al., 2007). However, these speleothems were sampled from coastal caves, and may not reflect rainfall conditions further inland in the Nejd (Fleitmann et al., 2007). Thus,

there is an outstanding need for local paleohydrological records to assess changes in moisture that may have driven the observed turnover in vegetation. Bulk nitrogen isotopes from the hyrax middens developed a local paleohydrological signal and suggest a transition to hyperaridity by 4000 cal yrs BP (Chase et al., 2012; Wang et al., 2014; Diaz et al., 2016). To investigate vegetation response to changing moisture conditions in the Nejd, we can use compound specific carbon and hydrogen isotopes from leaf wax *n*-alkanes ($\delta^{13}\text{C}_{\text{wax}}$ and $\delta\text{D}_{\text{wax}}$). The use of these geochemical proxies seeks to ascertain: (1) *How did local rainfall conditions change in the Nejd over the late Holocene?* (2) *Does this evidence support increasing aridity as a mechanism for floristic turnover during this time frame?*

Chapter 4: Modelling movement on the Dhofar landscape: climate change, human activity, and vegetation response

Domesticate animal grazing makes up $\frac{1}{4}$ of land surface use on the planet, and thus is an important source of food resources such as meat and dairy (Asner et al., 2004). Nomadic pastoralism, particularly in arid places, has a long-term history of resilience and sustainability and has been continuously practiced by hundreds of millions of people (Dyson-Hudson and Dyson-Hudson, 1980; Fratkin, 1997; Djohy et al., 2014; McCorriston et al., 2018). However, today much of these rangelands are actively being degraded (Sayre et al., 2012). Because rangelands are managed by humans, decisions regarding domesticate herding are influenced by governments and societal frameworks (Fratkin, 1997; El-Mahi, 2011). Moreover, changes in the economy as well as climatic changes can have significant impacts on these rangelands (Fratkin, 1997; El-Mahi, 2011; Ball and Tzanopoulos, 2020). Thus, the relationship between humans, the practice of pastoralism, and the environment is a complex system influenced by numerous environmental and cultural factors. Understanding these relationships is imperative to preserving this essential

lifeway under global climate change and changing land use. While paleoecological and archaeological data provides useful long-term records, these illustrate patterns in environmental and cultural changes. The mechanisms which create these patterns and their relationships with one another can be investigated with an Agent Based Model (ABM). ABM experiments are guided by these questions: *(1) How do changes in the amount and seasonality of rainfall affect the composition of vegetation communities? (2) How does more geographically extensive fog influence vegetation in the Nejd? (3) How does the amount of domesticated herds on the landscape, and thus grazing and browsing pressure, change the proportions of arboreal vegetation versus herbaceous plants?*

Chapter 2

DOI: <https://doi.org/10.1017/qua.2023.42>

In the dens of dassies: vegetation dynamics in Dhofar, Oman from the late Holocene to present inferred from rock hyrax middens

Arid regions are especially vulnerable to climate change and land use. Over one-third of Earth's population relies on these ecosystems. Modern observations lack the temporal depth to determine vegetation responses to climate and human activity, but paleoecological and archaeological records can be used to investigate these relationships. Decreasing rainfall across the late Holocene provides a case-study for vegetation response to changing hydroclimate. Rock hyrax (*Procavia capensis*) middens preserve paleoenvironmental indicators in arid environments where traditional archives are unavailable. Pollen from modern middens collected in Dhofar, Oman demonstrates the reliability of this archive. Pollen, stable isotope ($\delta^{13}\text{C}$, $\delta^{15}\text{N}$), and microcharcoal data from fossil middens reveal changes in vegetation, relative moisture, and fire from 4000 cal yr BP to present. Trees limited to moister areas (e.g., *Terminalia*) today existed further inland ~3100 cal yr BP. After ~2900 cal yr BP taxa with more xeric affiliations (e.g. *Senegalia*) had increased. Coprophilous fungal spores (*Sporormiella*) and grazing indicator pollen revealed an amplified signal of domesticated grazing ~1000 cal yr BP. This indicates that trees associated with semi-arid environments were maintained in the interior desert during ~3000-4000 years of decreasing rainfall, and that impacts of human activity intensified after the transition to a drier environment.

Introduction

Humans are unprecedented agents of landscape change. Anthropogenic climate change continues to accelerate, and other activities such as urban expansion and animal grazing will likely cause drastic changes in ecosystems (Maestre et al., 2016; Dahinden et al., 2017; IPCC, 2022). Dryland ecosystems comprise 41% of Earth's terrestrial surface, and 38% of the human population relies on them (Maestre et al., 2016). These ecosystems are especially sensitive to ecological change – small decreases in precipitation or increases in domesticated animal grazing can lead to a reduction in vegetation cover, with resultant impacts to water and food security (Asner et al., 2004; Maestre et al., 2016; Ball and Tzanopoulos, 2020;). Climate models predict globally increasing temperatures which have the net effect of decreasing relative moisture in arid places (Stavi et al., 2026). However, recent data are too brief to assess natural variability and long-term ecosystem dynamics (Dietl et al., 2014). There is a need for longer term records to investigate how changes in climate, particularly water availability, affect vegetation.

Southern Arabia is mainly hyperarid, but also hosts a biodiverse flora with a high level of endemism (Miller and Morris, 1988; Ghazanfar, 1998). The Dhofar Governorate of Oman is home to a unique cloud forest, with trees that intercept fog moisture from the seasonal Indian Ocean monsoon (*khareef*) (Hildebrandt et al., 2007). These conditions make the vegetation of Dhofar particularly sensitive to changes in temperature and precipitation: rainfall is correlated with vegetation cover, which is shown to be declining in the most arid locations in Dhofar (Ramadan et al., 2021). Recent studies have additionally highlighted the threat of overgrazing of native vegetation by domesticated animals due to rapid economic growth over the last few decades, which has led to increased stocking rates of cattle and camels in Dhofar (Ghazanfar, 1998; Galletti et al., 2016; Ball and Tzanopoulos, 2020). The preferential browsing of young shoots compared to adult trees prevents the regeneration of woody taxa, and there has been up to

10% loss of forest land cover in some areas of the cloud forest due to grazing alone (Galletti et al., 2016; Ball and Tzanopoulos, 2020). These changes have only been quantified over the last few decades as stocking rates reached current high levels (Galletti et al., 2016; Ball and Tzanopoulos, 2020). It is imperative to understand how both changes in climate and human activity dynamically influence vegetation, as human land use may amplify the effects of projected climate conditions.

One period that provides a case study for determining the vegetation response to increasing aridity is the end of the Holocene Humid Period. The termination of the Holocene Humid Period (~5.5 ka) led to decreased rainfall in southern Arabia and increasingly arid conditions (Renssen et al., 2003; Morrill et al., 2003; Fleitmann et al., 2007; Lézine et al., 2014; Ivory et al., 2021). Although this period has been well studied in places like North Africa, there are relatively few paleoclimate records from southern Arabia (Fleitmann et al., 2004; Fleitmann et al., 2007; Kröpelin et al., 2008). However, speleothem $\delta^{18}\text{O}$ records preserve changes in precipitation during the last deglaciation from multiple locations in southern Arabia. These records suggest a gradual decline in precipitation beginning at ~8-7 ka (Fleitmann et al., 2007; Lézine et al., 2014). While it is likely that conditions were already semi-arid in this region in the early Holocene, these paleoclimate records indicate conditions became increasingly dry across the Holocene such that perennial lakes disappeared and surface runoff became more limited (Fleitmann et al., 2007; Lézine et al., 2014; Hoorn and Cremaschi, 2004). The response of vegetation communities to these changes remains somewhat unclear.

To understand how ecosystems responded to decreasing rainfall over the mid- to late-Holocene, several previous paleoecological studies have been conducted in southern Oman and nearby Yemen. Estuarine cores from Oman provide near-continuous records of changes in coastal vegetation in the mid to late Holocene, which show an increase in more saline, drought-tolerant taxa (e.g., *Amaranthaceae*). This supports aridification by ~1.7-1.5 ka based on palynological and

sedimentological evidence (Lézine et al., 2002; Hoorn and Cremaschi, 2004; Lézine et al., 2017). There is also support for more wet phases that punctuated the trend in increasing aridity at ~2700-2300 cal yr BP and ~1700-1500 cal yr BP, when there was increased runoff to the estuaries (Hoorn and Cremaschi, 2004). However, information away from the coasts is patchy in both space and time. In Yemen, paleolakes provide insight into the wetter climate at the last deglaciation into the early Holocene, as no perennial lakes exist in this region today (Lézine et al., 1998; Lézine et al., 2007). Pollen and sedimentological records from these lakes indicate that even during maximum humid conditions, there were seasonal periods of high evaporation that led to a persistence of a semi-arid desert vegetation community in inland Yemen (Lézine et al., 2007). However, due to desiccation of most inland lakes by ~7 ka, evidence of vegetation change from sedimentary deposits in these areas after this time does not exist (Lézine et al., 2007). Pollen preserved in hyrax middens provide later records that suggest a semi-arid woodland with tropical trees such as *Terminalia* at 5 ka at Wadi Sana, Yemen (Ivory et al., 2021). Little information exists about vegetation changes further inland in Dhofar as aridification intensified from the mid-Holocene to present.

Archaeological evidence suggests changes in settlement and mobility in Dhofar during the Holocene, lending some insight into changes in human land use over this time frame (Harrower et al., 2014; McCorrison et al., 2018; McCorrison and Harrower, 2020). Nomadic pastoralism has been practiced in this region for at least 7000 years and continues to be a culturally important lifeway (McCorrison et al., 2018). Archaeological evidence based on the construction of megalithic monuments in the desert and the lack of permanent habitation sites indicate pastoral groups were highly mobile and grazed their animals far inland (Harrower et al., 2014; McCorrison et al., 2014; McCorrison et al., 2018). This was during an interval when paleoclimatic records suggest wetter than modern conditions (~7-5 ka) (Fleitmann et al., 2004; Fleitmann et al., 2007). During a period of increased aridity in the late Holocene (~2-1 ka),

pastoralists built more permanent settlements closer to the coast (McCorrison et al., 2014; McCorrison and Harrower, 2020). The ecological effects of ancient pastoralism and changes in settlement patterns are not well understood. Modern pastoral activity can have surprising impacts on vegetation in these arid regions that are not always degradational. For example, grazing and browsing can maintain grasslands and domesticated dung increases nutrient input to dry soils (Brierley et al., 2018). Assessing changes in vegetation in this region is important for understanding the persistence, and hopefully the continued sustainability, of pastoralism under changing climate conditions. Moreover, teasing apart climate and human-driven mechanisms of vegetation change is important for making more accurate predictions about changes to semi-arid pastoral landscapes, as well as designing sustainability initiatives to mitigate them.

In this study, we present pollen and bulk stable isotope data from rock hyrax middens collected in the Dhofar Governorate of Oman. We use thin (<5 cm) middens which represent individual, temporally averaged samples, with the oldest radiocarbon age at ~4000 cal yr BP. Rock hyrax middens serve as well-established paleoecological archives in arid ecosystems, preserving pollen, macrofossils, and isotopic information for thousands of years (Scott and Cooremans, 1992; Scott and Woodborne, 2007; Chase et al., 2012, Ivory et al., 2021). The records presented here provide paleoecological information after the onset of decreasing precipitation in this region at the end of the Holocene Humid Period to the present. While future conditions in Dhofar are likely to be drier than those seen in the last 4000 years, this record provides a long-term view of vegetation response to climate change in this unique, biodiverse dryland ecosystem (Dahinden et al., 2017). This can help inform predictions for southern Arabia as well as semi-arid drylands that are expected to experience aridification similar to that seen across the Holocene in Dhofar.

Modern Setting

The physiography of southern Oman is strongly characterized by the steep south-facing escarpments of the Dhofar Mountains. These mountains are mainly composed of Tertiary limestone, with a karst net that forms caves and rock shelters (Cremaschi, 2015; Miller and Morris, 1988). A fault system crosscuts the north-dipping limestone strata, which is mainly oriented east-west (Zerboni et al., 2020). At the highest elevations, approximately 850 m above sea level, the landscape becomes a plateau inset by northward-draining wadi systems (Miller and Morris, 1988; Zerboni et al., 2020). The Tertiary carbonates are incised by these dry riverbeds, which are covered with large gravel alluvium (Al-Mashaikhi et al., 2012). A lack of soil in the desert inland from the coast creates a landscape of large, bare carbonate outcrops that form the wadi walls (Zerboni et al., 2020).

The Dhofar Governorate is predominantly arid. The coastal region receives approximately 120-150 mm of precipitation per year and has a mean annual temperature of 25.7°C based on data from the Salalah airport weather station (1970-1990) (Fleitmann et al., 2004; Fleitmann et al., 2007; Cremaschi et al., 2015;). However, hyperarid conditions prevail further inland in the Nejd desert, which receives an average of 30 mm of precipitation per year based on observations from the Thumrait weather station (1980-2015) (Al-Mashaikhi, 2012). These two weather stations are denoted on the map (Figure 2-1). Most of the precipitation in this region occurs during the northern summer (June-September) (Fleitmann et al., 2007) when the Indian monsoon brings dense fog to the coastal regions of Dhofar, increasing relative humidity to as much as 97% (Patzelt, 2015). This fog forms as moisture-laden air passes over the cool surface waters off the coast (Miller and Morris, 1988). As the fog moves inland, it becomes trapped against the slopes due to a temperature inversion, blanketing the escarpment with thick cloud cover which generally does not extend past the crest of the escarpment (Miller and Morris, 1988).

The modern vegetation can be categorized into four ecological zones from south to north (coastal plain, escarpment, plateau, and Nejd desert), which encompass changes in elevation, climate conditions, as well as the dominant taxa (Miller and Morris, 1988). The coastal plain is a flat, low elevation band that stretches from the coast to the foothills of the escarpment. The vegetation in this zone is extremely sparse due to overgrazing and other human activities, but plants such as *Aerva javanica* and *Heliotropium* spp. can be found on rockier soils (Miller and Morris, 1988). The escarpment is home to the seasonal cloud forests comprised of deciduous trees, notably *Terminalia dhofarica* and *Maytenus dhofarensis*, with an understory of grasses (Poaceae) and other herbs (*Merremia* spp., *Heliotropium* spp.) (Patzelt, 2015). These trees, particularly *T. dhofarica*, are reliant on moisture from the monsoon fog. *Terminalia dhofarica* intercepts moisture directly from the air during the khareef to increase net water availability locally (Hildebrandt et al., 2007; Friesen et al., 2018). The plateau is a grassland with isolated trees such as *Ficus vasta* (Miller and Morris, 1988; Buffington and McCorriston, 2018). On the distal reaches of the plateau beyond monsoonal fog, *Boswellia sacra* (frankincense) is commonly found (Patzelt 2015). The furthest inland is the Nejd desert, which is the driest sector in the region (Al-Mashaikhi, 2012). This zone is characterized by isolated trees (*Senegalia* spp., *Boscia*, *Maerua*, *Ficus salicifolia*) and sparse herbaceous cover (*Heliotropium* spp., *Cornulaca*) (Miller and Morris, 1988; Ghazanfar, 2004; Patzelt, 2015). Table 2-1 highlights the dominant taxa in each of these areas.

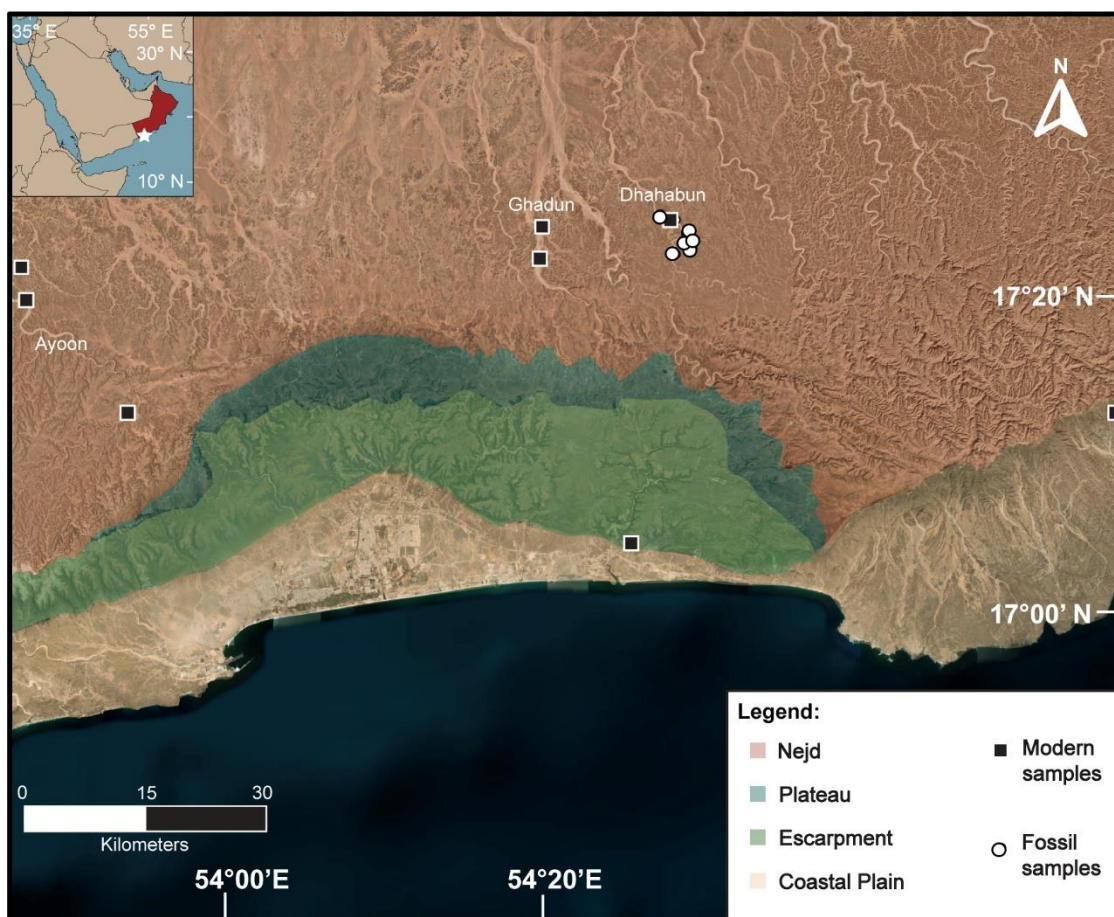


Figure 2-1: Map of Dhofar depicting the four ecological zones. The midden sampling locations are shown by the boxes. Inset shows the geopolitical boundaries of Oman on the Arabian Peninsula.

Table 2-1: The four ecological zones of Dhofar and their dominant vegetation taxa.

Ecological Zone	Description	Dominant vegetation
Coastal Plain	Low elevation, highly disturbed and sparsely vegetated	<i>Aerva javanica</i> , <i>Heliotropium spp.</i> ,
Escarpment	High elevation, mountainous, Seasonal cloud forest	<i>Terminalia dhofarica</i> , <i>Maytenus dhofarensis</i> , Poaceae, <i>Merremia spp.</i> , <i>Heliotropium spp.</i>
Plateau	High elevation, flat, grassland	Poaceae, <i>Ficus vasta</i> , <i>Boswellia sacra</i> , <i>Draceana</i>
Nejd	Desert, isolated trees and rare herbs	<i>Senegalia spp.</i> , <i>Boscia</i> , <i>Maerua</i> , <i>Ficus salicifolia</i> , <i>Heliotropium spp.</i> , <i>Cornulaca</i>

Hyrax middens as paleoenvironmental archives

Various types of animal middens have been successfully employed for paleoenvironmental analyses. These archives represent different spatial and temporal scales, dictated by the behavior of the animal and the manner in which they are deposited (Cole, 1990; Anderson and Van Devender, 1995; Scott et al., 2004; Chase et al., 2012). In the dry regions of western North America, packrat (*Neotoma*) midden studies have revealed changes in local flora within ~10-100 m of den sites through pollen and macrofossil studies, and more recently ancient DNA (Cole, 1990; Anderson and Van Devender, 1995; Fisher et al., 2009; Moore et al., 2020). Packrats collect plant matter and other materials, creating a “garbage pile” protecting the entrance of their dens (Cole, 1990). Through the defecation and urination of the packrats, this garbage pile will become an indurated mass, or midden (Cole, 1990; Anderson and Van Devender, 1995; Fisher et al., 2009). Analyses of modern packrat middens and local vegetation show high agreement, indicating that fossil middens are a reliable archive of past environments (Cole, 1990;

Anderson and Van Devender, 1995; Fisher et al., 2009). These samples are processed through dissolution in water, then a sieving process which separates macrofossil and microfossil fractions (Van Devender et al., 1994; Moore et al., 2020). Each midden is dated and treated as one sample at an individual point in time (Van Devender et al., 1994; Anderson and Van Devender, 1995).

Rock hyrax (*Procavia capensis*) middens have emerged as a powerful tool for similar paleoecological studies in the arid regions of Africa and Arabia (Scott and Woodborne, 2007; Chase et al., 2012; Ivory et al., 2021). Rock hyraxes are small mammals which resemble rodents but are in fact most closely related to elephants. They can eat a wide variety of plants and tolerate a large range of temperature and precipitation conditions (Sale, 1965; Rübsamen et al., 1982; Chase et al., 2012; Mohamed, 2019). Generally, middens are deposited in caves and rocky overhangs as compacted deposits of crystallized urine (hyraceum) and fecal pellets (Gil-Romera et al., 2010; Chase et al., 2012). Pollen and other paleoenvironmental indicators are brought into the caves on the feet or fur of hyraxes and blown in via aeolian deposition, then trapped in the sticky hyraceum (Chase et al., 2012). Plant matter consumed by the hyraxes also passes through their digestive systems and is preserved in their dung (Scott et al., 2004; Scott and Woodborne, 2007; Gil-Romera et al., 2010; Chase et al., 2012). Stable carbon isotope analyses of fecal pellets and hyraceum reflect the input of C₃ and C₄ vegetation, and nitrogen isotope studies can reveal changes in relative moisture (Chase et al., 2012; Ivory et al., 2021). Middens can differ in thickness and the amount of hyraceum versus fecal pellets, and thus can have varying degrees of dietary bias and represent disparate temporal scales (Scott and Cooremans, 1992; Scott et al., 2004; Gil-Romera et al., 2006; Scott and Woodborne, 2007; Chase et al., 2009; Chase et al., 2012).

In southern Africa, massive middens composed primarily of hyraceum have been discovered, providing paleoenvironmental insight for the late Pleistocene and Holocene (Chase et al., 2009; Carr et al., 2010; Chase et al., 2012). These types of middens can be sub-sampled for

isotope and pollen analyses akin to a sediment core and the data can be interpreted as a time series (Chase et al., 2012). However, thinner middens consisting of indurated dung material have also proved a useful archive of the same paleoecological indicators (Scott and Cooremans, 1992; Scott et al., 2004; Gil-Romera, 2006; Scott and Woodborne, 2007; Ivory et al., 2021). While these contain a higher dietary input from fecal material, analyses of modern dung middens from South Africa illustrate that their pollen spectra are negligibly different from pollen spectra of surface soils (Scott and Cooremans, 1992). Moreover, studies of hyrax diet and behavior from both Africa and Arabia demonstrate that hyraxes are generalists and have few dietary restrictions (Sale, 1965; Mohamed, 2019).

The methodology for processing these samples is also different. Hyraceum middens are typically radiometrically dated, drilled for isotopic analyses, then processed for pollen and other indicators through the midden's growth axis (Carr et al., 2010; Chase et al., 2012). Processing of thin, dung middens follows a protocol similar to the one described for packrat middens: they are first disaggregated in water then sieved to obtain a macrofossil fraction and microfossil fraction (Van Devender et al. 1994; Scott and Woodborne, 2007; Ivory et al., 2021). Because of the differences in material and sampling, thin middens are interpreted as single, variably time-averaged samples. Hyraceum middens can provide long term (10^3 - 10^4 years) paleoecological sequences with single datapoints averaged over $\sim 10^1$ - 10^2 years, whereas paleoecological data from dung middens are averaged over the period of midden deposition and include more dietary information (Scott and Cooremans, 1992; Gil-Romera, 2006; Scott and Woodborne, 2007; Chase et al., 2012; Ivory et al., 2021).

In this study, we obtained thin (<5cm) rock hyrax middens consisting of indurated dung pellets cemented with crystallized urine. To process these middens and conduct pollen analysis, we utilized the same approach that has been successful for both packrat middens and other fossil hyrax dung middens in South Africa (Van Devender et al., 1994; Scott and Woodborne, 2007;

Ivory et al., 2021). The presence of fecal matter introduces a degree of dietary bias in these samples. However, we conducted a comparison of pollen abundances from modern middens with botanical information from Dhofar and determined that signal recorded within the middens is a good representation of local vegetation. To assess the period over which thin middens accumulate, Ivory et al. (2021) obtained multiple radiocarbon dates from the same midden, which resulted in ages that were not significantly different. This analysis was conducted on multiple middens. Based on this analysis from nearby Yemen on similar middens, we assume the middens from our study represent decades to ~100 years of deposition. As such, we interpret each midden as one sample, and the data as an average of local vegetation over ~100 years.



Figure 2-2: Pictures of representative rock hyrax middens.

Methods

Pollen analysis was conducted on 13 modern hyrax middens across a large geographical area and spans the four ecological zones (Table 2-2). These were determined to be modern

through radiocarbon dating or if the samples were not compacted and included fresh dung, as was the case for all middens collected closer to the coast. In these regions, prevailing moist conditions during the monsoon season leads to the disintegration of middens; older middens are not typically preserved. Four samples were taken from the distal plateau (Wadi Ayun), two from a drainage system in the western Nejd (Wadi Ghadun), and three from the East Nejd (Wadi Dhahabun). Two samples were collected from the coastal plain close to the base of the escarpment. Two samples of fresh camel dung were also collected on the escarpment, where no hyrax middens were found. These samples were then compared to published botanical literature from the Dhofar region to assess the representativity of flora within this archive. (Miller and Morris, 1988; Ghazanfar, 1998; Ghazanfar, 1999; Raffaelli et al., 2003; Ghazanfar, 2004; Hildebrandt, 2007; Patzelt, 2015). The modern samples were also compared to four submodern middens from the East Nejd (110-160 cal yr BP) to assess historic changes in vegetation.

Additionally, pollen analysis was completed on fossil middens in the Nejd desert to establish a record of vegetation change over the last 4,000 years. To create the fossil pollen record, 26 rock hyrax middens were collected over three field seasons from February 2017 through October 2018 (Table 2-3). 22 fossil middens and one modern midden were collected from the East Nejd, while three additional modern midden samples from the distal plateau further to the west were used to compare a wide geographic range of modern vegetation to the recorded fossil vegetation (Figure 2-1). Surveying for middens consists of examining small natural caves in cliffs and looking for fecal pellets in and around these sheltered locations. The presence of these pellets helped identify caves which could contain middens. Once discovered, these middens were carefully extracted from the caves using a chisel and hammer, keeping them as intact as possible. The samples were then wrapped in plastic to avoid contamination before shipment. A photograph of a representative midden as well as a midden *in situ* are shown in Figure 2-2.

Table 2-2: Modern midden sampling locations, AMS radiocarbon dates, calibrated ages, and bulk stable isotope information.

Sample ID	Ecological Zone	Material	Latitude	Longitude	Age (cal yr BP)	$\delta^{13}\text{C}$ (‰)	$\delta^{15}\text{N}$ (‰)
WP19	Coastal Plain	Hyrax midden	17°12.804'	55°03.446'	modern (no date)	-27.54	7.14
WP18	Coastal Plain	Hyrax midden	17°12.854'	55°03.761'	modern (no date)	-27.84	6.03
C1 Camel	Escarpment	Camel pellet	17°4.655	54°27.068'E	modern (no date)	-29.81	6.35
C2 Camel	Escarpment	Camel pellet	17°4.655	54°27.068'E	modern (no date)	-30.07	8.01
ASO6	Distal Plateau	Hyrax midden	17°14.612'N	53°53.365'E	modern (no date)	-28.31	5.56
ASO3	distal plateau	Hyrax midden	17°14.618'N	53°53.380'E	modern (no date)	-27.05	4
ASO4	distal plateau	Hyrax midden	17°14.618'N	53°53.380'E	modern (no date)	-27.53	5.79
ASO7	distal plateau	Hyrax midden	17°14.618'N	53°53.380'E	modern (no date)	-26.24	4.01
WP79-2c	Nejd - west	Hyrax midden	17°20.987'	53°42.938'	0	-28.2	7.3
WP83-1	Nejd - west	Hyrax midden	17°24.138'	53°41.690'	0	-28.14	5.95
WP61-1	Nejd - east	Hyrax midden	17°24.865'	54°20.822'	0	-27.18	7.38
WP61-2	Nejd - east	Hyrax midden	17°24.865'	54°20.822'	0	-27.83	9.07
WP48-1B	Nejd - east	Hyrax midden	17°25.431'	54°29.385'	0	-28.12	7.98
ASO5	Nejd - east	Hyrax midden	17°23.123'N	54°29.767'E	110	-25.65	4.37
WP57-4	Nejd - east	Hyrax midden	17°23.210'	54°20.848'	130	-25.8	22.8
ASO1	Nejd - east	Hyrax midden	17°23.110'N	54°29.755'E	140	-25.96	6.99
WP45-2	Nejd - east	Hyrax midden	17°25.454'	54°29.296'	160	-27.37	4.69

Table 2-3: Fossil midden sampling locations, AMS radiocarbon dates, calibrated ages, and bulk stable isotope information.

Sample ID	Latitude	Longitude	UGAMS #	Material Dated	¹⁴ C Date (yr BP)	δ ¹³ C (‰)	δ ¹⁵ N (‰)	2σ range (yr BP)		Median Age (cal yr BP)
WP135-1	17°14.618'N	53°53.380'E	42490	fecal pellets	n/a	-27.53	5.79	n/a	n/a	n/a (modern)
WP135-2	17°14.618'N	53°53.380'E	42491	fecal pellets	n/a	-27.05	4	n/a	n/a	n/a (modern)
P135-3	17°14.618'N	53°53.380'E	42492	fecal pellets	n/a	-26.24	4.01	n/a	n/a	n/a (modern)
WP48-1B	17°25.431'N	54°29.385'E	32591	fecal pellets	modern	-28.12	7.98	n/a	n/a	0
WP144-4	17°24.000'N	54°30.580'E	44358	fecal pellets	130±20	-24.91	6.58	268	11	107
WP108-1B	17°23.123'N	54°29.767'E	37185	fecal pellets	110±20	-25.65	4.37	261	27	109
WP107-2B	17°23.110'N	54°29.755'E	37187	fecal pellets	140±20	-25.96	6.99	277	7	114
WP142-B	17°24.007'N	54°30.376'E	44357	fecal pellets	100±20	-26.03	8.01	257	32	115
WP45-2	17°25.454'N	54°29.296'E	32588	fecal pellets	160±25	-27.37	4.69	283	0	177
WP153-2	17°23.843'N	54°30.563'E	44360	fecal pellets	340±20	-26.98	7.51	472	315	384
WP155-2B	17°24.513'N	54°30.555'E	42501	fecal pellets	510±20	-26.3	7.45	545	511	529
WP38-3a	17°25.684'N	54°28.774'E	29897	fecal pellets	710±25	-21.9	15.4	682	570	665
WP146	17°23.523'N	54°31.010'E	42500	fecal pellets	800±20	-24.86	5.88	730	680	706
WP50-2	17°25.694'N	54°28.851'E	29898	hyraceum	970±25	-24	20.9	927	793	853
WP155-2C	17°24.513'N	54°30.555'E	44353	fecal pellets	1540±20	-25.49	8.36	1514	1356	1403
WP38-2	17°25.684'N	54°28.774'E	29900	fecal pellets	1570±25	-23.7	21.3	1521	1390	1461
WP147-1	17°23.331'N	54°30.724'E	44355	fecal pellets	1580±20	-26.32	7.41	1522	1404	1466
WP50-3a	17°25.694'N	54°28.851'E	29896	hyraceum	1640±25	-24.3	30	1585	1412	1522
WP138	17°23.150'N	54°29.825'E	42505	fecal pellets	1680±20	-26.24	10.33	1688	1532	1566
WP151	17°23.305'N	54°30.724'E	42507	fecal pellets	1690±20	-26.2	7.4	1689	1535	1574
WP145-4	17°23.733'N	54°30.996'E	42506	fecal pellets	1740±20	-25.69	6	1704	1549	1638
WP111-2E	17°23.142'N	54°29.869'E	44361	fecal pellets	1760±20	-26.94	9.65	1711	1590	1651
WP155-D	17°24.513'N	54°30.555'E	44359	fecal pellets	2820±20	-26.87	9.29	2994	2860	2920
WP103-2C	17°25.338'N	54°29.861'E	37186	fecal pellets	2940±20	-24.13	8.22	3167	3004	3103
WP149-2	17°23.298'N	54°30.711'E	42503	fecal pellets	3030±20	-25.82	9.68	3336	3167	3233
WP155-F	17°24.513'N	54°30.555'E	44362	fecal pellets	3690±20	-25.85	10.85	4140	3932	4038

Palynological analysis

This study involves a sampling protocol for thin (<5cm) middens. A minimum of 100 g of material, representing the entire vertical thickness of the midden, was disaggregated in 1 L of deionized water. This solution was sieved at 500 µm to remove fecal pellets and separate macrobotanicals. The <500 µm fraction was then used for pollen and microcharcoal analyses. A standard volume (45 mL) from each disaggregated sample was processed using the extraction

method of Faegri and Iversen (1989). Hydrochloric acid was used to remove carbonates and hydrofluoric acid to remove silicates. Acetolysis removed most organic material from the samples. The samples were sieved at 180 μm and 10 μm to remove large particulates and clays, respectively. *Lycopodium* spores were added to each sample to calculate pollen concentrations. The pollen residue was suspended in glycerin and mounted on glass slides for microscopy, and an average of 354 pollen grains (including fern spores) per sample were counted. For four samples, pollen counts fell below 300 but were still >250 grains. For the two samples, WP107-2B and WP149-2, 44 and 186 grains were counted, respectively, due to issues of preservation. Microcharcoal pieces that were >10 μm were also counted.

Pollen identifications were made using the African Pollen Database (Lézine et al., 2021), the pollen atlas of Bonnefille and Riollet (1980), as well as a collection of reference slides from the Penn State Paleocology Lab. Pollen taxa were categorized by plant habit, with the most predominant types being arboreal, herbs, and indeterminate, with indeterminate indicating there are multiple plant habits represented by that taxon. Taxonomic nomenclature and plant habit follow the African Pollen Database (APD; Vincens et al., 2007; Lézine et al., 2021). Pollen morphotypes for the genus *Senegalia* were differentiated based on their exine texture. Smooth exines were classified as *Senegalia* I, gemmate as *Senegalia* II, and reticulate as *Senegalia* III (Guinet and Vassal, 1978).

Certain groups of taxa were defined based on their affiliations to wetter or more dry areas in Dhofar, as well as whether they are considered grazing indicators. Grazing indicators in this setting are plant taxa that are avoided by domesticated animals, and therefore tend to be in higher abundances relative to other plants in highly grazed areas. Of these taxa, *Dodonaea viscosa*, *Cassia*-type, *Heliotropium*, and *Cornulaca/Aerva*-type are observed in the pollen record (Dereje and Udén, 2005; Brinkmann et al., 2009). Mesic affiliated taxa are arboreal pollen taxa which are generally found in moister areas of Dhofar, such as the escarpment and plateau; these are

identified as *T. dhofarica*, *Boscia/Cadaba*, *Maytenus*, *Ficus*, and *Boswellia sacra* (Miller and Morris, 1988; Patzelt, 2015). Nejd Associations are defined here as the most common pollen taxa found today in the dry Nejd: Amaranthaceae, *Senegalia* I, *Commiphora*, *Salvadora persica*, and *Senegalia* III (Miller and Morris, 1988; Patzelt, 2015).

Raw pollen counts were converted to relative abundances using a total of pollen grains and fern spores (APD). Concentrations were calculated by first determining the particles per milliliter of disaggregated sample, then using the sample mass that was rehydrated to calculate particles per gram of sample. A pollen diagram based on the relative abundances (%) was generated in Tilia (Grimm, 1987), and pollen zones were quantitatively determined using the CONISS program (Grimm, 1987). CONISS cluster analysis is stratigraphically constrained and uses the sum of squares (Grimm, 1987). Detrended Correspondence Analysis (DCA) was conducted using the ‘vegan’ package in R (Oksanen et al., 2019; RStudio Team, 2020). Taxa with maximum abundances less than 2% within a single sample and taxa with only one occurrence were excluded from the DCA and the CONISS. The relative abundances were Wisconsin-transformed and detrended using 26 segments. The axes were rescaled using four iterations. Sample and taxa scores were plotted on the first two axes, and the samples were assigned symbols according to their CONISS cluster membership.

Radiocarbon dating and stable isotopes

After the middens had been disaggregated, the sieved >500-micron fraction was separated and dried. This fraction included plant macrobotanicals and fecal pellets. 10 fecal pellets were randomly selected from the sieved material and homogenized, then sent to the University of Georgia Center for Applied Isotope Studies for Accelerator Mass Spectrometry (AMS) radiocarbon dating. Ten pellets were used to obtain an average age. There is the

possibility that these pellets were deposited and not cemented by hyraceum for a period of time, and thus have ages not directly representative of fossil pollen in the hyraceum fraction. However, given the nature of the middens as thin, dung-rich accumulations it is likely they formed within a relatively brief amount of time (10^1 - 10^2 years). Because of this, we interpret the data as averaged across this time frame (Scott and Woodborne 2007; Ivory et al. 2021). For two samples (WP38-3a 4-6 and WP50-2 0.5-2), radiocarbon dates were obtained on hyraceum drilled out of the solid sample prior to disaggregation. Calibrated ages were determined using Calib 8.20 (CALIB rev. 8) and the Intcal20 calibration curve (Reimer et al. 2020).

Bulk $\delta^{13}\text{C}$ and $\delta^{15}\text{N}$ were also measured on the same homogenized samples at the same laboratory using Gas Chromatography Isotope Ratio Mass Spectrometry (GC-IRMS) (Table 2-3). Bulk $\delta^{13}\text{C}$ values measured on fecal pellets should be largely reflective of the carbon isotopes of undigested plant material and can be used to infer changes in C3 and C4 vegetation (Ehleringer et al., 1997; Chase et al., 2012). Analyses of rock hyrax middens in southern Africa and Yemen have demonstrated a link between bulk $\delta^{15}\text{N}$ and relative moisture, wherein the nitrogen isotope composition in the feces reflects that of the consumed plant tissue, which is absorbed from the pool of nitrogen in the soil (Chase et al., 2012; Craine et al., 2015; Ivory et al., 2021). This relationship has also been observed feces from other herbivores (Díaz et al., 2016). Generally, $\delta^{15}\text{N}$ is negatively correlated with mean annual precipitation (MAP) on a global scale, and thus has an inverse relationship with soil moisture (Chase et al., 2012; Wang et al., 2014). However, nitrogen cycling in soils is a complicated process, which may be driven by other mechanisms in arid regions (Wang et al., 2014; Craine et al., 2015; Díaz et al., 2016).

To evaluate the relationship between $\delta^{15}\text{N}$ and moisture in the middens, we compared the bulk $\delta^{15}\text{N}$ with speleothem records of $\delta^{18}\text{O}$ from Qunf and Defore Caves (Fleitmann et al., 2004; Fleitmann et al., 2007). While these indicators reflect different aspects of hydroclimate, speleothem $\delta^{18}\text{O}$ can be used as a proxy for precipitation, specifically monsoon rainfall, which

represents most of the MAP in this region (Fleitmann et al., 2007). Values of $\delta^{15}\text{N}$ traditionally have an inverse relationship with MAP, but this correlation may change in very arid places (Wang et al., 2014; Chase et al., 2012; Díaz et al., 2016). The Qunf cave ($17^{\circ}10'\text{N}$, $54^{\circ}18'\text{E}$) $\delta^{18}\text{O}$ data was sourced from the National Oceanographic and Atmospheric Administration (NOAA) paleoclimatology database. To obtain sub-modern (~50- 200 BP) $\delta^{18}\text{O}$ values which are missing due to a hiatus at Qunf Cave, data were extracted from a speleothem from nearby Defore cave ($17^{\circ}07'\text{N}$, $54^{\circ}05'\text{E}$) which covers this interval (Fleitmann et al. 2004).

The temporal resolution of the Qunf cave speleothem record was much higher than the middens, which are temporally averaged (Fleitmann et al., 2004; Fleitmann et al., 2007; Ivory et al., 2021). To help account for this, the 1σ range (68.3% probability) of the calibrated ages for the midden samples was used determine an age range over which to average the $\delta^{18}\text{O}$ data from the speleothem record. A set of three samples (WP38-3a 4-6, 665 cal yr BP; WP50-2 0.5-2, 853 cal yr BP; WP38-2B, 1461 cal yr BP) with particularly high measured values of $\delta^{15}\text{N}$ (6.7-12.6‰ above the average of 9.5‰) were not included in this analysis. Two of these (WP38-3a 4-6 and WP50-2 0.5-2) were measured on hyraceum rather than fecal pellets. Rock hyraxes concentrate their urine to preserve water as an adaptation to their arid environment, which likely affects the $\delta^{15}\text{N}$ value (Rübsamen et al., 1982; Chase et al., 2012). The third sample (WP38-3a 4-6, 21.3 ‰) was removed as it fell far beyond the calculated standard deviation (7.90 ± 3.43 ‰). Modern samples and five samples with median ages 1566-1922 cal yr BP were also excluded due to a lack of coverage in the speleothem $\delta^{18}\text{O}$ data. The averaged speleothem $\delta^{18}\text{O}$ values were then plotted against the bulk $\delta^{15}\text{N}$ from each midden. For samples with overlapping 1σ ranges, each $\delta^{15}\text{N}$ value was plotted individually. Error bars representing the 95% confidence interval were added for the $\delta^{18}\text{O}$ averages, then a linear regression was conducted (Figure 2-7).

Results

Modern pollen

On the coastal plain near the base of the escarpment, the samples are dominated by *Dracaena* (31.0%), Poaceae (17.6%), and *Senegalia* III (6.8%). The pollen taxa in highest abundance from the camel dung collected in the escarpment mountains were Poaceae (67.6%), *T. dhofarica* (7.4%), and *Suaeda* (6.3%). In the distal plateau samples, the most abundant taxa are *Salvadora persica* (17.7%), Poaceae (9.2%), *Dodonaea viscosa* (8.3%), *Cocculus pendulus* (7.9%), and *Senegalia* III (7.3%). Here the abundance of *Boswellia sacra* is highest (6.5%). In the western Nejd, *Salvadora persica* (19.0%), *Ficus* (14.0%), Poaceae (10.3%), *Senegalia* III (9.5%), and *Ziziphus*-type (8.9%) are all relatively abundant. Cyperaceae pollen is also in a relatively higher proportion (7.8%). Modern East Nejd samples are characterized by *Polycarpon*-type (*Reseda*) (39.2%), *Kohautia* (12.9%), Poaceae (8.7%), and *Senegalia* III (7.2%). The submodern samples from East Nejd have a lower pollen abundance of *Polycarpon*-type (*Reseda*) (12.0%) and *Kohautia* (1.7%). *Senegalia* III (9.7%) is higher in abundance. The samples contain higher percentages of *Ficus* (8.2%) and Poaceae (15.2%) (Figure 2-3).

CONISS cluster analysis reveals two compositionally distinct groups of samples; those collected from the escarpment and coastal plain ecological zones cluster as one group and samples from the Nejd and distal plateau locations cluster as the other (Figure 2-3). In the DCA, Nejd samples cluster with common modern taxa observed within 100 m of the midden caves such as *Senegalia* (4.3%) and *Salvadora persica* (12.6%) (Figure 2-4). Two samples of fresh camel dung collected from the escarpment region have pollen representative of modern cloud forest taxa, notably *T. dhofarica* (7.4%). Grazing indicator pollen taxa are in highest abundance today in samples from the distal plateau (13.2%). Submodern (110-160 cal yr BP) samples in the East

Nejd reveal higher abundances (10.7%) of grazing indicators compared to modern abundances in this region (7.9%).

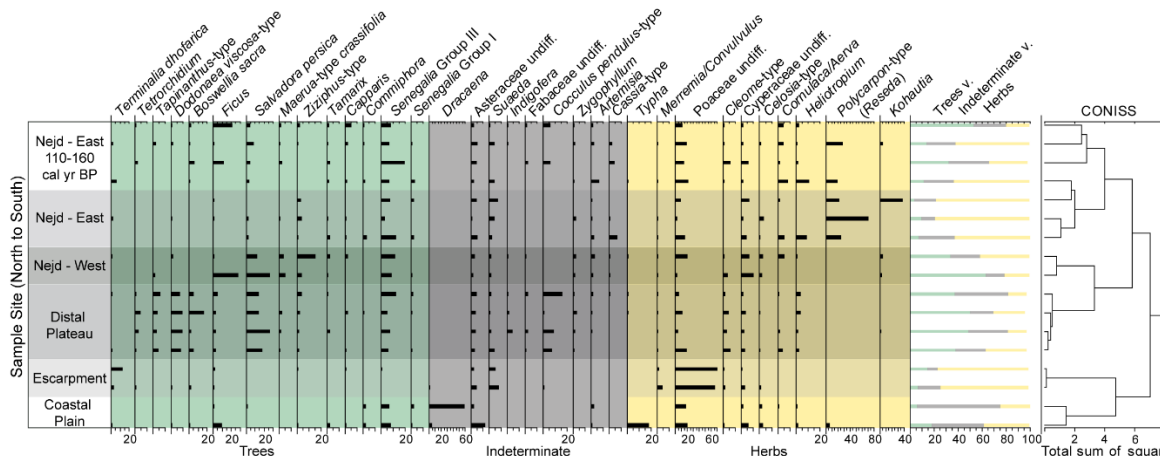


Figure 2-3: Pollen diagram of modern hyrax middens and two camel dung samples, in order from North to South. The middens are grouped by their ecological zone (East Nejd, West Nejd, Distal Plateau, Escarpment, Coastal plain). The two escarpment samples are camel dung specimens. Submodern hyrax middens are included with their median calibrated ages. Pollen abundances are on the x-axis. The green shade indicates tree pollen habits, grey indeterminate habits, and yellow are herbaceous pollen habits. The CONISS dendrogram is plotted on the right.

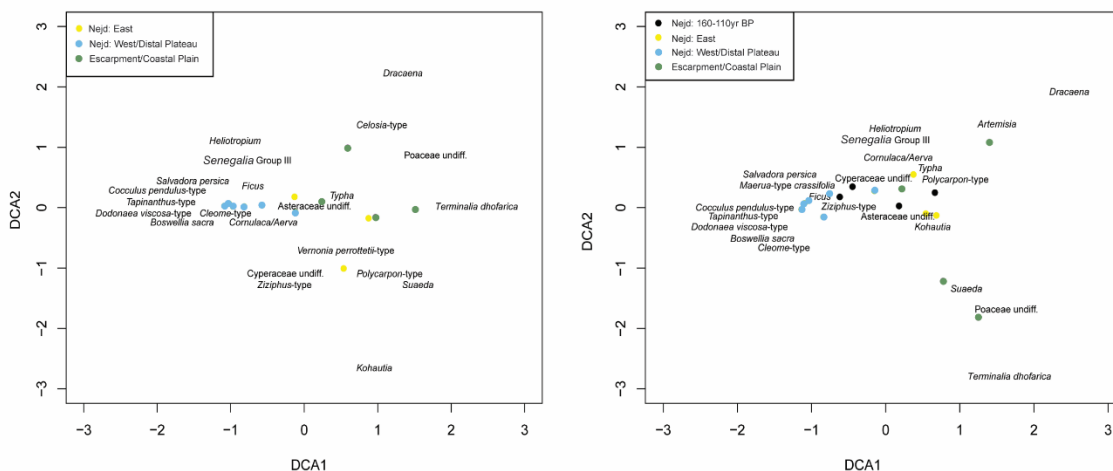


Figure 2-4: Detrended Correspondence Analysis (DCA) of all modern samples (right) and including submodern samples (left). Samples are color coded by their ecological zone.

Fossil pollen zones

Pollen analysis of the fossil middens revealed a diverse flora, with 134 total pollen taxa identified. Preservation was variable among the samples, with a range of percent broken grains of 0-11.9%. Most samples (23) had good preservation (broken grains <10%), while three had higher abundances of broken pollen grains (WP45-2, WP153-2, and WP38-3a 4-6). The average pollen concentration of the samples was 12825.13 (particles/g). Zonation of the pollen stratigraphy was determined using the CONISS dendrogram, which splits the assemblages into two distinct sets of samples, fossil samples and the modern. The fossil samples are then subdivided into groups A and B, then again into A1, A2, B1, and B2. These subzones were based on the two next highest branch heights in the dendrogram. The percentages given are zonal average abundances, except for those that refer to a single sample and are specified as such. Pollen taxa were grouped within the pollen diagram by plant habit (APD; Vincens et al. 2007; Lézine et al. 2021). The trends described in this section refer to the pollen diagram in Figure 2-5.

Zone A1 (4038-3233 cal yr BP): This pollen zone includes the two oldest samples. Herbaceous pollen comprised 4.0-17.0% of total pollen in each sample, while arboreal pollen was 27.0-57.0% of the total pollen. The most abundant herbaceous taxa were Poaceae (3.0%) and *Kohautia* (1.7%), but these were fairly low in abundance compared to the rest of the pollen record. *Boswellia sacra* (10.8%), *Ficus* (17.9%), and *Boscia/Cadaba* (5.2%) pollen were the most dominant tree taxa. The liana *Cocculus pendulus* was also a dominant pollen taxon (10.8%) in this zone.

Zone A2 (3103-1466 cal yr BP): There are eight samples within this zone, which bracket a 1100-year gap from 2920 cal yr BP to 1651 cal yr BP. The oldest sample (3103 cal yr BP) contained notably high abundances of Combretaceae pollen (31.2%), which mainly consisted of *T. dhofarica* (30.9%). The third sample occurred after the gap in the record, and at this time there

was a transition to increased abundances of herbaceous pollen taxa (21.2%) on average in the rest of the samples. There was a pronounced increase in *Kohautia* pollen (10.3%), as well as an increase in pollen from Poaceae (8.2%) in the younger six samples. Tree pollen (30.7%) decreased from the previous zone but remained abundant. *Ficus* (7.7%) decreased in this zone.

Zone B1 (1461-115 cal yr BP): This zone contains nine samples. Herbaceous pollen taxa (21.8%) remained similarly abundant from the prior zone, while tree pollen (18.7%) decreased further in abundance. The transition to this zone was dominated by pronounced increases in *Commiphora* (11.3%) and Cyperaceae (22.3%) pollen in the oldest sample. Pollen from the Amaranthaceae family (12.0%) also increased during this interval.

Zone B2 (114-107 cal yr BP): This pollen zone consists of 3 submodern samples. Herbaceous pollen taxa (22.9%) were still abundant, but there was also a significant increase in tree pollen (29.1%). *Ficus* (12.0%) pollen was the most abundant tree taxon. Poaceae pollen (10.6%) became more abundant than in previous intervals, while Amaranthaceae pollen (5.3%) decreased.

Modern: This zone consists of all the modern samples from both the East Nejd and the distal plateau. These samples were characterized by high abundances of tree pollen (37.9%). Herbaceous pollen (22.5%) remained at a consistent abundance with the previous zone. There was a marked increase in pollen from the trees such as *Salvadora persica* (15.1%) and *Dodonaea viscosa* (6.7%), as well as an increase in *Senegalia* III (4.4%). Poaceae pollen (12.2%) increased from the previous zone, while Cyperaceae pollen (2.9%) decreased.

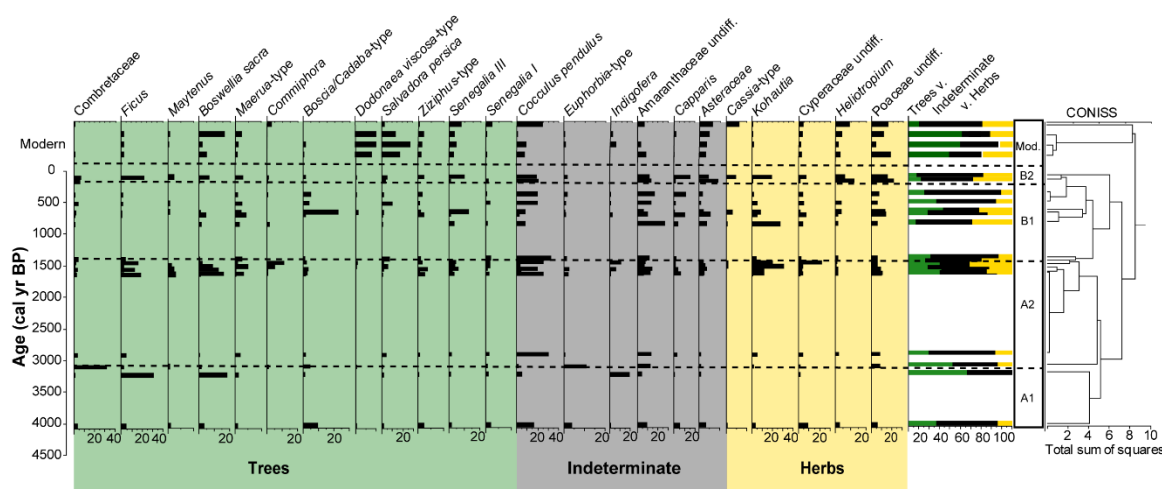


Figure 2-5: Pollen diagram of selected taxa from East Nejd fossil middens. Abundances are plotted on the x-axis and age in calibrated years BP on the y-axis. The four modern samples are plotted individually. The green shade indicates tree pollen habits, grey indeterminate habits, and yellow taxa with herbaceous pollen habits. Pollen zones determined via CONISS cluster analysis are represented by the column on the right.

Fossil midden detrended correspondence analysis (DCA)

The first two axes of the DCA performed on the fossil midden samples is shown in Figure 2-6. The first DCA axis had an eigenvalue of 0.3129, and a length of 2.3642 standard deviations. The second DCA axis had an eigenvalue of 0.2203, and the axis length was 2.5927 standard deviations. Modern samples and sub-modern samples (107-114 cal yr BP) from Zone B2 clustered together near positive values on DCA axis 1. The older samples (Zones A2, A1, and B1) clustered near negative values on DCA axis 1.

$\delta^{15}\text{N}$ (10.9‰). The linear regression explained 49.71% of the variance in the $\delta^{15}\text{N}$ data (Figure 2-7).

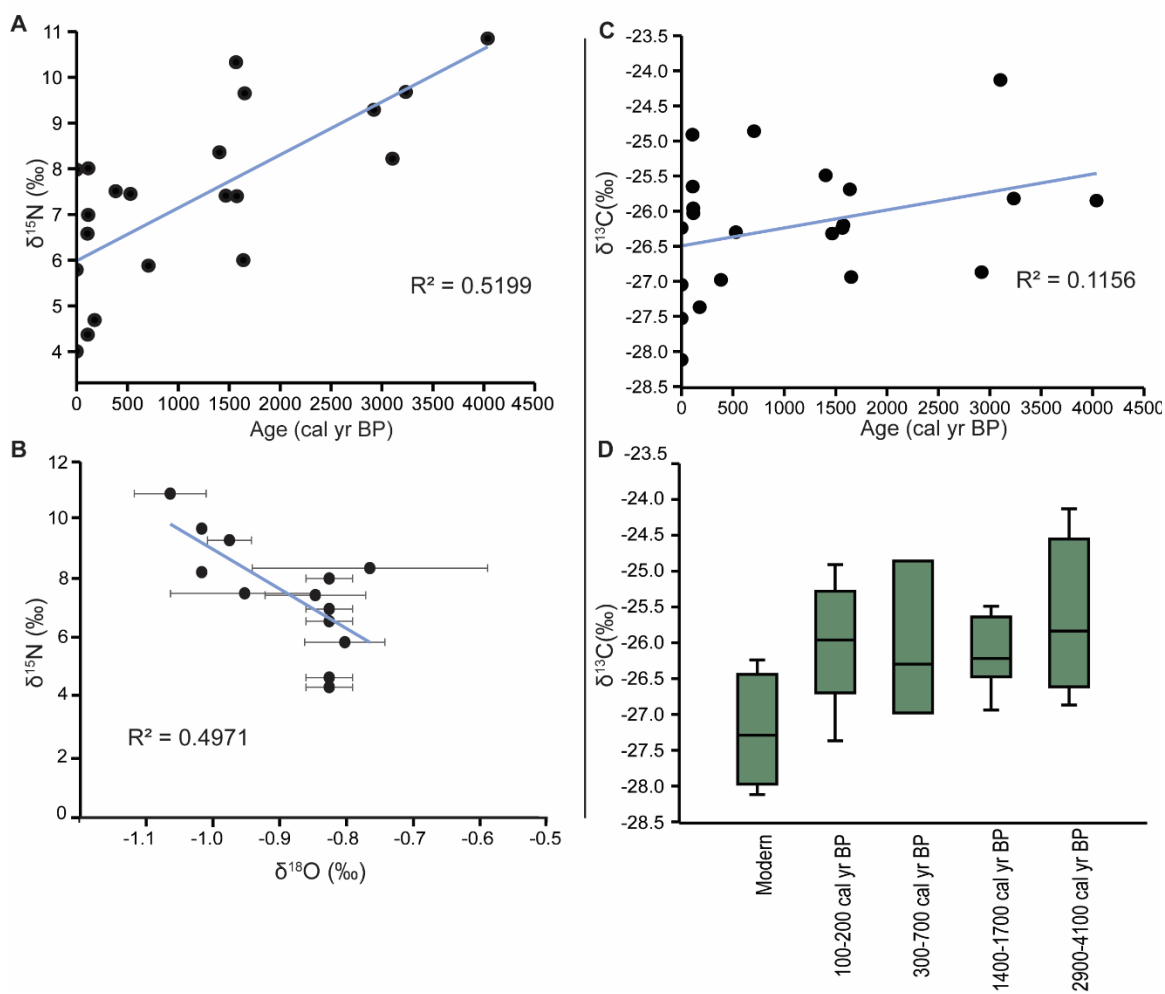


Figure 2-7: Panel A plots the $\delta^{15}\text{N}$ values of the middens by age in calibrated years BP. Panel B plots average speleothem $\delta^{18}\text{O}$ against midden N. Panel C is a plot of the bulk $\delta^{13}\text{C}$ values by midden age in calibrated years BP. Panel D shows a boxplot of midden $\delta^{13}\text{C}$ values by age bin.

Discussion

Hyrax midden pollen and modern vegetation

The pollen data from the modern hyrax middens were closely aligned with documented vegetation in each ecological zone, and thus captured a local signal of vegetation (Table 2-1). On the coastal plain, Poaceae (18.92%), *Draceana* (31.01%), and *Senegalia* III (6.81%) are most abundant. The vegetation in this region has been significantly reduced due to overgrazing by domesticated animals and other human activity, resulting in a desert grassland with sparse *Senegalia tortilis* trees (Miller and Morris, 1988). In the escarpment samples, Poaceae (67.6%) and *T. dhofarica* (7.4%) were found in high pollen abundance. *Suaeda* (6.3%) is common among coastal vegetation communities, and the escarpment samples come from the southernmost area nearest the coastal plain (Figure 2-1) (Miller and Morris, 1988; Patzelt, 2015). One of these samples contained 12.1% *T. dhofarica* pollen. These samples were camel dung and therefore indicate direct consumption, introducing a dietary bias which created larger pollen abundances than those that result from aeolian deposition (Scott and Cooremans, 1992). While there is likely dietary contribution of pollen into the hyrax middens, this camel dung was collected from an animal actively browsing on the escarpment and on *T. dhofarica* plants. The pollen abundances in these samples can be used as a tentative benchmark for what could be expected for high dietary input of *T. dhofarica* pollen in the hyrax middens (Scott and Cooremans, 1992; Gil-Romera et al., 2010; Chase et al., 2012). *Terminalia dhofarica* is limited to the escarpment woodlands today (Miller and Morris, 1988; Hildebrandt et al., 2007; Patzelt, 2015).

The distal plateau samples are dominated by the tree taxa *Salvadora persica* (17.7%) as well as Poaceae (9.2%) pollen. The plateau ecological zone is a grassland with sparse trees (Miller and Morris, 1988). *Salvadora persica* is found along wadi drainage systems, preferring

wetter soils (Miller and Morris, 1988). *Boswellia sacra* (Frankincense), is higher in abundance in the distal plateau samples (6.5%), which is this plant's preferred habitat (Miller and Morris, 1988; Patzelt, 2015). All the Nejd samples contain high abundances of *Senegalia* III (7.2-9.7%). *Senegalia* vegetation communities are prolific throughout the desert of Dhofar (Miller and Morris, 1988; Ghazanfar, 2004). Modern samples from East Nejd have a significant contribution from the pollen taxa *Polycarpon*-type (*Reseda*) (39.2%). A member of the genus *Reseda*, *R. sphenocleoides*, is common in the dry wadi drainage systems of the Nejd (Raffaelli et al., 2003). Cyperaceae pollen is found in a higher proportion in the West Nejd (7.8%). Generally, sedges found in the inland desert are members of the genus *Cyperus*, particularly *Cyperus conglomeratus*, which is found even among the sand dunes of the Rub al' Khali desert, or the Empty Quarter (Miller and Morris, 1988). Semi-aquatic varieties of Cyperaceae are found on the coast, typically near estuaries (Miller and Morris, 1988; Hoorn and Cremaschi, 2004).

The CONISS results for the samples presented distinguished all the modern Nejd samples, which cover a wide geographic area, from the submodern samples (110-160 cal yr BP). Additionally, the CONISS results distinguished all other samples by geographical location (and ecological zone). The DCA of the modern samples illustrates this ecological gradient, where samples cluster near taxa that today are abundant in their respective ecological zone. These statistical analyses suggest that middens preserve a pollen signal of the local vegetation within a reasonable degree of reliability (Figure 2-3 and Figure 2-4).

Fossil pollen interpretation

We interpret the dated middens as averaged time slices representing approximately decades to ~100 years of deposition. The fossil pollen record reveals variability between samples of similar ages. While the samples come from the same wadi drainage system, there is still some

geographic distance between sample sites (~0.25-4.4 km). Variability in their pollen compositions may reflect the vegetation in the immediate vicinity outside of the caves as well as dietary biases from hyrax foraging (Scott and Woodborne, 2007; Chase et al., 2012; Ivory et al., 2021). Having a higher sample density of middens with similar ages but from slightly disparate locations thus gives a broader picture of the vegetation in the East Nejd at a particular time. Moreover, it is important to note that despite the dissimilarities between samples of similar ages, the CONISS statistical analysis reveals that their overall compositions are most similar to one another in comparison to all other samples.

The fossil pollen record demonstrates a change in the vegetation communities such that arboreal taxa with mesic affiliations on the modern landscape (i.e., Combretaceae, *Maytenus*) were more prevalent ~3000-4000 cal yr BP. After 1500 cal yr BP more xeric taxa (i.e., *Senegalia*, *Kohautia*) became more abundant, and the density of vegetation was much sparser (Figure 2-5 and Figure 2-8). In the DCA, samples grouped near pollen taxa that characterized their composition, which captured this ecological gradient through time along the first axis (Figure 2-6) (McCune and Grace, 2002). Taxa associated with the Nejd today, such as *Senegalia* III, *Salvadora persica*, and Poaceae were on the positive side of DCA axis 1 near the modern and sub-modern samples (~100-120 cal yr BP). Emblematic taxa of the older groups were *Boscia/Cadaba* and the Combretaceae family (mainly *Terminalia*), neither of which exist in the Nejd today (Patzelt, 2015).

In the early part of the pollen record (4038-2920 cal yr BP), there was a higher proportion of tree pollen taxa (~20-57%) on the landscape relative to herbaceous taxa (0-16%). Trees such as *Boscia/Cadaba* and *Ficus* were more abundant on average until approximately 3000 cal yr BP. These trees are common on the landscape today but are typically found in moister places (Miller and Morris, 1988; Patzelt, 2015). There was also a high abundance of Combretaceae pollen in the sample dated to 3100 cal yr BP. Although multiple members of this family are found throughout

the Afrotropics, only *T. dhofarica* is native to Dhofar (Miller and Morris, 1988; Patzelt, 2015). This makes *T. dhofarica* the most likely candidate to have been present during this interval. *Terminalia dhofarica* is an insect-pollinated plant, which are often underrepresented in pollen spectra. Although no modern middens were found in *Terminalia* woodland to understand the representativity of its pollen in middens, abundances of *T. dhofarica* from within fresh camel dung collected during browsing on an individual tree resulted in values of 12.1%. To the extent that these samples can be used to benchmark the data from the hyrac middens, we tentatively interpret the even higher values in this fossil sample of >30% to indicate a local presence of this tree in the East Nejd ~3100 cal yr BP (Miller and Morris, 1988; Lippi et al., 2007; Oberpreiler et al., 2009; Chase et al., 2012).

The sample at 3100 cal yr BP also contained high abundances (39.9%) of other mesic tree taxa including *Boscia/Cadaba*-type. This supports the idea that during the period of deposition of this sample a major vegetation change took place where woodlands more like those currently growing in the modern escarpment were supported in the Nejd. Further, this sample had a high concentration of microcharcoal (36,605 particles/g) (Figure 2-8). Modern vegetation in the Nejd is severely fuel-limited due to the sparseness of the vegetation. The presence of increased charcoal during a time of denser vegetation suggests that vegetation during this interval was continuous enough to be more conducive to burning (Blackford, 2000, Chase et al., 2009, Genet et al., 2021).

Though paleoecological records in this region are fragmentary, several suggest wetter conditions in coastal southern Arabia and more pervasive woodlands in the desert of Yemen ~10-4 ka (Lézine et al., 2002; Parker et al., 2006; Fleitmann et al., 2007; Ivory et al., 2021). Speleothem $\delta^{18}\text{O}$ from Qunf cave indicates higher precipitation starting at ~10 ka, which then began to decrease around 7-8 ka until present (Fleitmann et al., 2007). Sedimentological and pollen evidence from the United Arab Emirates illustrates the presence of interdunal lakes during

a wetter early Holocene, which become dessicated by the late Holocene ~4000 cal yr BP and a C4 dominated plant community becomes established (Parker et al., 2006). Pollen records from coastal estuaries demonstrate changes mainly in wetland and mangrove taxa, however, they provide some evidence that communities further inland included tropical taxa from ~6000-4500 cal yr BP (Lézine et al., 2002). Pollen from hyrax middens in Yemen indicate a diverse, semi-arid woodland further inland in the modern-day desert at Wadi Sana during the mid-Holocene (6-4.7 ka), with high local abundances of *Terminalia* (Ivory et al., 2021). The pollen data presented here complements these records, suggesting a denser arboreal community was present in the Nejd in Dhofar from ~4000-3000 cal yr BP.

After the gap in the hyrax midden record (~1500 cal yr BP), the composition of the vegetation communities was much different. Between ~2900 and 1500 cal yr BP, there was a taxonomic turnover characterized by a pronounced increase in herbaceous pollen taxa (Amaranthaceae and Poaceae) and tree pollen taxa (*Senegalia* III and *Salvadora persica*) indicative of modern Nejd communities (Figure 2-8). Species of *Senegalia* are widespread in Dhofar but are most common in the Nejd and make up most of the trees in this zone (Miller and Morris, 1988). The herbaceous Amaranthaceae family is also dominant in this part of the record. Many of the species of Amaranthaceae in Dhofar are weeds in cultivated areas or grow on disturbed ground, as well as in xeric environments (Miller and Morris, 1988). Additionally, after 1500 cal yr BP, microcharcoal concentrations were much lower (94.9 p/g). This decrease in charcoal in combination with indications of xeric vegetation suggests a change in fire dynamics to a regime more like the modern day with less fuel for natural wildfires (Figure 2-8).

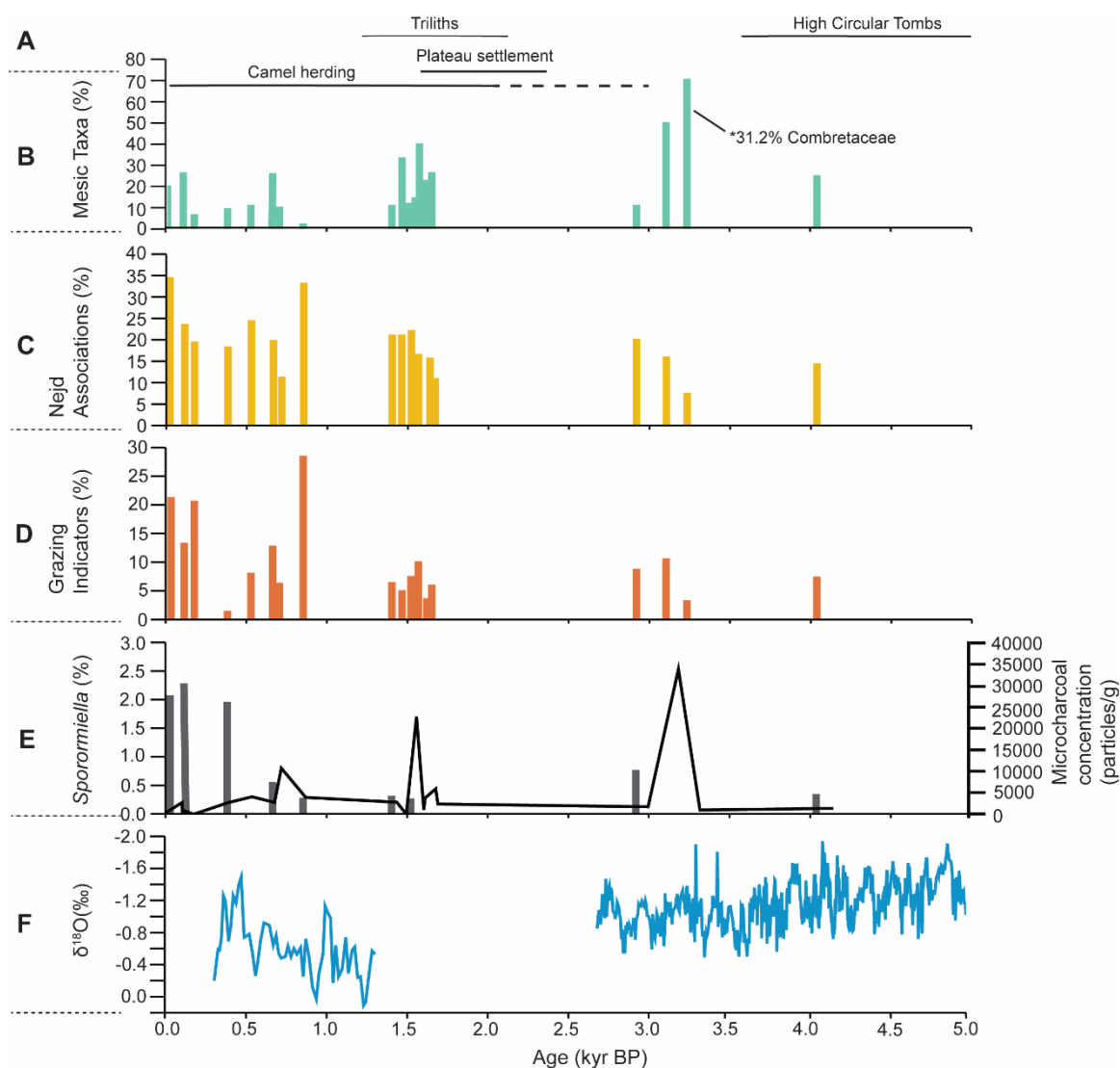


Figure 2-8: A. Archaeological periods of monument building and settlement, along with the earliest evidence for the introduction of domesticated camels in Dhofar (2000 yrs BP) and elsewhere in Arabia (3000 yrs BP). B. Mesic Taxa relative abundances (%): *Ficus*, *Boswellia sacra*, *Boscia/Cadaba*, *Maytenus*. C. Nejd Associations relative abundances (%): *Amaranthaceae*, *Salvadora persica*, *Senegalia I*, *Senegalia III*, *Commiphora*. D. Grazing Indicators relative abundances (%): *Dodonaea viscosa*-type, *Cornulaca/Aerva*, *Cassia*-type, *Heliotropium*. E. Gray bars showing *Sporormiella* relative abundance (%) and black line indicating microcharcoal concentrations (particles/g). F. Speleothem $\delta^{18}O$ from Fleitmann et al. 2007

Monsoon dynamics and aridity

Regional paleoclimate records suggest a gradual decrease in rainfall across the Holocene in southern Arabia. The mechanism behind this decline has traditionally been interpreted as the southward migration of the Intertropical Convergence Zone (ITCZ) following decreasing northern hemisphere summer insolation during the mid-Holocene (Fleitmann et al., 2007; Lézine et al., 2014; Nicholson, 2018). More recently, climatologists suggest that this latitudinal shift in the rain belt is driven by the development of the African Westerly Jet (AWJ) and subsequent movement of the African Easterly Jet (Nicholson, 2018). Moreover, the vertical rising of the ITCZ over the ocean amplifies this effect by widening the rain belt and increasing the duration of the rainy season (Nicholson, 2018). These two processes lead to the intensification of the summer monsoon over land. The speleothem $\delta^{18}\text{O}$ records from Dhofar suggest the variation in rainfall over this time are related to changes in Northern Hemisphere insolation (Fleitmann et al., 2007).

The presence of *T. dhofarica* in the Nejd at 3100 cal yr BP, and the high abundances of other relatively mesic taxa (ex. *Boscia/Cadaba*), suggests that the range of semi-arid woodlands was more expansive in the early part of the late Holocene (4000-3000 cal yr BP). These taxa were locally abundant in the Nejd at this time, at least 25-30 km further inland than their modern extent. A stronger monsoon during this interval would have brought increased precipitation and/or fog, and likely supported more arboreal vegetation further inland than today (Ivory et al., 2021). While fog is an important climatic factor for modern woodland vegetation in the region, speleothem oxygen isotopes provide a record of rainfall, they do not provide direct information about fog (Fleitmann et al., 2004; Fleitmann et al., 2007). Speleothem growth occurs when water seeps into the cave, and in Dhofar this is strongly tied to the summer monsoon which brings in both fog and rainfall (Fleitmann et al., 2007). Thus, speleothem $\delta^{18}\text{O}$ is an indicator of this

moisture source rather than rainfall or fog alone. Regardless, pollen evidence suggests more expansive semi-arid woodlands than seen today.

Additionally, although the hyrax midden record only provides snapshots of vegetation from collected intervals, there is evidence of some level of resilience of woodland taxa to increasing aridification during the late Holocene. For example, *T. dhofarica* was locally present in the desert at 3100 cal yr BP, ~3000-4000 years after the onset of decreasing precipitation regionally (Fleitmann et al., 2004; Lézine et al., 2007). Transient climate model simulations indicate that there were abrupt changes in rainfall as the ITCZ retreated southward and the monsoon weakened (Lézine et al., 2017). These model results, compared with mangrove pollen data from the coast, suggest an abrupt decrease in rainfall at 4000 cal yr BP (Lézine et al., 2002; Lézine et al., 2017). In the early part of the record, the mangroves contained pollen of *Rhizophora*, a coastal, brackish taxon that requires some freshwater input (Lézine et al., 2017), which became extremely rare after ~4000 cal yr BP and was replaced by more saline and drought-tolerant species (Lézine et al., 2002). This suggests a transition to more arid conditions in Oman (Lézine et al., 2017). However, the arboreal community further north in the East Nejd persisted for another ~1000 years after this transition, suggesting a resilience to increasing aridity in the late Holocene.

The gap in the hyrax midden record from 2920 cal yr BP to 1651 cal yr BP is coeval with a hiatus in the Qunf cave speleothem record (Fleitmann et al., 2004). Regional paleoclimate records from Arabia, Africa and western Asia indicate this was an especially dry period, and it may be that the interior Nejd did not have enough food and water resources to sustain a hyrax population during this period (Gasse and van Campo, 1994; Fleitmann et al., 2004; Ivory and Lézine, 2009; Gil-Romera et al., 2010). Hyraxes obtain most of their water from foraged vegetation, especially in arid regions (Sale, 1965; Chase et al., 2012; Mohamed, 2019). When drought conditions occur and herbaceous plants do not grow or desiccate on the landscape, the

trees become a critical source of both food and water (Sale, 1965). Hyraxes have even been observed stripping bark from trees such as *Senegalia* in southern Africa when under severe drought stress (Sale, 1965). The reduction of the trees during this interval, as seen in the shift in vegetation once middens are again deposited, suggests that hyraxes may have lacked these necessary resources during this arid interval. The alternative hypothesis would be that this gap is simply the result of insufficient sampling. While this is certainly possible, there are many independent lines of evidence indicating that it may have been too dry and resource depleted in the Nejd during this interval. Additionally, the middens that are dated to ~1500 cal yr BP after this hiatus co-occur with the redeposition of speleothems at Qunf cave as well as an observed wet phase in the coastal estuaries (Hoorn and Cremaschi, 2004; Flietmann et al., 2007).

Bulk $\delta^{15}\text{N}$ data from hyrax middens has previously been interpreted to indicate local changes in moisture availability. Soil and plant foliar $\delta^{15}\text{N}$ have an established inverse relationship with water availability that has also been demonstrated in herbivore feces (Chase et al., 2012; Wang et al., 2014; Carr et al., 2016; Díaz et al., 2016). $\delta^{15}\text{N}$ is also negatively correlated with MAP globally (Wang et al., 2014). In our record, $\delta^{15}\text{N}$ became more depleted over time, which would counterintuitively suggest increasing water availability over this study interval. In contrast, all other evidence, from regional precipitation records to the change in vegetation in this area, strongly indicate drying (deMenocal et al., 2000; Flietmann et al., 2007; Lézine et al., 2017; Ivory et al., 2021). However, the inverse relationship between water availability and $\delta^{15}\text{N}$ observed in previous studies may not apply in hyperarid regions.

A study by Díaz et al. (2016) looked at plant and herbivore feces $\delta^{15}\text{N}$ across an aridity gradient in the Atacama Desert. They observed a unimodal relationship between herbivore fecal $\delta^{15}\text{N}$ and moisture availability. Wang et al. (2014) observed this same curve across an aridity gradient in savannah grassland in both soil $\delta^{15}\text{N}$ and plant foliar $\delta^{15}\text{N}$. Likewise, this study demonstrated a positive correlation between soil and plant $\delta^{15}\text{N}$ and MAP at an arid location. This

suggests that after a certain threshold, different controls on the nitrogen cycle become more dominant, such as loss of gaseous nitrogen or nitrogen fixation by bacteria (Wang et al., 2014). The relationship between hyrax midden bulk $\delta^{15}\text{N}$ and speleothem $\delta^{18}\text{O}$ from this study provides further evidence of an inverse relationship between fecal pellet bulk $\delta^{15}\text{N}$ and speleothem $\delta^{18}\text{O}$. This implies a positive correlation between bulk $\delta^{15}\text{N}$ and MAP in Dhofar and thus continued aridification, over the last 4000 years (Figure 2-7).

Human-environment interactions

Archaeological evidence attests to the movement of ancient pastoralists across the Dhofar region (Harrower et al., 2014; McCorrison et al., 2014; McCorrison et al., 2018; McCorrison et al., 2020). Generally, there is sparse evidence for prolonged habitation in any one spot, suggesting pastoralists were highly mobile (McCorrison et al., 2018). Small monuments were constructed across Dhofar over the last 7000 years (McCorrison et al., 2014; McCorrison et al., 2018). This was punctuated by one period of visible settlement by cattle herders on the plateau at ~2 ka, where there are permanent structures documenting ~200 years of abandonment and re-occupation (McCorrison et al., 2018; McCorrison et al., 2020). These sites were near more stable water sources, but there is no evidence for the development of settled agriculture (McCorrison et al., 2020).

Historically, there has been a lack of understanding regarding how pastoralist practices impact vegetation, and past theoretical frameworks often focused on exploitation and depletion of habitat resources (i.e., the “tragedy of the commons”) (Hardin, 1968; Warren, 1995). However, recent studies have demonstrated the sustainability of pastoralism even under increasing aridity (Brierley et al., 2018). Linking paleoecological records with archaeological data allows for an increased understanding of long-term human-environment interactions in pastoralist systems. In

the early part of the hyrax midden pollen record, there is evidence for more continuous arboreal vegetation cover, and archaeological evidence suggests mobility of pastoralist groups until ~2350 cal yr BP (Harrower et al., 2014; McCorrison et al., 2018). Mesic trees were present further inland in the Nejd even after 3000-4000 cal yr BP of drying and 4000 years of a mobile herding practice in Dhofar. This suggests that pastoralists did not degrade woodland vegetation at this time.

Beginning around 1000 cal yr BP, there was a pronounced increase in grazing indicator pollen taxa (12.5%). Likewise, at approximately 500 cal yr BP, there was an increase in the abundance of *Sporormiella* (1.9-2.3%), a fungus found in the dung of large herbivores which in Dhofar is found abundantly in camel dung (Ivory et al., 2021). The observation of *Sporormiella* in the middens likely occurs through hyraxes walking across soil where camels are present, as the fungus would be trapped in the dung that is on the ground, as well as aeolian transport. The increase in grazing indicator taxa and *Sporormiella* may indicate an intensification of land use in the inland desert, particularly camel herding, beginning 1000-500 cal yr BP. While the distribution of grazing indicator taxa would have also been influenced independently by other ecological or climatic controls, the combination of the higher abundances of these particular pollen taxa and *Sporormiella* point to an increase in domesticate herbivores on the landscape. These pollen taxa are low in abundance in the earlier part of the record (6.6%), suggesting that animal grazing on the vegetation would have been relatively low until ~1000 cal yr BP.

In the modern cloud forests on the escarpment, higher stocking rates of camels increase the abundance of unpalatable plant species, or grazing indicators, and decrease plant diversity (Ball and Tzanopoulos, 2020). Preferential grazing of the softer shoots and saplings of *T. dhofarica* by camels is already being shown to affect the regeneration of these key trees (Ball and Tzanopoulos, 2020). Maintaining these high browsing pressures under anthropogenic climate change may ultimately lead to the degradation of the cloud forest (El-Sheikh, 2013; Ball and

Tzanopoulos, 2020). However, it is important to note the long-term sustainability of pastoralism under lower stocking rates as shown through the archaeological record and the paleoecological evidence presented here. The earliest evidence for domesticated camel herding in Dhofar is from 2 ka, but there is no observable increase in grazing indicators or *Sporormiella* for another 1000 to 500 years in the collection region of our samples (McCorrison et al., 2018).

Conclusion

The pollen data from the rock hyrax midden record demonstrates a turnover from a more mesic, arboreal vegetation community to the more xeric community that characterizes the Nejd today. While the nature of the termination of the Holocene Humid Period is debated, an arboreal community persisted in the Nejd for approximately 3000-4000 cal yr BP after the onset of decreasing rainfall (Fleitmann et al., 2007). Bulk stable isotope data from the middens indicates a transition to hyperaridity over this time frame. This combined data suggests some resilience of this biodiverse dryland community under increasing aridity conditions. The end of the hiatus in the midden record and its co-occurrence with the renewal of speleothem growth and increased runoff at the coast suggest this overall trend was perhaps punctuated by a wetter phase beginning ~1500 cal yr BP (Hoorn and Cremaschi, 2004; Fleitmann et al., 2007).

Modern human land use enhances the risk of vegetation degradation, and anthropogenic climate change is likely to push this region into novel climate spaces (Dahinden et al., 2017; Ball and Tzanopoulos, 2020). There is an outstanding need to mitigate the effects of global climate change and reduce degradational impacts from human land use to help maintain this biodiverse and vulnerable vegetation community. Evidence for the practice of nomadic pastoralism in southern Arabia dates to at least 7000 cal yr BP (Martin, 2020). Indicators of more intense human landscape use do not appear in the paleoecological record generated from the middens until 1000-

500 yr BP. The lack of evidence for human impacts on vegetation for the bulk of the record highlights continued sustainability of pastoralism in this region under changing climate conditions. In terms of vegetation composition, the modern samples were considerably different compared to the fossil samples, indicating the recent economic growth and substantially higher stocking rates are an unprecedented driver of vegetation change in Dhofar. It is important to consider the context provided by these long-term records when discussing human activity and impacts to the landscape: though animal grazing may be degradational to the modern vegetation, it has not always been in the past, and there may be conservation options that preserve the practice of nomadic pastoralism in Dhofar and other drylands.

Chapter 3

The only thing certain in grad school is death and (leaf) waxes: Late Holocene hydrologic variability and ecosystem structure

Over 1/3 of the Earth's population relies on dryland ecosystems for food and water resources, however, these ecosystems are especially sensitive to changes in climate. Recent observational data are insufficiently brief to constrain how changes in hydrology influence plant communities in these regions. In southern Arabia, paleoecological data show woodland communities transitioned to more dry, herbaceous plants, presumably as rainfall decreased across the Holocene. However, there are currently no reconstructions of rainfall to assess the relationship between hydrology and ecology. Here, we employ leaf wax *n*-alkane distributions, $\delta^{13}\text{C}_{\text{wax}}$, and $\delta\text{D}_{\text{wax}}$ analysis to reconstruct changes in C3/C4 vegetation and local changes in moisture availability from rock hyrax (*Procapra capensis*) middens in Dhofar, Oman. These complementary signals, in tandem with a previously published pollen record, can be used to develop a more complete picture of hydrologic change and vegetation response. To constrain interpretations of this signal in fossil middens, *n*-alkane analyses were conducted on modern herbarium specimens of plants collected in Dhofar. *N*-alkane distributions from these specimens reveal leaf wax homologues in xeric plants are longer than in mesic plants. Across the fossil middens (4038-109 cal yrs BP), the proportions of these homologues do not show major changes in xeric versus mesic plants. Further, $\delta^{13}\text{C}_{\text{wax}}$ values suggest there was no change in the overall distributions of C3 and C4 vegetation. Limited $\delta\text{D}_{\text{wax}}$ from the middens confirms an overall drying trend in the late Holocene that was punctuated by a wetter pulse at ~1.6 ka. These results indicate that despite changes in moisture availability across the late Holocene, the structural composition of the plant communities and C3/C4 vegetation remained stable. Thus, we infer that

vegetation change associated with late Holocene drying involved reshuffling of community composition rather than major changes to vegetation structure.

Introduction

Drylands support over 40% of the Earth's population, therefore understanding the ways in which changes in water availability will affect these ecosystems is critical. Decreases in rainfall can have a significant impact on vegetation density in arid places (Maestre et al., 2016). Global climate models predict an overall increase in aridity globally due to changes in rainfall as well as increased evapotranspiration from higher temperatures (Asner et al., 2004; Maestre et al., 2016; Dahinden et al., 2017; IPCC, 2022). Predicted higher variability in rainfall as well as an increase in extreme events such as droughts are expected to also stress dryland ecosystems (Asner et al., 2004; Maestre et al., 2016; IPCC, 2022). Prior studies have suggested that 10-20% of drylands are already severely degraded, and this is likely to increase with climate change, resulting in altered species composition and reduction of vegetation cover which provide food, fodder, lumber to hundreds of millions of people (Asner et al., 2004; Maestre et al., 2016; Ball and Tzanopoulos, 2020).

The Dhofar region of Oman is a biodiverse dryland that is home to cloud forest woodlands, which rely on moisture from dense fog brought in seasonally by the Indian Monsoon (Fleitmann et al., 2007; Hildebrandt et al., 2007; Friesen et al., 2018). These woodlands are both ecologically and economically important; they serve as a critical resource for both people and animals (El-Mahi, 2011; Hildebrandt et al., 2007; Ball and Tzanopoulos, 2020). More broadly, vegetation across Dhofar provides grazing resources for domesticated animals, particularly camels (McCorrison et al., 2020). This region is expected to enter novel climate space by the end of this

century (Dahinden et al., 2017), and large-scale changes in vegetation have already occurred in this region over the last few decades. For example, cloud forest woodlands have contracted in space and have been degraded over the last few decades due to increased human land use (El-Mahi, 2011; Ball and Tzanopoulos, 2020; McCorriston et al., 2020).

Modern observational data is too brief to assess long-term trends in climate change and vegetation response. While modern data can assess the impacts of extreme events on vegetation, which generally occurs in a timeframe of months to a few years, anthropogenic climate change will occur over decades to centuries, and thus more data is needed to capture these long-term dynamics (Dietl et al., 2014; Afuye et al., 2021). Paleoenvironmental records can be used to understand these relationships over long periods of time. Regional paleoclimate studies generally agree that rainfall decreased across the Holocene in northern Africa and southern Arabia as the Indian Monsoon system weakened (Morrill et al., 2003; Renssen et al., 2003; Fleitmann et al., 2007; Lézine et al., 2014; Nicholson, 2018). However, there are currently very few paleoecological records investigating climate-vegetation dynamics in southern Arabia (Lézine et al., 2002; Lézine et al., 2017; Ivory et al., 2021; Hoorn and Cremaschi, 2004).

In southern Arabia from the mid to late Holocene, vegetation responses to increased aridity are described by pollen records that are patchy in both space and time. Pollen studies from paleolakes and hyrax middens from nearby Yemen suggest a contraction of semi-arid woodlands inland across the Holocene (Lézine et al. 2017; Ivory et al. 2021). Most paleoenvironmental data from Oman comes from speleothem records or sediment core records from the coast (Hoorn and Cremaschi, 2004; Fleitmann et al., 2007; Lippi et al., 2007; Bellini et al., 2020; Horisk et al., 2023). Omani mangrove records demonstrate an increase in xeric, saline-tolerant taxa on the coast over this time frame (Lézine et al. 2002). Oxygen isotopes from the speleothems indicate an overall trend of decreasing rainfall across the Holocene, while sedimentological information from the estuarine records highlights wetter pulses that punctuate this long-term trend (Hoorn and

Cremaschi, 2004; Fleitmann et al., 2007; Lippi et al., 2007; Bellini et al., 2020). Given the sparse data, the impact of long-term changes in precipitation on vegetation further inland in this region is not well-understood.

Rock hyrax middens serve as a powerful paleoecological archive in arid regions which lack more traditional archives such as lakes or bogs. Pollen studies from hyrax middens in both Africa and Arabia have successfully reconstructed ancient vegetation change across the Holocene and late Pleistocene (Scott and Cooremans, 1992; Chase et al., 2012; Ivory et al., 2021; Horisk et al., 2023). A pollen record from rock hyrax middens in Dhofar demonstrated changes in vegetation in the inland desert (Nejd) across the late Holocene (Horisk et al., 2023), indicating an overall shift to more xeric, herbaceous taxa at ~1.6 ka. More recent explorations of geochemical tools within the middens have demonstrated the efficacy of bulk stable isotopes in assessing past changes in vegetation and moisture as well as leaf wax biomarkers (Carr et al., 2010; Chase et al., 2012; Carr et al., 2016). Herein lies an opportunity to develop a long-term paleoecological record to disentangle climatic drivers of vegetation change in an inland, biodiverse dryland community.

Background

Modern environment

The Dhofar region is semiarid on the coast (~120-150mm/yr) to hyperarid further inland in the desert (~30mm/yr). The vegetation is highly biodiverse: at least 817 species have been documented in Dhofar alone, many of which are endemic, and this represents over half of the total flora in the county (Patzelt, 2014). Moreover, it is estimated that nearly 14% of the total vegetation in Oman is range-restricted, and thus at increased risk under changing climate conditions (Patzelt, 2014). The vegetation is highly dependent on the annual precipitation, which

comes mainly from the Indian Monsoon system (Miller and Morris, 1988; Fleitmann et al., 2007; Hildebrandt et al., 2007; Ball and Tzanopoulos, 2020).

The vegetation in the Dhofar region is composed of four ecological zones from the Arabian Sea inland: the coastal plain, the escarpment, the plateau, and the Nejd (Figure 3-1; Miller and Morris, 1988). The coastal plain today is sparsely vegetated due to grazing of domesticated animals and other human land use such as urbanization and infrastructure (Miller and Morris, 1988; El-Mahi, 2011). Near estuaries, vegetation is dominated by grasses (Poaceae), some sedges (Cyperaceae), *Salvadora persica* trees, and semi-aquatic plants such as *Typha* (Ghazanfar, 1999; Buffington and McCorrison, 2018). The escarpment sharply increases in elevation and is home to a semiarid cloud forest (Miller and Morris, 1988; Patzelt, 2015; Ball and Tzanopoulos, 2020). This unique woodland can intercept fog brought in by the Indian Monsoon and flourishes seasonally (Hildebrandt et al., 2007; Friesen et al., 2018). This community consists of trees that require seasonal moisture such as *Terminalia dhofarica*, *Maytenus dhofarensis*, *Boscia arabica*, and *Ziziphus spina-christii* (Miller and Morris, 1988; Patzelt, 2015; Buffington and McCorrison, 2018). Taxa affiliated with this zone are considered more mesic for this region, as they have access to more rainfall annually and are nearer to permanent freshwater sources.

The plateau is a flat, high-elevation band that is mainly grassland (Poaceae) with isolated tree taxa such as *Senegalia* and shrubs (eg. *Euphorbia* spp.; Miller and Morris, 1988; McCorrison et al., 2020). The Nejd lies furthest inland and is mainly desert, with isolated trees and shrubs that dot the cliff sides and dry wadi riverbeds. Notable taxa in this zone are frankincense trees (*Boswellia sacra*) and *Senegalia*, as well as herbs like *Cleome* and *Heliotropium* (Miller and Morris, 1988). *Cadaba heterotricha* is a shrub which is rare in this region today, but typically found in drier wadi beds in the Nejd (Miller and Morris, 1988; Buffington and McCorrison, 2018). Most taxa in the Nejd, with the exception of those that grow

surrounding freshwater springs in oases are considered xeric and exist in hyperarid conditions beyond the reach of the monsoon.



Figure 3-1: Map of the Dhofar region indicating the four ecological zones. Black squares are modern samples, white circles represent fossil samples. The stars denote the weather stations in Salalah and Thumrait.

Leaf wax *n*-alkanes

N-alkanes are long-chain hydrocarbons that are a component of plant leaf waxes (Killops and Killops, 2013). Those sourced from higher terrestrial plants show a strong odd over even preference for number of carbon atoms and tend to form longer chains (C₂₅-C₃₅) (Killops and

Killops, 2013; Bush and McInerney, 2013). These biomarkers are insoluble in water and preserve well over long periods of time, and the isotopes of both carbon and hydrogen within these compounds record past changes in vegetation and rainfall, respectively (Killops and Killops, 2013; Sachse et al., 2012; Bush and McInerney, 2015). This makes *n*-alkanes a useful biomarker that can be extracted from geological materials for paleoecological analyses (Bush and McInerney, 2015; Eglinton and Eglinton, 2008).

Compound-specific $\delta^{13}\text{C}_{\text{wax}}$ is sensitive to atmospheric CO_2 , the photosynthetic pathway of the plant (C3, C4, or CAM), as well as aridity (Sage, 2004; Eglinton and Eglinton, 2008). In C3 plants, more negative $\delta^{13}\text{C}_{\text{wax}}$ values occur under higher humidity (Rao 2017). The C4 photosynthetic pathway is mostly found in grasses and sedges and evolved to limit water loss via transpiration, thus, these plants are better adapted to warmer and more arid climates (Keeley and Rundel, 2003; Sage, 2004; Feakins et al., 2020). Crassulacean acid metabolism (CAM) is used in plants that conduct CO_2 fixation at night and is most predominant in succulents (Keeley and Rundel, 2003).

More negative $\delta^{13}\text{C}_{\text{wax}}$ values (avg. -36‰) are associated with C3 vegetation, while less negative values (avg. -21.5‰) are associated with C4 plants (Castañeda et al., 2009; Rao et al., 2017). Fractionation of carbon isotopes occur during plant uptake and fixation of atmospheric carbon (Diefendorf et al. 2010). The degree of fractionation can vary based on precipitation and other environmental conditions, as well as plant functional type (Diefendorf et al. 2010). Overall, however, $\delta^{13}\text{C}_{\text{wax}}$ reflects the relative proportions of C3/C4 vegetation (Chikaraishi and Naraoka, 2007; Rao, 2017; Liu and An, 2020).

The hydrogen in *n*-alkanes is ultimately sourced from meteoric water, thus the isotopic composition is generally controlled by environmental factors such as latitude, humidity, and temperature (Dansgaard, 1964; Liu and Yang, 2008; Feakins and Sessions, 2009; Polissar and Freeman, 2010). The amount effect summarizes the change in δD of precipitation: as the amount

of rainfall increases, the δD of precipitation decreases (Dansgaard, 1964). δD_p also decreases as an air mass moves inland or higher up in altitude, preferentially raining out isotopically heavy water and leaving behind isotopically light vapor (Dansgaard, 1964; Herrmann et al., 2017). Meteoric waters enter soils, where evaporation can impact the isotopic composition of this new isotopic pool, especially in arid ecosystems (Feakins and Sessions, 2010).

Plants take up water from the soil, which does not cause any fractionation, and use it to synthesize leaf wax *n*-alkanes. The biosynthesis of these compounds causes significant fractionation to the hydrogen isotopes, which varies between C3/C4/CAM plants as well as between plant habits (Sachse et al., 2012). Because of this, δD_{wax} values are often corrected using mixing-models which consider photosynthetic pathways and plant groups such as trees and herbs (Feakins et al., 2013). Transpiration of leaf waters can also impact resultant δD_{wax} values, such that the *n*-alkanes will record an enrichment in deuterium relative to meteoric waters (Feakins and Sessions, 2010). Additionally, biosynthesis of these lipid molecules causes significant isotopic fractionation, which varies taxonomically (Sachse et al., 2012; Feakins, 2013). Overall, less negative values of δD_{wax} indicate more arid conditions, making the δD_{wax} and $\delta^{13}C_{wax}$ records from *n*-alkanes complementary paleoenvironmental signals (Sachse et al., 2012; Rao et al., 2017). These compounds have been shown to preserve in rock hyrax middens over geologic timescales in South Africa and can be used to strengthen paleoecological studies in southern Arabia (Carr et al., 2010; Chase et al., 2012; Carr et al., 2016).

Methods

Rock hyrax middens

Approximately 100g of material from 14 hyrax middens were disaggregated in 1L of deionized water for pollen analysis as presented in Horisk et al. (2023). The rehydrated urine was sieved at 500 μm to remove fecal pellets and other macrobotanicals, and 10 fecal pellets from each sample were homogenized and radiocarbon dated at the University of Georgia Center for Applied Isotope Studies via Accelerated Mass Spectrometry (AMS) radiocarbon dating. A standard 40 mL of the liquid <500 μm fraction was then used to obtain pollen data. The archived portion of this rehydrated hyraceum was employed to extract leaf wax *n*-alkanes as well as to conduct $\delta\text{D}_{\text{wax}}$ and $\delta^{13}\text{C}_{\text{wax}}$ analyses. The use of the liquid fraction ensures the two datasets are directly comparable.

To obtain the Total Lipid Extract (TLE), 50 mL of the liquid fraction was frozen and then freeze-dried in ashed 500 mL beakers. Approximately 20 mL of a 2:1 azeotrope of Dichloromethane (DCM) to Methanol (MeOH) was added to the beaker and sonicated for 30 minutes, and the extracted TLE was pipetted into 50 mL vials. This process was repeated three times. A portion of the TLE (~8 mL) was archived before conducting further analysis. The TLE was separated into an acid and neutral fraction by adding water and salt through Bligh-Dyer separation, using the Wakeham and Pease (2004) protocol. Approximately 60 mL of TLE was added to a separatory funnel along with ~20 mL of 5% NaCl solution. The separatory funnel was inverted and degassed 5-7 times, and the bottom fraction was collected into an ashed flask. This process was repeated an additional two times to obtain the neutral fraction. To collect the acid fraction, the remaining 5% NaCl solution was acidified using HCl to reach a pH of ~2, then extracted three times using DCM.

The neutral fraction was separated into compound fractions via silica gel column chromatography. The column was constructed using a glass pipette and ashed silica gel and an ashed glass wool plug. The first fraction was eluted using hexane, and a second fraction was extracted using 2:1 DCM to MeOH. The hexane fraction (F1) was dried gently with N₂ in a FlexiVap, then 200 µL of hexane were quantitatively added to the vial prior to Gas Chromatography-Flame Ionization Detector (GC-FID) analysis. *n*-alkane peaks were identified and quantified on the GC-FID using a 2 µL injection volume and a calibration curve with 5, 10, 25, and 50, and 100 ng/µL standards, and the response curve was generated after each batch of samples. The standard deviation of the peak areas for the standards ranged from 0.15 to 1.3 pA*min, which is an error of approximately 7%.

The concentrations reported here are volumetric, since a liquid sample was used. However, we normalized abundance to a mass of organic material extracted, weighed some of the freeze-dried samples and conducted a unit conversion. These ranged from 0.20 to 1.8 µg/g of *n*-alkanes in relation to the mass of dried organic material. The middens analyzed by Carr et al. (2010) had average *n*-alkane concentrations of 0.005 to 0.157 µg/g. One explanation for this discrepancy would be higher fecal pellet concentration in the middens of this study, and thus more leaf material from hyrax browsing. Moreover, if the yield was incomplete, sample amount would be underestimated. However, when middens were processed via sonication extraction and silica gel column separation alone (without a Bligh-Dyer separation), our *n*-alkane yields were much lower (<0.02 µg/g), suggesting that the addition of the Bligh-Dyer step to the methodology improves yields for midden samples with low concentrations. Additionally, we were able to do manual injections of our samples into the GCC III open split to the Finegan Delta Plus XP IRMS, which enabled us to concentrate our samples to a smaller volume than those possible for instruments with autosamplers.

Ten of these samples were shipped to the University of California Davis Stable Isotope Facility for $\delta^{13}\text{C}_{\text{wax}}$ analyses. The resulting dataset had a standard deviation of $\pm 0.82\%$ and an overall accuracy of $\pm 0.29\%$. We obtained $\delta\text{D}_{\text{wax}}$ measurements on five samples at Penn State in the Deines Stable Isotope Laboratory. For each sample, 4 $\mu\text{L}/100 \mu\text{L}$ was injected into the GCC III open split to a Finegan Delta Plus XP isotope-ratio mass spectrometer (IRMS). The A6 standard (A.Schimmelmann, Indiana University) was used, and the lowest peak area that produced reliable values was ~ 6 Vs. Due to this analytical constraint, only measurements above 6 Vs were considered for analysis. The instrument $\delta\text{D}_{\text{wax}}$ measurements were converted to VSMOW scale and analytical uncertainty was calculated using the methods of Polissar and Andrea (2014). This includes calculating standard deviation of replicate measurements ($n \geq 4$ for each sample), then propagating errors from measured and known values on the VSMOW scale (Polissar and Andrea, 2014). This uncertainty was estimated as the standard error of the mean and was between ± 4.1 - 6.2% .

Modern herbarium plant specimens

Plant specimens from herbarium sheets collected in Dhofar in 2018 and housed in the Ohio State University Archeobotany Lab were sampled for geochemical analyses. For *n*-alkane analyses, 94-699 mg of leaf material was extracted using Accelerated Solvent Extraction (ASE), then separated into a hexane fraction and 1:1 DCM:MeOH fraction via the same silica gel column chromatography protocol used for the midden samples. The hexane fraction was evaporated using the FlexiVap, and 50 μL of hexane were quantitatively added to each sample for GC-FID analysis. A 2 μL injection was used and calibration standards of 5, 10, 25, 50, and 100 $\text{ng}/\mu\text{L}$ were employed to create a calibration curve.

Results

Modern herbarium plant specimens

The *n*-alkanes from leaves from herbarium specimens were identified and quantified on the GC-FID, and values ranged from 0.72-380 ng/ μ L. In six samples, concentrations of the long-chain odd *n*-alkanes were too low and not identified by the instrument (labelled “n/a” in Table 3-1). The proportions of the C27, C29, and C31+C33 *n*-alkanes in each sample were plotted in a histogram and on ternary diagrams (Fig. 3-2 and 3-3)

The histogram in Figure 3-2 illustrates that the C27 and C29 *n*-alkanes were highest in relative abundance in comparison to the combined abundances of C31+ C33 homologues from tree taxa (*Terminalia dhofarica*, *Salvadora persica*, *Boscia arabica*, *Ziziphus spina-christii*) on average (C27=21.0%, C29=29.5%, C31+C33=37.5%). The C31+ C33 homologues were most abundant (C31+C33=76.8%) among the herbaceous taxa (*Lasiurus scindicus* [Poaceae], *Cleome brachycarpa*, *Cenchrus ciliaris* [Poaceae], *Heliotropium fartakense*) compared to the other two homologues (C27=8.1%, C29=9.3%). Amongst the trees, *Ziziphus spina-christii* had a higher proportion of the C31+C33 *n*-alkanes (70.0%) in comparison to all other taxa (8.9-60.0%). The highest abundance of the C31+C33 homologues was in the shrub *Cadaba heterotricha* (~99.5%).

In general, taxa with xeric affinities (*Cadaba heterotricha*, *Lasiurus scindicus*, *Cleome brachycarpa*, *Cenchrus ciliaris*, *Heliotropium fartakense*) had higher proportions of the C31+ C33 chains (>50%). Taxa with mesic affiliations (*Terminalia dhofarica*, *Salvadora persica*, *Boscia arabica*, *Ziziphus spina-christii*), except for *Ziziphus spina-christii*, were more abundant in the C27 and C29 chains (C27+C29 > 50%).

Table 3-1: *N*-alkane chain lengths for herbarium plant samples.

ID	Species	Family	Mass (mg)	C27 (ng/g)	C29 (ng/g)	C31 (ng/g)	C33 (ng/g)
1	<i>Croton oblongifolius</i>	Euphorbiaceae	301	n/a	n/a	n/a	n/a
2	<i>Pulicaria glutinosa</i>	Asteraceae	201	n/a	n/a	n/a	n/a
3	<i>Cadaba heterotricha</i>	Capparaceae	434	5.20	11.00	180.00	240.00
4	<i>Euphorbia granulata</i>	Euphorbiaceae	84	15.00	30.00	100.00	20.00
5	<i>Salsola rubescens</i>	Amaranthaceae	421	1.90	2.10	0.52	0.12
6	<i>Terminalia dhofarica</i>	Combretaceae	94	20.00	32.00	12.00	0.79
7	<i>Heliotropium fartakense</i>	Boraginaceae	384	3.00	5.00	24.00	2.30
8	<i>Salvadora persica</i>	Salvadoraceae	404	2.20	3.00	2.40	0.30
9	<i>Cleome sp.</i>	Capparaceae	102	2.50	18.00	21.00	7.80
10	<i>Pluchea dioscoridis</i>	Asteraceae	423	n/a	n/a	n/a	n/a
11	<i>Halothamnus bottae</i>	Amaranthaceae	313	n/a	n/a	n/a	n/a
12	<i>Cadaba farinosa</i>	Capparaceae	201	1.30	0.72	n/a	n/a
13	<i>Cleome brachycarpa</i>	Capparaceae	239	13.00	27.00	270.00	330.00
14	<i>Ziziphus spina-christi</i>	Rhamnaceae	284	7.30	21.00	48.00	8.00
15	<i>Ficus cordata</i>	Moraceae	699	n/a	n/a	n/a	n/a
16	<i>Boscia arabica</i>	Capparaceae	272	27.00	79.00	68.00	3.10
17	<i>Cocculus pendulus</i>	Menispermaceae	100	n/a	n/a	n/a	n/a
18	<i>Indigofera coerulea</i>	Fabaceae	271	1.10	1.20	0.79	0.11
19	<i>Lasiurus scindicus</i>	Poaceae	223	3.30	n/a	5.90	14.00
20	<i>Cenchrus ciliaris</i>	Poaceae	106	18.00	45.00	n/a	48.00

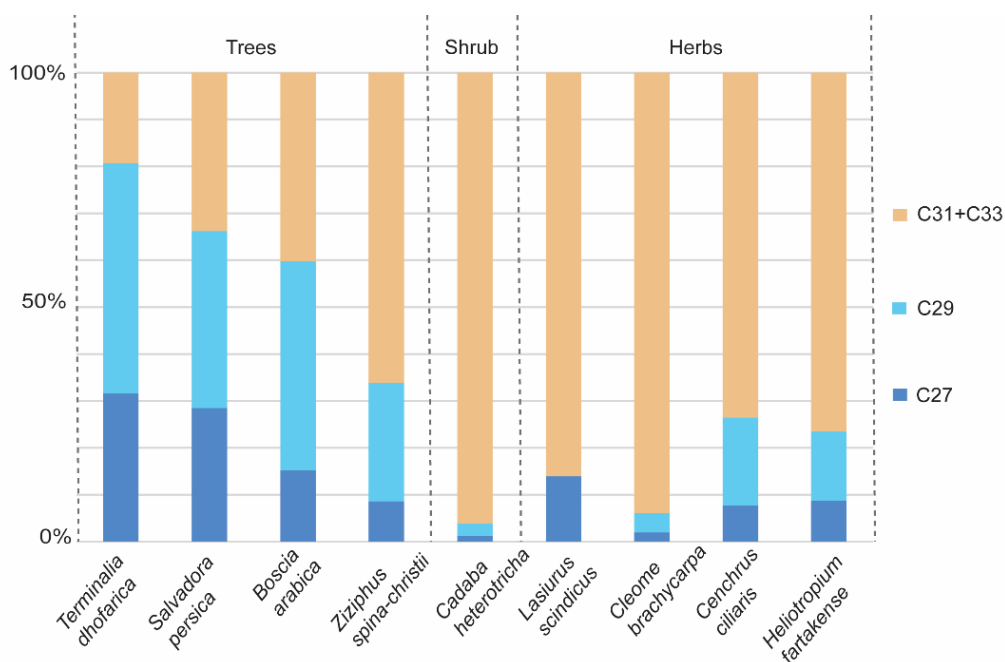


Figure 3-2: Proportions of the C27, C29, and C31+C33 *n*-alkanes in plant herbarium specimens. The C27 and C29 compounds are generally associated with trees, and the C31+C33 with herbs and grasses. From left to right are the **Trees**: *Terminalia dhofarica*, *Salvadora persica*, *Boscia arabica*, *Ziziphus spina-christii*; **Shrub**: *Cadaba heterotricha*; **Herbs**: *Cleome*, *Cenchrus ciliaris*, *Euphorbia granulata*, *Heliotropium fartakense*, *Cleome brachycarpa*

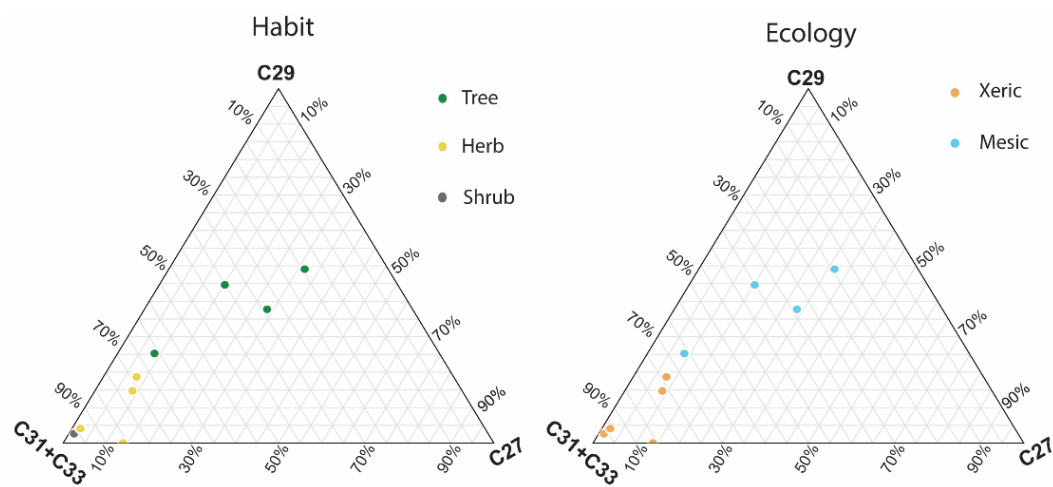


Figure 3-3: Ternary plots showing the proportions of the C27, C29, and C31+C33 *n*-alkanes in plant herbarium specimens. The left panel is color-coded by plant habit (tree, herb, or shrub) and the right panel is color-coded based on ecological affinity in the region (more mesic or xeric).

Rock hyrax middens

The concentrations of *n*-alkanes from the hyrax middens ranged from 0.82 to 270 ng/ μ L (Table 3-2). One modern and five fossil samples had high enough concentrations of the C31 *n*-alkane to yield compound specific $\delta^{13}\text{C}_{\text{wax}}$ values. These values ranged -34.72 to -28.14‰. Peak areas of the C31 *n*-alkane ranged from 2.42 to 40.56 Vs. The average $\delta\text{D}_{\text{wax}}$ values of the C31 *n*-alkane from one modern and three fossil middens ranged from -153.8 to -121.1‰ vs VSMOW. Sample 103-2C (3103 cal yr BP) did not yield any peaks above the analytical threshold, but samples 135-1, 146, 111-2E, and 155-D (0, 706, 1651, and 2920 cal yr BP, respectively) yielded 2-4 replicates with a high enough peak area.

Discussion

Interpreting plant community change through *n*-alkane distributions

The proportions of the C27, C29, and C31+C33 *n*-alkanes in the modern plant specimens largely reflect their plant habit, whether they are classified as herbs or trees/shrubs, which supports previous studies in other regions (Smith et al., 2007; Carr et al., 2014; Bush and McInerney, 2015). One notable exception, the shrub *Cadaba heterotricha*, had the highest proportion of C31+C33 *n*-alkanes. This plant is found only in the drier wadis of Dhofar and has xerophyte characteristics such as trichomes (Miller and Morris, 1988). Xerophytic plants tend to produce a higher concentration of *n*-alkanes and are typically abundant in the C31 chain length (Boom et al., 2014; Carr et al., 2014). The taxon *Ziziphus spina-christii* had the lowest relative abundances of the C27 and C29 chains in comparison to other trees. This plant typically has an arboreal habit and is distributed mainly throughout the monsoon-affected (mesic) areas of Dhofar (Miller and Morris, 1988). However, it can also grow as a shrub, and like *C. heterotricha* this shrub habit may explain the higher relative abundances of the longer chains (Miller and Morris, 1988).

When modern plant specimens were distinguished by their ecological affinity, whether they are generally associated with more mesic (*Terminalia dhofarica*, *Salvadora persica*, *Boscia arabica*, *Ziziphus spina-christii*) or xeric habitats (*Cadaba heterotricha*, *Lasiurus scindicus*, *Cleome brachycarpa*, *Cenchrus ciliaris*, *Heliotropium fartakense*) in Dhofar, xeric plants were also more abundant in C31+C33 homologues (79.5%). Plants that were affiliated with more mesic environments had a higher proportion of C27 and C29 chains (25.1% and 30.8%; Miller and Morris, 1988). These results indicate that in Dhofar, both plant habit and ecology impact the

distribution of *n*-alkanes, which would then be preserved in paleoecological archives and can aid in interpretations of vegetation change (Smith et al., 2007; Boom et al., 2014; Carr et al., 2014).

Applications of leaf wax isotopes for rock hyrax middens

While previous studies have extracted high enough concentrations of *n*-alkanes from hyrax middens for compound specific carbon isotope analyses, there is yet no published δD_{wax} data from fossil hyrax middens (Carr et al., 2010; Chase et al., 2012; Boom et al., 2014; Carr et al., 2014; Carr et al., 2016). The method used for this study has proven to yield higher concentrations of *n*-alkanes, and thus reproducible δD_{wax} values. Published *n*-alkane concentrations from hyrax middens are as low as 0.0002 $\mu\text{g/g}$ (Carr et al., 2010). In comparison, ocean cores and terrestrial sediments range from 0.4-1.3 $\mu\text{g/g}$ (Carr et al., 2010). Compound specific hydrogen isotope values have been successfully measured on samples with low concentrations of terrestrial *n*-alkanes, but these were two orders of magnitude larger than the previous midden studies (Carr et al., 2014; Aichner et al. 2015).

Paleohydrology and vegetation change in the late Holocene

The *n*-alkane chain length proportions from fossil hyrax middens had some variability, but generally remained dominated by C31+C33 chain lengths (Figure 3-4; ~60%). Samples with higher proportions of the smaller chains (C27 and C29) often correlate to high percentages of tree pollen. This revealed that overall, little change occurred in the predominant vegetation over this period from ~4 cal yr BP to modern, and that the plant community remained dominated by herbaceous plants. Further, other indications of changes in the proportion of vegetation types, including bulk $\delta^{13}\text{C}$, and $\delta^{13}\text{C}_{\text{wax}}$, do not indicate a notable shift. Taken together, this suggests that

the overall structure of the ecosystem in relation to C3 and C4 plants and woody versus herbaceous taxa, did not significantly change. In contrast, the pollen data produced from the same middens implied considerable turnover in the plant community, and the composition of the pollen flora in each pollen zone was demonstrated to be statistically different through time (Horisk et al., 2023). In particular, the pollen record shows that from ~4-3.1 ka, there were higher abundances of arboreal vegetation associated with escarpment woodlands and edaphically wetter locations like *Terminalia*, *Maytenus*, and *Boscia* (Horisk et al., 2023). After ~1.6 ka, there was a large shift to predominantly herbaceous taxa, such as Poaceae and *Heliotropium* (Horisk et al., 2023).

Although the results of the pollen, *n*-alkane abundance patterns, and $\delta^{13}\text{C}$ data from the same middens seem to disagree, we suggest that pollen and *n*-alkanes provide separate pieces of information about regional vegetation that are not truly at odds but represent different spatial and taxonomic scales. For example, the pollen from the middens may represent a more regional signal, capturing vegetation changes on the plateau, while the *n*-alkanes more closely represent the local plant community. In this scenario, pollen deposition into the middens would be primarily aeolian and represent a larger catchment area. This is supported by other midden studies which suggest more environmental deposition, rather than dietary consumption, in recent *Procapra* dung samples (Scott and Cooremans, 1992; Scott and Woodborne, 2007). In contrast, the bulk of the *n*-alkanes may have largely been deposited through dietary consumption of plant materials, which is supported by the previous study of Carr et al. (2010). The lack of large changes to the vegetation locally as suggested by the geochemical data is also aligned with macrobotanical data from the middens, which do not show any change through time (Sekulić, 2020).

While the alkane data provides a broad picture of local abundances of xeric vegetation structure, they do not provide detailed information about the taxonomy of plants more regionally as revealed by pollen data. The significant changes in the pollen composition over this interval

suggest there was turnover in the ecosystem composition over the late Holocene. At a coarse resolution, the vegetation structure, in terms of the distribution of herbaceous versus arboreal plants, did not shift significantly in the Nejd over the last 4000 years. However, it is likely that there was a higher density of mesic, arboreal vegetation on the plateau and escarpment from ~4-3 ka.

Further, we suggest that turnover in plant communities over the late Holocene in the Nejd was driven by variability in rainfall across the late Holocene. Although only two samples were available prior to 1.6ka, δD_{wax} (-144.7‰ to -153.8‰) values were relatively depleted in comparison to the more recent values, indicating relatively higher moisture availability (Figure 3-5; Sachse et al., 2012). This brief period of increased water availability punctuated the overall drying trend across the mid- to late Holocene (Fleitmann et al., 2004; Fleitmann et al., 2007). In contrast, the two more recent δD_{wax} samples at 706 and 0 cal yr BP were both enriched relative to the older samples by ~20-30‰, indicating less moisture availability and modern-like conditions by ~700 years ago.

The $\delta^{13}\text{C}_{\text{wax}}$ results suggest an admixture of C4 grasses and C3 woody plants, with a predominance of n-alkane homologues associated with C4 vegetation from ~4-3 kyr. The $\delta^{13}\text{C}_{\text{wax}}$ values at ~1.6 kyr were more variable, with one more depleted (111-2E; -31.78‰) and one more enriched (151; -28.14‰). The variability between these two samples may be a product of some temporal and spatial heterogeneity between the two samples, but on average represent a mixed C3/C4 cover (Chikaraishi and Naraoka, 2007; Rao, 2017; Liu and An, 2020). The sub-modern sample (108-1b, 109 cal yr BP) has a similar value to the older samples, and one modern sample (48-1b) shows a 2‰ depletion in line with the Suess Effect (Keeling, 1979; Feakins et al., 2015).

Given the $\delta^{13}\text{C}_{\text{wax}}$ results, we assume an average fractionation factor (ϵ) to make a tentative comparison to modern meteoric δD values. Feakins et al. (2013) report an average ϵ value of -150‰ in C3 monocots and -134‰ in C4 monocots. Due to the mix of this vegetation in

our record, we apply a simple average of these two values for an ϵ of -142‰. These values were plotted in comparison to modern measurements on both meteoric and groundwater in Dhofar (Figure 3-6; Strauch et al., 2014; Friesen et al., 2018). These show that samples dated to 2920 and 1651 cal yr BP have more depleted values of the δD_{wax} that are similar to modern Nejd groundwater (approximately -40 to -20‰). This could indicate groundwater recharge in the Nejd at this time, or perhaps more input from cyclone events. Modern meteoric water from cyclones is far more depleted in hydrogen and oxygen than monsoon precipitation (δD values -80 to -50‰; Strauch et al., 2014; Friesen et al., 2018). These events originate in the Arabian Sea and occur generally once every three years, with a severe storm once in every five (Kwarteng et al., 2009). Cyclonic events cause increased runoff, which is indicated by sedimentological records from coastal estuaries at ~1.6 kyr (Hoorn and Cremaschi, 2004).

The younger samples (706 cal yr BP and modern) were in the range of modern monsoon rainfall values and runoff (approx. -5 to 20‰). Thus, more enriched values in the younger samples could indicate a change in water source to runoff from monsoon rainfall occurring on the escarpment and/or increased evapotranspiration. In comparison to cyclones, winds from the monsoon transport moisture from the southern Indian Ocean (Fleitmann et al., 2007). Due to this larger transport distance, the moisture that is released over Dhofar has a more enriched hydrogen isotope composition due to the latitudinal effect (Dansgaard, 1964; Fleitmann et al., 2007).

The speleothem record from Qunf Cave indicates decreasing rainfall across the Holocene through gradual $\delta^{18}\text{O}$ enrichment (Fleitmann et al., 2007). The δD_{wax} data suggests a wetter pulse, which may be indicative of groundwater recharge or an uptick in cyclonic events at ~1.6ka. This aligns with local sedimentological and pollen evidence from an estuary near the coast, which demonstrates increased surface water flow at ~1.6ka (Hoorn and Cremaschi, 2004). All three records independently indicate it was dryer by ~1 kyr to ~700 yr in Dhofar, and particularly locally in the Nejd (Smith and Freeman, 2006; Fleitmann et al., 2007; Sachse et al., 2012). Taken

together, this information suggests that despite an overall drying trend across the Holocene, we capture shorter-term variability in rainfall.

While the pollen habits (trees, indeterminate, herbs) suggested large changes in community composition over the late Holocene, the geochemical data help fill in a picture wherein there was little to no changes in local structure, with arid and semi-arid desert scrub taxa dominated over the entire interval. This implies some resistance in the Nejd vegetation communities to large-scale changes with hydroclimate variability and increasing aridity, which global climate models predict will become more severe in the next century (Dahinden et al., 2017). However, substitutions within the major plant habit groups may result in the loss of species that are used as fodder for domesticated animals (e.g. *Terminalia*, *Salvadora persica*) or are economically important (e.g. Frankincense) across the vegetation zones, which could drastically impact economic resources, foodways, and timber (Asner et al., 2004; El-Mahi, 2011; Ball and Tzanopoulos, 2020). Overgrazing and other human activity could potentially intensify this, thus mitigating these impacts should be a focus of conservation efforts.

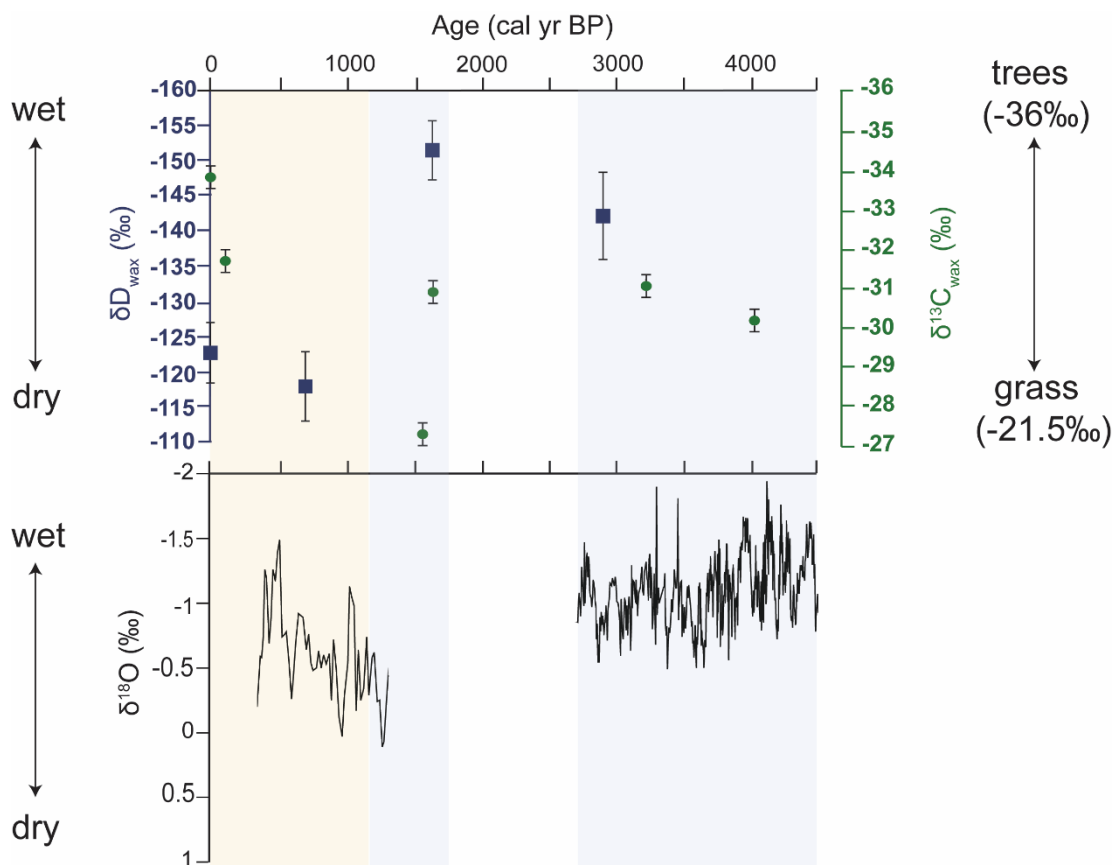


Figure 3-5: Top panel: δD_{wax} (blue) and $\delta^{13}C_{wax}$ data (green) plotted against midden sample age (cal yrs BP). Bottom panel: $\delta^{18}O$ data replotted from the Qunf cave speleothem record of Fleitmann et al. 2007. Blue bars represent periods where local and regional records indicate it is relatively wetter, compared to yellow bar which is a time frame that is generally accepted to be the driest time.

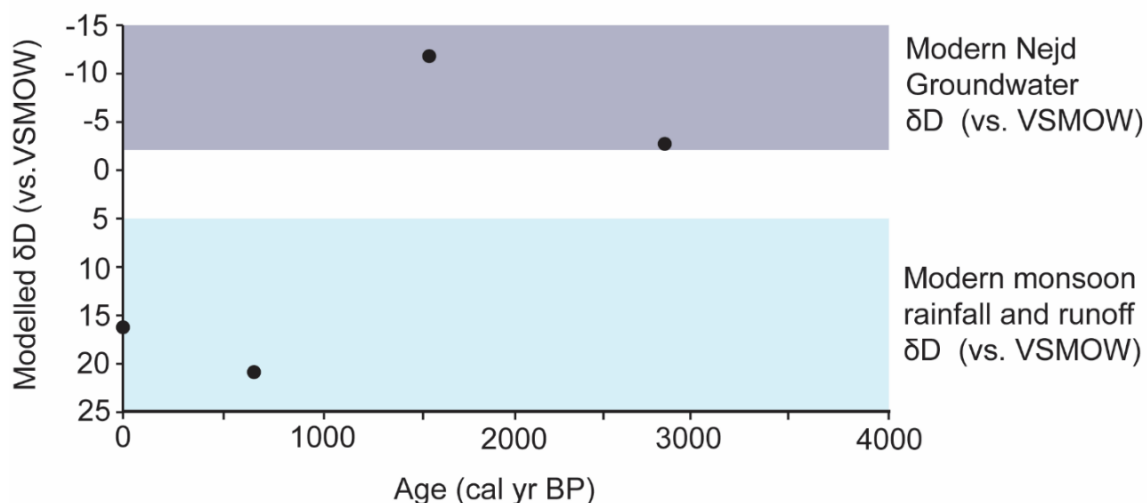


Figure 3-6: δD_{wax} data with applied ϵ value based on average of the C3 and C4 plant ϵ values described in the literature. Purple bar represents range of isotopic values from modern Nejd groundwater and the blue from modern monsoon rainfall and runoff, as presented by Strauch et al. (2014) and Friesen et al. (2018).

Conclusion

Dryland ecosystems are essential to nearly half of the Earth's population but are also the most at risk under changing climate conditions (Asner et al., 2004; Maestre et al., 2016). Global anthropogenic climate change is accelerating, and paleoecological records allow us to determine long-term patterns in changing climate and vegetation response. These can help scientists constrain future predictions of climate change impacts (Asner et al., 2004; Maestre et al., 2016; Dahinden et al., 2017). Rock hyrax middens have proven a powerful archive of both pollen and geochemical indicators for paleoecological studies in arid regions (Chase et al., 2012; Carr et al., 2016). In Dhofar, a more complete picture of vegetation change over the late Holocene and a link

to changing hydroclimate was revealed by plant biomarkers and stable isotopes derived from middens.

δD_{wax} data demonstrated that over the course of regional drying, driven by Indian Monsoon dynamics, there may have been a shorter wet period at $\sim 1.6\text{ka}$ (Fleitmann et al., 2004; Hoorn and Cremaschi, 2004; Fleitmann et al., 2007). The leaf wax *n*-alkanes and $\delta^{13}\text{C}_{\text{wax}}$, in comparison with the pollen record, indicated that these hydrological changes drove changes in the composition of the local vegetation, but not the overall structure of the plant communities. This suggests resilience of dryland vegetation to state-shifts under increasing aridity, which global climate models predict will be amplified by climate change (Dahinden et al., 2017). More work is necessary to fully constrain local paleohydrological change in this region, which can be achieved through the previously outlined midden processing methods that yielded reproducible δD_{wax} data.

Chapter 4

Modelling movement on the Dhofar landscape: climate change, human activity, and vegetation response

Abstract

Humans are profound agents of landscape change. Both climate and human-driven processes dynamically interact and influence vegetation. Pastoralism, particularly nomadic pastoralism, has been practiced in dryland ecosystems for thousands of years. Recent work has shown the complex, and often beneficial, ways this practice can affect plant communities. Through paleoecological and archaeological information, one can reconstruct patterns in human activity, changes in climate, and changes in vegetation. However, this does not reveal the ways in which these processes develop over time. A model can be employed to better understand the ways in which climate and people interact and affect vegetation. An Agent-Based Model was developed using modern climate and vegetation data from Dhofar, Oman, as well as information about pastoralist movement decisions. Through adjusting both climate parameters such as amount of rainfall, as well as browsing and grazing pressure, and running experiments over 1000 years, we were able to reveal the ways in which climate change influences human movement, and in turn creates patterns in vegetation structure across the landscape. Overall, the amount of rainfall and length of the Indian monsoon season are the most important for tree and grass growth. The density of animals on the landscape, even when increased to values beyond what is seen in Dhofar today, does not instigate changes to the vegetation. Additionally, when people are added to the landscape under changing monsoon conditions, there are significant changes to vegetation patterns. These results show that both climate change and human activity influence vegetation,

and pastoralism in Dhofar can be integrated into and play an active role in sustainability initiatives.

Introduction

Domesticated animal grazing makes up $\frac{1}{4}$ of land surface use on the planet, and thus is an important source of food such as meat and dairy (Asner et al., 2004). Nomadic pastoralism, particularly in arid places, has a long-term history of sustainability and has been continuously practiced by hundreds of millions of people for at least ten thousand years (Dyson-Hudson and Dyson-Hudson, 1980; Fratkin, 1997; Djohy et al., 2014; McCorrison et al., 2018). However, today much of this rangeland is actively being degraded (Sayre et al. 2012). Because rangelands are managed by humans, decisions regarding domesticated herding are influenced both by governments and societal frameworks (Fratkin, 1997; El-Mahi, 2011). Moreover, changes in the economy as well as climatic changes can have significant impacts on these rangelands (Fratkin, 1997; El-Mahi, 2011; Ball and Tzanopoulos, 2020). Thus, the relationship between humans, the practice of pastoralism, and the environment is a complex system influenced by numerous environmental and cultural factors. Understanding these relationships is imperative to preserving these environments and this essential lifeway under global climate change and changing land use.

In Dhofar, browsing and grazing by domesticated animals are reducing tree cover despite the persistence of pastoralism in this region for thousands of years (Martin et al., 2009; McCorrison et al., 2018; Ball and Tzanopoulos, 2020). There have been significant changes over the last century, both ecological and economic, which have led to this modern unsustainable relationship (El-Mahi, 2011). The stocking rates of domesticated animals, particularly camels, have increased exponentially in the last couple of decades (El-Mahi, 2011; Ball and Tzanopoulos,

2020). Moreover, there has been an increase in land use and disturbance through urban expansion (El-Mahi, 2011). In addition to these anthropogenic considerations, pastoralism emerged within the context of large environmental changes over the Holocene (Lézine et al., 2002; Fleitmann et al., 2004; Hoorn and Cremaschi, 2004; Fleitmann et al., 2007; Lézine et al., 2017). These have created novel parameters involved in pastoralist decisions and ecosystem dynamics. There exists a need to disentangle the impacts of climate, vegetation changes, and the grazing and browsing of domesticates on the landscape to understand the potential consequences of anthropogenic climate change.

While paleoecological and archaeological data provide useful long-term records, these illustrate patterns in environmental and cultural changes. The mechanisms which create these patterns and their relationships with one another are unknown. In this study, we use agent-based modelling (ABM) as a useful tool for understanding drivers of vegetation change in a mechanistic way. In particular, we use an ABM to assess the sensitivity of vegetation structure to various factors, both climate and grazing, to answer the following questions:

1. How do changes in rainfall amount and distribution affect the composition of vegetation communities?
2. How does the number of livestock / grazing and browsing pressure, alter the vegetation in comparison?
3. With increasing herds, is a threshold observed after which structural vegetation changes begin?

Background

Biodiverse plant communities in Dhofar

The vegetation in the Dhofar region is typically described by four ecological zones: the coastal plain, the escarpment, the plateau, and the Nejd (Figure 4-1; Miller and Morris, 1988). The coastal plain today is sparsely vegetated due to grazing of domesticated animals and other human land use such as urbanization and infrastructure (Miller and Morris, 1988; El-Mahi, 2011). The escarpment sharply increases in elevation and is home to a semi-arid cloud forest (Miller and Morris, 1988; Patzelt, 2015; Ball and Tzanopoulos, 2020). This unique woodland can intercept fog brought in by the Indian Monsoon and flourishes seasonally (Hildebrandt et al., 2007; Friesen et al., 2018). The plateau is a flat, high elevation band that is mainly grassland with isolated trees (Miller and Morris, 1988; McCorrison et al., 2020). The Nejd lies furthest inland and is mainly desert, with sparse trees and shrubs (Miller and Morris, 1988).



Figure 4-1: Map of Dhofar with ecological zones and locations of Salalah and Thumrait weather stations.

Climate and vegetation dynamics

The mean annual precipitation (MAP) in Dhofar varies considerably from the coast to the inland Nejd. The coast and escarpment regions are within reach of the Indian Monsoon (khareef), which brings dense fog from June to September. MAP as recorded by the Salalah weather station on the coast is ~120 mm/yr. This fog is prevented from extending further inland into the Nejd due to a thermal inversion that blocks convection (Abdul-Wahab, 2003; Hildebrandt et al., 2007). Beyond the reach of the khareef in the Nejd, MAP is much lower, ~20-30 mm/yr according to data from the Thumrait weather station (Almazroui et al., 2012). Cyclone events can bring upwards of 400 mm of precipitation, and occur roughly once every three years, with extreme events once every five years (Kwarteng et al., 2009). A true periodicity in cyclonic events has not yet been ascertained, but they cause large runoff and contribute to groundwater in the Nejd (Kwarteng et al., 2009; Friesen et al., 2018).

Climate, particularly moisture during the khareef, has a profound relationship with vegetation in Dhofar. The hydrological conditions in the cloud forests are influenced by fog harvesting by cloud forest trees, particularly *Terminalia dhofarica*, which can increase net precipitation by as much as ~250% and decreases loss from evapotranspiration (Hildebrandt et al., 2007; Friesen et al., 2018; Ball and Tzanopoulous, 2020). In the Nejd today, groundwater aquifers, recharged mainly through cyclone events, provide necessary moisture for the sparse, xeric vegetation (Al- Mashaikhi et al., 2011; Strauch et al., 2014; Friesen et al., 2018).

Over the Holocene, there have been significant changes in rainfall in Dhofar, which have in turn driven changes in vegetation (Morrill et al., 2003; Renssen et al., 2003; Fleitmann et al., 2004; Fleitmann et al., 2007; Horisk et al., 2023). Speleothem carbonate oxygen isotopes from the coastal region of Dhofar indicate a weakening Indian monsoon over the last 7-8 kyrs, which currently provides 70-80% of the MAP to the region (Fleitmann et al., 2007). Estuarine records

also suggest drying, punctuated by wetter pulses at ~2.7-2.3ka and ~1.7-1.5ka (Hoorn and Cremaschi, 2004). Bulk $\delta^{15}\text{N}$ data from fossil middens collected from the inland desert (Nejd) indicate a shift to hyperarid conditions over the late Holocene, and $\delta\text{D}_{\text{wax}}$ information from these same middens also show the drying trend and a wetter pulse at ~1.6 ka (Hoorn and Cremaschi, 2004; Horisk et al., 2023). Overall, the evidence suggests recent pastoral practices developed during increasing aridity across the Holocene, and experienced brief, wetter periods (Morrill et al., 2003; Fleitmann et al., 2007; Hoorn and Cremaschi, 2004).

The pollen data from the rock hyrax middens suggests considerable changes in vegetation composition in the Dhofar over the late Holocene, at approximately ~3-4 ka, after the onset of decreasing rainfall (Fleitmann et al., 2007). These data suggest denser vegetation, dominated by more arboreal plant taxa, were common inland at ~4000-3100 cal yrs BP. At ~2900 cal yrs BP, arboreal plants significantly decreased, and a more herbaceous, xeric-affiliated plant community emerged. However, bulk $\delta^{13}\text{C}$, $\delta^{13}\text{C}_{\text{wax}}$, and *n*-alkane homologue distributions drying did not result in a shift from C3 to C4 vegetation or from mesic to xeric ecological affinity. This implies that the large increase in trees occurred closer to the coast, while vegetation in the desert remained relatively arid. In contrast, by 1000 ka, indicators of human activity became more abundant in the record, and there was a particularly large shift in the plant community within the last century alone (Horisk et al., 2023).

Pastoralism through the Holocene

Pastoralists in Dhofar have had a close connection with the landscape for thousands of years (Martin et al., 2009; McCorriston et al., 2018). Today, overstocking of domesticates is leading to changes in the composition of vegetation communities and is preventing regeneration

of important cloud forest taxa (Ball and Tzanopoulos, 2020). It is now critical to understand if there is a threshold for vegetation resilience under different browsing pressures, especially under predicted climate change conditions that will lead to a decrease in moisture in an already moisture-limited environment (Maestre et al., 2012; Ault et al., 2016; Almazroui, 2012; Majdi et al., 2022).

The archaeological data indicate several changes in the mobility of pastoralist groups across the late Holocene. Most megalithic structures from ~5-4 ka were funerary in nature and are observed across Dhofar and into Yemen, indicating some cultural connection across this area (Harrower et al., 2014; McCorrison et al., 2014; Steimer, 2022). This tradition continued with trilith construction, a stone monument whose purpose is yet unknown, and was built solely in the Nejd (Newton and Zarins, 2010; McCorrison et al., 2014; Harrower et al., 2014; Garba, 2019). However, from ~2-1 ka, there is a notable shift: pastoralists began building permanent settlement structures on the plateau, closer to the coast. This suggests a reduction in mobility, and perhaps a congregation near more water resources. Nomadism into the Nejd began again after this and continues to this day (Ball and Tzanopoulos, 2020; McCorrison et al., 2023).

Agent-based modelling

The ABM for this project provides a variety of ways to study the complex system of climate, human behavior, and vegetation, specifically in Dhofar. The model allows the manipulation of environmental and human-influenced variables. The output from these experiments is the proportion of the vegetation types in patches, allowing us to assess the relationship between climate change and vegetation response. The hydrological controls on

vegetation in each ecological zone can be tested through adjusting the extent of the khareef into the Nejd, the amount of rainfall, and the length of the monsoon season.

The way in which pastoralist groups move across the landscape is a complex decision-making process involving both social and ecological factors (Rodriguez-Lopez et al., 2021). In Dhofar, environmental considerations include the vegetation of the different ecological zones and thus available biomass for domesticated animals, as well as access to water (McCorrison et al., 2018; Ball and Tzanopoulos, 2020). In broad terms, the ABM has built-in environmental parameters, independent agents with user-defined behaviors, all of which interact over defined time steps (Romanowska et al., 2021). These interactions influence the proportion of vegetation in each patch.

Methods

A suite of seven ABM experiments were designed to test the sensitivity of vegetation to different climate parameters as well as human activity. The current ABM is based on contemporary climate and general pastoralist movement decisions specific to Dhofar. We use the modern values of climate variables generated from weather stations in Dhofar as a starting point, or control, to simulate sensitivity to increasing and decreasing rainfall, as an analog for potential past or future climate states. Each experiment is designed to test the influence of various parameters on the vegetation fraction simulated in the model runs, which are the proportions of grass, trees, and bare ground averaged across the patches of an ecological zone (Nejd, Escarpment, Coast). The manipulated parameters included rainfall amount (Rainfall experiment), khareef season length (Khareef season experiment), geographic extent of khareef fog (Khareef extent experiment), as well as cattle and camel herds (Grazing and Browsing pressure

experiments). We also assessed the impact of rainfall and cloud extent on average soil moisture in each zone.

The ABM simulates changes in three ecological zones: the coast, the escarpment (which includes the plateau), and the Nejd desert. Each zone is affected by rainfall, monsoon fog, and has prescribed soil moisture parameters based on modern climate data and geomorphology. These zones are delineated areas made up of 1 km² patches, where each patch has a certain proportion of vegetation (grass, tree, bare ground) based on the plant communities in the different zones. Grass and trees are prescribed colonization rates based on how quickly they grow. The entire model is 100x100 kilometers and consists of 10,000 patches.

Random yearly rainfall datasets are generated using modern data from weather stations in Dhofar. These represent a typical monsoon season from mid-July to mid-September. Monsoon fog is simulated using a raster generated from near-infrared bands of Landsat data, which produces a normal distribution of fog within the coast and escarpment regions (Ball and Tzanopoulos, 2020). Each vegetation fraction can intercept fog moisture depending on the proportion of trees. This is based on ecohydrological studies of the Dhofar cloud forest which illustrate the relationship between cloud forest trees (esp. *Terminalia*) and fog interception (Hildebrandt et al., 2007; Friesen et al., 2018). Soil moisture is a simple bucket model, with input from rainfall and fog interception and loss through evapotranspiration and runoff.

The agents of the model are cattle and camel groups. These will move within a prescribed visual radius based on the dietary needs of the specific animal and the ideal vegetation. The model experiments were run on a weekly time-step for 1000 years, and 30 iterations of each experiment were conducted to ensure reproducibility. Vegetation fraction output values were recorded every 100 years and averaged across the 30 iterations.

The rainfall experiment utilized a multiplier to increase or decrease the rainfall amounts for each cell based on modern conditions. Rainfall was decreased by 0.5x, then increased by up to 4x modern conditions in 0.5 increments. A value of 1.5x modern Nejd rainfall (~30mm/yr) equates to about 45mm of precipitation, which may be a reasonable assumption for late Holocene conditions which were already arid (Fleitmann et al. 2004; Fleitmann et al. 2007). We then extended the experiment to 4x rainfall, up to ~120mm of precipitation in the Nejd, or near semi-arid conditions, to assess if there were significant differences in the vegetation under much wetter conditions, such as may have occurred during the Holocene Humid Period.

The Khareef extent experiment increased the geographic extent of monsoon clouds from modern up to 40 km inland by 5 km increments into the Nejd. The effect of the duration of the monsoon on the vegetation fractions was tested in the Khareef season experiment: the 14-week season was decreased by one two-week increment to 12 weeks. The season was then lengthened by two-week increments at the beginning, the end of the season, and then both ends, up to a total season length of 26 weeks.

The Browsing and Grazing Pressure experiment increased the number of cattle and camel herds from 0 to 3000 by 250 herds each. 3000 herds equate to approximately 500,000 animals in total. The number of herds is used as a proxy for grazing and browsing pressure on the landscape. The Grazing Pressure experiment excluded camels to disentangle grazing versus browsing impacts on the vegetation. These experiments are described in Table 4-1. The Khareef extent experiment was also run with a constant of 2500 herds to investigate how changes in climate and vegetation conditions influenced movement decisions, as well as how human activity and animal browsing/grazing impacted the vegetation under these conditions.

Table 4-1: Table describing each of the model experiments.

	Experiment	Parameter	Values	Increment	Units
1	Rainfall	rainfall_multiplier	0.5-4x	0.5x	mm
2	Khareef Extent*	fog_extent	0-40 km	5 km	kilometers
3	Rainfall and Khareef Extent	rainfall_multiplier fog_extent	0.5-1.5x 0-35 km	0.5x 5	mm kilometers
4	Khareef Season	start-week end-week	12-26 weeks	2	weeks
5	Browsing and Grazing Pressure	cattle and camels	0-2500	125 each	herds
6	Grazing Pressure	cattle	0-3000 herds	500	herds

*Run with and without herds (constant 2500 herds of cattle)

Results

The Rainfall experiment without herds showed no change in the relative vegetation fractions of vegetation in the Nejd (Figure 4-2). The escarpment tree fraction approximately doubled (~20-40%) with 4x modern rainfall amount, while grass and bare ground slightly

decreased. On the coastal plain, grass increased from ~32-68% and bare ground decreased with increasing rainfall from 1x to 4x rainfall. With 0.5x rainfall (half as much rain as modern conditions), there was approximately 10% less grass on the coast and ~6% less trees on the escarpment. In the Nejd, there was only ~2% decrease in the grass fraction. The Khareef extent experiment had no effect on the tree fraction in the Nejd but resulted in a moderate increase in the grass fraction with an increase in khareef extent of 40km further inland (~5-17%; Figure 4-4). The combined Rainfall and Khareef extent experiment produced results similar to those of the rainfall experiment across all zones.

In the Khareef season experiment, Nejd vegetation did not notably change, as the khareef is geographically limited to the coast and escarpment regions under control conditions. In these experiments, Nejd grass varies by $\pm 4\%$. On the escarpment, there is a logarithmic growth in the proportion of trees from ~32% to ~76% as khareef length increases from 14 to 26 weeks (Figure 4-3). With a shorter khareef season of 12 weeks, trees are half as abundant (~14%) as modern conditions (~32%). The overall length of the monsoon season is the primary driver of this change, whether the season starts earlier or ends later does not have an effect. On the coast, the grass fraction increases by a maximum of ~10% from the shortest monsoon season to the longest.

Grazing Pressure experiments (cattle only) show little to no impact on the vegetation fractions in each ecological zone. There is no change on the escarpment or in the Nejd and a small decrease (7%) in the grass fraction on the coast as herd density increases from 1500 to 3000 herds. Browsing and Grazing Pressure experiments, or an increase in both cattle and camel herds, do not change the vegetation in any of the zones.

By combining Khareef extent with browsing and grazing pressure from domesticated animal herds, the impact to vegetation is more notable in comparison to without animals (Figure 4-4). In the Nejd, grass has a slightly higher initial proportion (~8-9%) and increases as the

khareef reaches further inland to over 30% of the vegetation. On the escarpment, the tree fraction increases to ~50% of the total vegetation in comparison to ~25% without herds by 35 km extension of the monsoon. Grass on the coast is slightly elevated by up to ~5%, however values overall are comparable to the zero-herd experiment. The results of the 40km combined experiment are still pending confirmation.

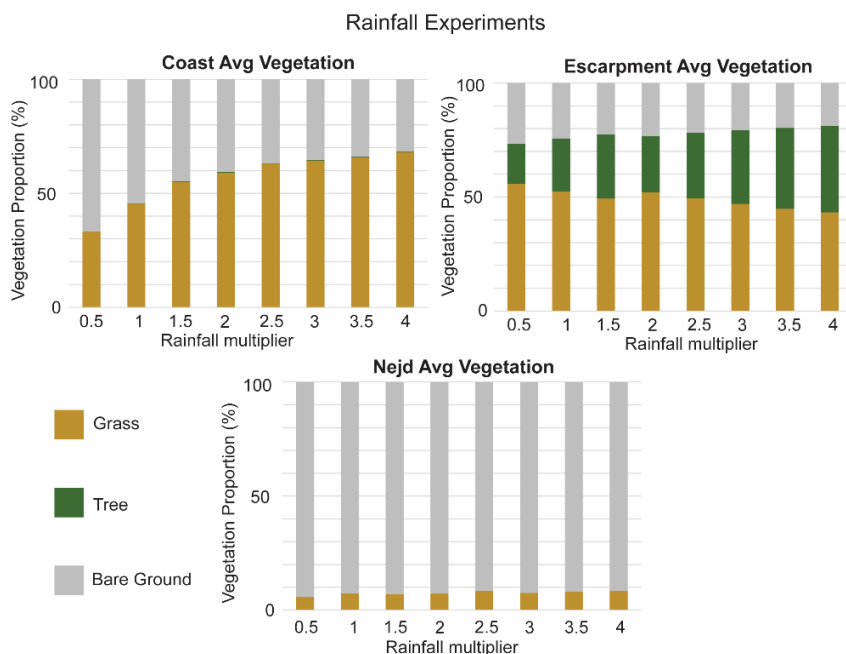


Figure 4-2: Rainfall experiment results: average vegetation fractions with increasing rainfall by vegetation zone

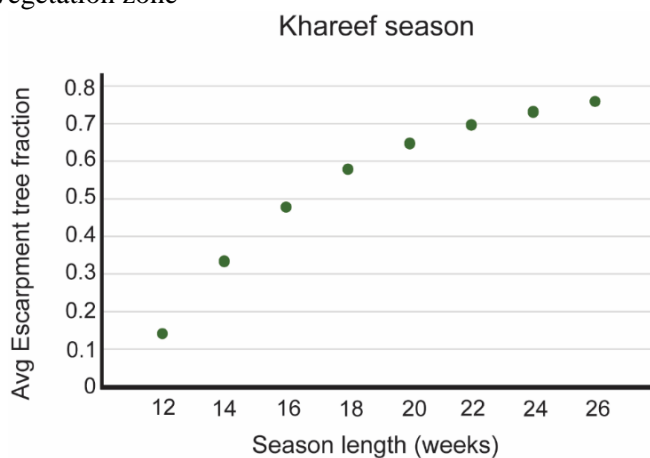


Figure 4-3: Average tree fraction on the escarpment with increasing khareef season length (weeks)

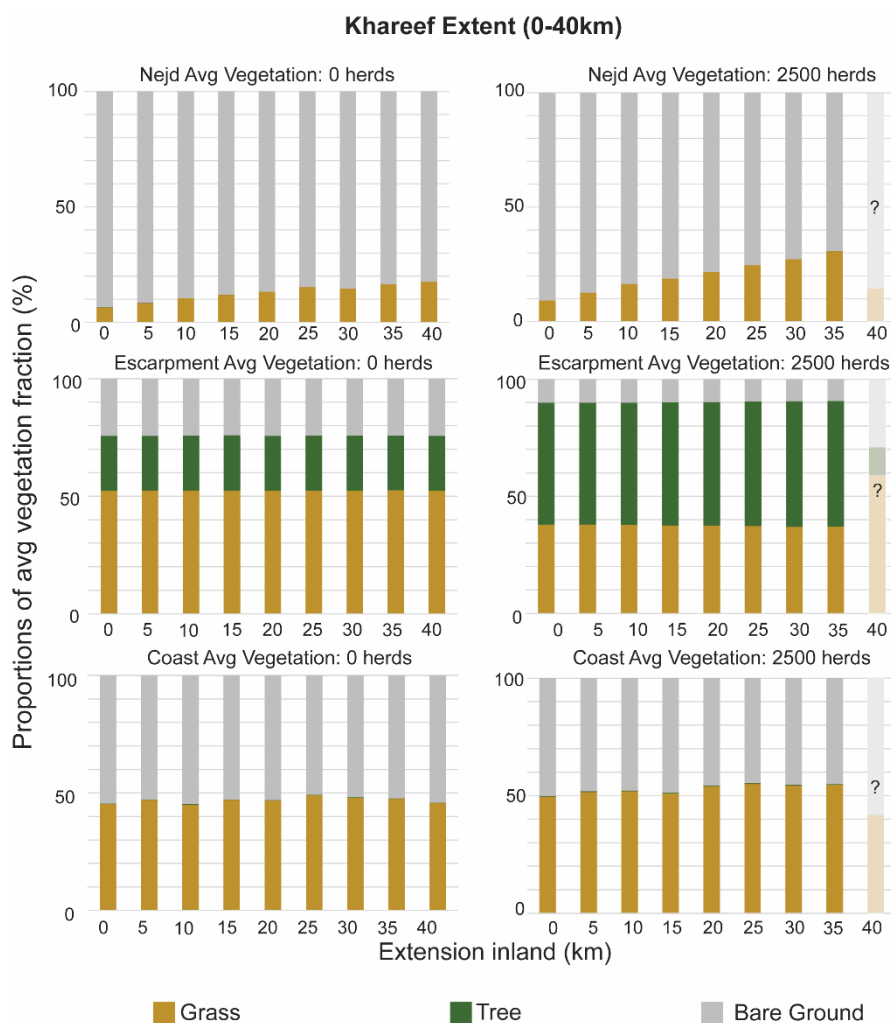


Figure 4-4: Left column: Khareef extent experiment run without herds; Right column: Khareef extent experiment run with a constant of 2500 cattle herds. From top to bottom are the Nejd, Escarpment, and Coast vegetation zones. The vertical axes represent the average vegetation proportion and the horizontal axes are khareef extent in kilometers.

Discussion

The results of the ABM experiments suggest that rainfall amount and monsoon seasonality are the primary climatic controls on vegetation in the different ecological zones. Increases in grass on the coast and in the Nejd, as well as a higher proportion of trees on the escarpment, are strongly linked with higher amounts of rainfall and a longer monsoon season (Figures 4-2 and 4-3). In the Nejd, vegetation remains unchanged until the khareef extends into this area. Khareef fog extending into the Nejd has the effect of increasing grass in the Nejd and increasing trees on the escarpment.

In contrast, reductions in rainfall and khareef season length seem to have contrasting effects in the Nejd versus on the escarpment. For example, less rain and a shorter khareef have little impact on Nejd vegetation. This suggests some potential resilience in the driest communities in Dhofar to decreased moisture to the levels evaluated in these simulations. However, these same moisture reductions led to significant decreases in trees on the escarpment and grass on the coast, suggesting less resilience to decreasing moisture in the vegetation wetter environments in the region. As global model projections suggest increased seasonality in rainfall and overall higher aridity in the region by the end of the century, this may suggest an imminent threat to the long-term stability of these biodiverse escarpment plant communities (Asner et al., 2004; Maestre et al., 2016; Dahinden et al., 2017; IPCC, 2022).

The ABM experiments also support interpretations of paleoecological studies linked with paleoclimate records from speleothems. These suggest that higher rainfall and/or reduced seasonality of the Indian Monsoon from the early to mid-Holocene (10-7 ka) led to expansion of woody ecosystems and grasslands in some areas (Fleitmann et al., 2004; Fleitmann et al., 2007; Ivory et al., 2021; Horisk et al., 2023). However, the model results support that the pollen record from hyrax middens represents a more regional signal, and that the high abundances of

Terminalia and other mesic tree pollen likely reflects a larger population of trees on the escarpment from 4-3 ka, rather than locally in the Nejd. This conclusion is supported by the presence of abandoned termite mounds which have been interpreted to indicate expansion of grasses and escarpment trees (McCorrison et al., 2020). The lack of major changes in the Nejd vegetation in the experiments is also in agreement with the macrobotanical and geochemical information from the middens, which show little to no change in the Nejd community over time (Sekulić, 2020).

The cattle grazing pressure experiment made little to no change in the vegetation with up to 3000 herds cattle, or ~500,000 animals. On its surface, these results may seem contradictory given connections by recent studies between current high herd densities and vegetation degradation. For example, as of 2021, estimates suggest that there are ~421,000 cattle and ~285,000 camels in Oman countrywide (NCSI, 2023). Degradation of the *Terminalia* woodlands on the escarpment under these high stocking rates has been well documented (Ball and Tzanopoulos, 2020). Juvenile trees are most susceptible to grazing and browsing, which inhibits regeneration of the forests (Pour et al., 2012; Ball and Tzanopoulos, 2020). Moreover, modern urbanization on the coastal plain is limiting the amount of biomass for browsing and grazing, which may condense herds on the lush escarpment and amplify the impacts of domesticated animals in this zone (El-Mahi, 2011). Therefore, it may be that the dispersal of herds on the landscape may be a primary factor in impacting plant communities, rather than the number of animals alone. Alternatively, it is possible that the model is oversimplified in that the carrying capacity of cattle is unrealistic.

In the experiment that combines interactions between the extent of the khareef with animal herds, there are notable changes to vegetation density throughout Dhofar. For example, higher grass in the Nejd as the khareef extends further inland. Additionally, a higher proportion of

trees are found under these conditions on the escarpment. While it might seem counterintuitive that trees are more common when animal browsing and grazing increases, we suggest that as fog extent increases, resulting in more grass in the Nejd, it is likely that the cattle herds begin to disperse more into this area, allowing grasses and trees to recover on the escarpment (McCorrison et al., 2018).

The results from these experiments support interpretations of the paleoclimate record wherein from the early to mid-Holocene, the monsoon was stronger, either through a longer season or increased rainfall, and may have extended further into the Nejd than it does today. The archaeological record indicates nomadic pastoralists were moving across the Nejd desert with their animals and leaving behind stone monuments (Martin, 2009; McCorrison et al., 2014; Steimer, 2022). These climate conditions would have supplied the preferred grassy fodder for cattle.

In the model, high numbers of domesticated animal herds do not seem to influence the overall proportions of vegetation. These results are hopeful indications of resilience of dryland plant communities to degradation with changing climate and domesticated grazing/browsing. Additionally, cattle grazing may positively impact tree growth on the escarpment. Conversely, with increasing aridity and seasonality of rainfall (longer dry seasons) under modern climate change conditions, there could be a significant threat to the overall state within each zone. Moreover, the taxonomic-scale changes revealed by the pollen record suggest species-specific resources are threatened by both climate change and human land use.

Conclusion

The results from ABM simulations of the socio-ecological system of Dhofar, Oman revealed interesting information that provides a framework for understanding dryland vegetation under changing climate and human activity. Rainfall and the length of the monsoon season primarily drive vegetation change in the different ecological zones, and increasing aridity poses a risk to the long-term stability of these communities. Domesticated animal herds can also introduce unique feedbacks with changing climate. Promisingly, however, large amounts of animal herds do not seem to drive significant changes in vegetation.

The model strengthens our interpretation of the paleoecological record in Dhofar. The lack of large-scale structural changes in the vegetation fractions (e.g. going from predominantly trees to grass) with substantial changes in climate agrees with evidence from the geochemical and macrobotanical evidence from the middens. This indicates the pollen record is a regional signal, and the mesic, arboreal vegetation early in the record represents trees from closer to the coast, likely on the plateau. The taxonomic turnover in this record also suggests threats to economically and culturally important plants, such as frankincense, as well as plants like *Terminalia dhofarica* which is critical to the cloud forest ecosystem (Miller and Morris, 1988; Hildebrandt et al., 2007).

In addition to changes in vegetation over the late Holocene, there have been very recent changes to woodland communities (Ball and Tzanopoulos, 2020; McCorrison et al., 2020). Local memory confirms the cloud forest once extended onto the plateau and has contracted significantly in the last few decades, and ecological studies have revealed they are actively being degraded (Ball and Tzanopoulos, 2020; McCorrison et al., 2020). Given this information, and the model results, conservation efforts might focus on increasing the dispersal of animal herds on the landscape or rotating the areas for browsing/grazing. Decreasing stocking rates and increasing supplemental feeding could also reduce anthropogenic pressure on the landscape.

Chapter 5

Conclusion

The studies presented in this dissertation tell the story of resilience and persistence in Dhofar. The use of the different methods paints a holistic picture of vegetation response to both climatic and anthropogenic pressures across the late Holocene and gives some insight into the future of this biodiverse ecosystem. While the plant communities in the Nejd proved resistant to large-scale changes under both changing hydroclimate conditions and modelled browsing and grazing pressures, there were changes in the species composition of the flora and changes in woodlands on the escarpment. Emerging parameters with climate change and human land use are thus likely to threaten these taxon-specific resources, such as frankincense or the cloud forest tree, *Terminalia dhofarica*, based on this observed turnover in the pollen record. Moreover, modern reduction in the cloud forest vegetation suggests that this has already begun (Ball and Tzanopoulos, 2020; McCorrison et al., 2020).

Rock hyrax middens preserved a host of information in a dryland where paleoecological archives are sparse. The pollen record demonstrated significant turnover in the composition of the flora and suggests the presence of a denser woodland on the escarpment and plateau ~4-3 ka. The taxa within the plant community then became predominantly xeric after ~1.6ka. The geochemical information from *n*-alkanes revealed that at the larger scale there was little to no change in the structure of the plant community in the Nejd (i.e. from more C3 to C4 or woody to grassy). Based on this, we can infer that the Nejd was already xeric by 4 ka but also resilient to large-scale changes despite several thousand years of decreasing rainfall (Fleitmann et al., 2007). The taxonomic turnover within the pollen record was further linked to hydrologic variability across the late Holocene – hydrogen isotopes from the *n*-alkanes suggest a wetter pulse punctuated the

overall drying trend ~1.6 ka, and near modern conditions by ~700 years ago. The substitutions of taxa imply that species-specific resources are likely to change with continued anthropogenic climate change.

The ABM experiments suggest that rainfall and khareef season length are the main climatic controls on vegetation in Dhofar. Interestingly, high browsing and grazing pressure does not initiate large changes in the proportions of vegetation. This suggests that modern reduction of woody vegetation cover may be linked to a concentrated distribution of herds on the escarpment, or the perhaps the preferential browsing of young saplings is not accurately represented by the model (Ball and Tzanopoulos, 2020). Moreover, the addition of a large number of cattle herds with a geographic extension of the khareef significantly increases the proportion of trees on the escarpment. This suggests that some amount of grazing is in fact beneficial to woodland growth. These results indicate that pastoralist practices in and of themselves are not necessarily destructive of vegetation communities and can actually positively shape escarpment woodlands.

This study illustrates the way climatic variables and human activity create complex feedbacks in shaping plant communities. Overall, this dryland ecosystem has proven resilient to large-scale state shifts across the late Holocene, which casts some hope in our projections of the future. However, loss of specific taxa may exacerbate the impacts of both climate change and human land use. For example, *Terminalia dhofarica* increases net precipitation in the cloud forest (Hildebrandt et al., 2007; Friesen et al., 2018). To lose this key species would reduce the water available to the vegetation in that zone, which may be catastrophic. The cloud forest is a large draw for tourism and provides food for domesticated herds and is thus a critical economic resource. Considering the results of the model experiments, conservation and sustainability initiatives may focus on the distribution of herds on the landscape, in addition to reducing the number of herds, to reduce the amount of grazing and browsing pressure on the cloud forest.

Hyrax middens in Dhofar and elsewhere in Arabia hold the potential to greatly expand our understanding of the interactions between climate, plants, and people. Pollen and macrobotanical information demonstrate changes, or the lack thereof, in the surrounding flora. With new processing methods for geochemical indicators, there is the opportunity to continue to develop hydroclimate records, which can then be directly linked with vegetation change. Additionally, modelling the impacts of fire and cyclones in this system may reveal more nuance than the current suite of parameters in the ABM. There are still many questions to be asked, and more beauty and intricacy to be revealed.

References Cited

- Abbas, H., Qaiser, M., & Alam, J. (2010). Conservation status of *Cadaba heterotricha* Stocks (Capparaceae): An endangered species in Pakistan. *Pakistan Journal of Botany*, 42(1), 35-46.
- Abdul-Wahab, S. A. (2003). Analysis of thermal inversions in the Khareef Salalah region in the Sultanate of Oman: Thermal inversions. *Journal of Geophysical Research: Atmospheres*, 108(D9). <https://doi.org/10.1029/2002JD003083>
- Afuye, G. A., Kalumba, A. M., & Orimoloye, I. R. (2021). Characterisation of Vegetation Response to Climate Change: A Review. *Sustainability*, 13(13), 7265. <https://doi.org/10.3390/su13137265>
- Aichner, B., Feakins, S. J., Lee, J. E., Herzsuh, U., & Liu, X. (2015). High-resolution leaf wax carbon and hydrogen isotopic record of the late Holocene paleoclimate in arid Central Asia. *Climate of the Past*, 11(4), 619–633. <https://doi.org/10.5194/cp-11-619-2015>
- Albalawi, E. K., & Kumar, L. (2013). Using remote sensing technology to detect, model and map desertification: A review. *Journal of Food, Agriculture and Environment*. 11. 791-797.
- Al-Mashaikhi, K., Oswald, S., Attinger, S., Büchel, G., Knöller, K., & Strauch, G. (2012). Evaluation of groundwater dynamics and quality in the Najd aquifers located in the Sultanate of Oman. *Environmental Earth Sciences*, 66(4), 1195–1211. <https://doi.org/10.1007/s12665-011-1331-2>

- Almazroui, M., Islam, M. N., Jones, P. D., Athar, H., & Rahman, M. A. (2012). Recent climate change in the Arabian Peninsula: Seasonal rainfall and temperature climatology of Saudi Arabia for 1979–2009. *Atmospheric Research*, *111*, 29–45.
<https://doi.org/10.1016/j.atmosres.2012.02.013>
- Anderson, M. J. (2003). Analysis of Ecological Communities. *Journal of Experimental Marine Biology and Ecology*, *289*(2), 303–305. [https://doi.org/10.1016/S0022-0981\(03\)00091-1](https://doi.org/10.1016/S0022-0981(03)00091-1)
- Armitage, S. J., Jasim, S. A., Marks, A. E., Parker, A. G., Usik, V. I., & Uerpmann, H.-P. (2011). The Southern Route “Out of Africa”: Evidence for an Early Expansion of Modern Humans into Arabia. *Science*, *331*(6016), 453–456.
<https://doi.org/10.1126/science.1199113>
- Asner, G. P., Elmore, A. J., Olander, L. P., Martin, R. E., & Harris, A. T. (2004). Grazing systems, ecosystem responses, and global change. *Annual Review of Environment and Resources*, *29*(1), 261–299. <https://doi.org/10.1146/annurev.energy.29.062403.102142>
- Ault, T. R., Mankin, J. S., Cook, B. I., & Smerdon, J. E. (2016). Relative impacts of mitigation, temperature, and precipitation on 21st-century megadrought risk in the American Southwest. *Science Advances*, *2*(10), e1600873.
<https://doi.org/10.1126/sciadv.1600873>
- Avanzini, A. (2008). *A port in Arabia between Rome and the Indian Ocean, 3rd C. BC-5th C. AD: Khor Rori report 2*. L’Erma di Bretschneider.
- Ball, L., & Tzanopoulos, J. (2020). Livestock browsing affects the species composition and structure of cloud forest in the Dhofar Mountains of Oman. *Applied Vegetation Science*, *23*(3), 363–376. <https://doi.org/10.1111/avsc.12493>

- Bar-Matthews, M., Ayalon, A., & Kaufman, A. (1997). Late Quaternary Paleoclimate in the Eastern Mediterranean Region from Stable Isotope Analysis of Speleothems at Soreq Cave, Israel. *Quaternary Research*, 47(2), 155–168.
<https://doi.org/10.1006/qres.1997.1883>
- Baudena, M., Boni, G., Ferraris, L., von Hardenberg, J., & Provenzale, A. (2007). Vegetation response to rainfall intermittency in drylands: Results from a simple ecohydrological box model. *Advances in Water Resources*, 30(5), 1320–1328.
<https://doi.org/10.1016/j.advwatres.2006.11.006>
- Bellini, C., Pavan, A., Pignotti, L., Gonnelli, T., & Lippi, M. M. (2020). Food plants in pollen records from ancient Southern Arabia: The evidence from Sumhuram (Southern Oman). *Journal of Arid Environments*, 177, 104131.
<https://doi.org/10.1016/j.jaridenv.2020.104131>
- Binford, L. R. (1990). Mobility, housing, and environment: a comparative study. *Journal of Anthropological Research*, 46(2), 119-152.
- Blackford, J. J. (2000). Charcoal fragments in surface samples following a fire and the implications for interpretation of subfossil charcoal data. *Palaeogeography, Palaeoclimatology, Palaeoecology*, 164(1–4), 33–42. [https://doi.org/10.1016/S0031-0182\(00\)00173-5](https://doi.org/10.1016/S0031-0182(00)00173-5)
- Bliege Bird, R., McGuire, C., Bird, D. W., Price, M. H., Zeanah, D., & Nimmo, D. G. (2020). Fire mosaics and habitat choice in nomadic foragers. *Proceedings of the National Academy of Sciences*, 117(23), 12904–12914. <https://doi.org/10.1073/pnas.1921709117>
- Böll, A., Lückge, A., Munz, P., Forke, S., Schulz, H., Ramaswamy, V., Rixen, T., Gaye, B., & Emeis, K.-C. (2014). Late Holocene primary productivity and sea surface temperature

variations in the northeastern Arabian Sea: Implications for winter monsoon variability: Late Holocene winter monsoon variations. *Paleoceanography*, 29(8), 778–794.

<https://doi.org/10.1002/2013PA002579>

Bonabeau, E. (2002). Agent-based modeling: Methods and techniques for simulating human systems. *Proceedings of the National Academy of Sciences*, 99(suppl_3), 7280–7287.

<https://doi.org/10.1073/pnas.082080899>

Boom, A., Carr, A. S., Chase, B. M., Grimes, H. L., & Meadows, M. E. (2014). Leaf wax n-alkanes and $\delta^{13}\text{C}$ values of CAM plants from arid southwest Africa. *Organic Geochemistry*, 67, 99–102. <https://doi.org/10.1016/j.orggeochem.2013.12.005>

Borgogno, F., D’Odorico, P., Laio, F., & Ridolfi, L. (2007). Effect of rainfall interannual variability on the stability and resilience of dryland plant ecosystems: Plant ecosystems and rainfall variability. *Water Resources Research*, 43(6).

<https://doi.org/10.1029/2006WR005314>

Brierley, C., Manning, K., & Maslin, M. (2018). Pastoralism may have delayed the end of the green Sahara. *Nature Communications*, 9(1), 4018. <https://doi.org/10.1038/s41467-018-06321-y>

Brinkmann, K., Patzelt, A., Dickhoefer, U., Schlecht, E., & Buerkert, A. (2009). Vegetation patterns and diversity along an altitudinal and a grazing gradient in the Jabal al Akhdar mountain range of northern Oman. *Journal of Arid Environments*, 73(11), 1035–1045.

<https://doi.org/10.1016/j.jaridenv.2009.05.002>

Buffington, A., & McCorriston, J. (2019). Wood exploitation patterns and pastoralist–environment relationships: Charcoal remains from Iron Age Šhakal, Dhufar, Sultanate of

Oman. *Vegetation History and Archaeobotany*, 28(3), 283–294.

<https://doi.org/10.1007/s00334-018-0682-y>

Burns, S. J., Fleitmann, D., Matter, A., Neff, U., & Mangini, A. (2001). Speleothem evidence from Oman for continental pluvial events during interglacial periods. *Geology*, 29(7), 623. [https://doi.org/10.1130/0091-7613\(2001\)029<0623:SEFOFC>2.0.CO;2](https://doi.org/10.1130/0091-7613(2001)029<0623:SEFOFC>2.0.CO;2)

Burns, S. J., Matter, A., Frank, N., & Mangini, A. (1998). Speleothem-based paleoclimate record from northern Oman. *Geology*, 26(6), 499. [https://doi.org/10.1130/0091-7613\(1998\)026<0499:SBPRFN>2.3.CO;2](https://doi.org/10.1130/0091-7613(1998)026<0499:SBPRFN>2.3.CO;2)

Bush, R. T., & McInerney, F. A. (2015). Influence of temperature and C 4 abundance on n - alkane chain length distributions across the central USA. *Organic Geochemistry*, 79, 65–73. <https://doi.org/10.1016/j.orggeochem.2014.12.003>

Carr, A. S., Boom, A., & Chase, B. M. (2010). The potential of plant biomarker evidence derived from rock hyrax middens as an indicator of palaeoenvironmental change. *Palaeogeography, Palaeoclimatology, Palaeoecology*, 285(3–4), 321–330. <https://doi.org/10.1016/j.palaeo.2009.11.029>

Carr, A. S., Boom, A., Grimes, H. L., Chase, B. M., Meadows, M. E., & Harris, A. (2014). Leaf wax n-alkane distributions in arid zone South African flora: Environmental controls, chemotaxonomy and palaeoecological implications. *Organic Geochemistry*, 67, 72–84. <https://doi.org/10.1016/j.orggeochem.2013.12.004>

Carr, A. S., Chase, B. M., Boom, A., & Medina-Sanchez, J. (2016). Stable isotope analyses of rock hyrax faecal pellets, hyraceum and associated vegetation in southern Africa: Implications for dietary ecology and palaeoenvironmental reconstructions. *Journal of Arid Environments*, 134, 33–48. <https://doi.org/10.1016/j.jaridenv.2016.06.013>

- Castañeda, I. S., Werne, J. P., Johnson, T. C., & Filley, T. R. (2009). Late Quaternary vegetation history of southeast Africa: The molecular isotopic record from Lake Malawi. *Palaeogeography, Palaeoclimatology, Palaeoecology*, 275(1–4), 100–112. <https://doi.org/10.1016/j.palaeo.2009.02.008>
- Charpentier, V. (2023). Hunter-gatherers of the “empty quarter of the early Holocene” to the last Neolithic societies: Chronology of the late prehistory of south-eastern Arabia (8000–3100 BC). *Proceedings of the Seminar for Arabian Studies*, 38, 93–113.
- Chase, B. M., Meadows, M. E., Scott, L., Thomas, D. S. G., Marais, E., Sealy, J., & Reimer, P. J. (2009). A record of rapid Holocene climate change preserved in hyrax middens from southwestern Africa. *Geology*, 37(8), 703–706. <https://doi.org/10.1130/G30053A.1>
- Chase, B. M., Scott, L., Meadows, M. E., Gil-Romera, G., Boom, A., Carr, A. S., Reimer, P. J., Truc, L., Valsecchi, V., & Quick, L. J. (2012). Rock hyrax middens: A palaeoenvironmental archive for southern African drylands. *Quaternary Science Reviews*, 56, 107–125. <https://doi.org/10.1016/j.quascirev.2012.08.018>
- Chikaraishi, Y., & Naraoka, H. (2007). $\Delta^{13}\text{C}$ and δD relationships among three n-alkyl compound classes (n-alkanoic acid, n-alkane and n-alkanol) of terrestrial higher plants. *Organic Geochemistry*, 38(2), 198–215. <https://doi.org/10.1016/j.orggeochem.2006.10.003>
- Claussen, M., Bathiany, S., Brovkin, V., & Kleinen, T. (2013). Simulated climate–vegetation interaction in semi-arid regions affected by plant diversity. *Nature Geoscience*, 6(11), 954–958. <https://doi.org/10.1038/ngeo1962>
- Clements, F. E. (1916). *Plant succession: an analysis of the development of vegetation* (No. 242). Carnegie Institution of Washington.

- Cremaschi, M., Zerboni, A., Charpentier, V., Crassard, R., Isola, I., Regattieri, E., & Zanchetta, G. (2015). Early–Middle Holocene environmental changes and pre-Neolithic human occupations as recorded in the cavities of Jebel Qara (Dhofar, southern Sultanate of Oman). *Quaternary International*, 382, 264–276.
<https://doi.org/10.1016/j.quaint.2014.12.058>
- Cressman, R., & Krivan, V. (2006). Migration Dynamics for the Ideal Free Distribution. *The American Naturalist*, 168(3), 384–397.
- Cronk, L. (1991). Human Behavioral Ecology. *Annu. Rev. Anthropol.*, 20, 25–53.
- Dahinden, F., Fischer, E. M., & Knutti, R. (2017). Future local climate unlike currently observed anywhere. *Environmental Research Letters*, 12(8), 084004.
<https://doi.org/10.1088/1748-9326/aa75d7>
- Dansgaard, W. (1964). Stable isotopes in precipitation. *tellus*, 16(4), 436–468.
- Davies, C. P. (2006). Holocene Paleoclimates of Southern Arabia from Lacustrine Deposits of the Dhamar Highlands, Yemen. *Quaternary Research*, 66(3), 454–464.
<https://doi.org/10.1016/j.yqres.2006.05.007>
- deMenocal, P., Ortiz, J., Guilderson, T., Adkins, J., Sarnthein, M., Baker, L., & Yarusinsky, M. (2000). Abrupt onset and termination of the African Humid Period: Rapid climate responses to gradual insolation forcing. *Quaternary Science Reviews*, 19, 347–361.
[https://doi.org/10.1016/S0277-3791\(99\)00081-5](https://doi.org/10.1016/S0277-3791(99)00081-5)
- Dereje, M., & Uden, P. (2005). The browsing dromedary camel I. Behaviour, plant preference and quality of forage selected. *Animal Feed Science and Technology*, 12.

- Díaz, F. P., Frugone, M., Gutiérrez, R. A., & Latorre, C. (2016). Nitrogen cycling in an extreme hyperarid environment inferred from $\delta^{15}\text{N}$ analyses of plants, soils and herbivore diet. *Scientific Reports*, 6(1), 22226. <https://doi.org/10.1038/srep22226>
- Diefendorf, A. F., Mueller, K. E., Wing, Scott. L., Koch, P. L., & Freeman, K. H. (2010). Global patterns in leaf ^{13}C discrimination and implications for studies of past and future climate. *Proceedings of the National Academy of Sciences*, 107(13), 5738–5743. <https://doi.org/10.1073/pnas.0910513107>
- Dietl, G. P., Kidwell, S. M., Brenner, M., Burney, D. A., Flessa, K. W., Jackson, S. T., & Koch, P. L. (2014). Conservation Paleobiology: Leveraging Knowledge of the Past to Inform Conservation and Restoration. 25. *Annual Review of Earth and Planetary Sciences*, 43, 79-103.
- Dinies, M., Plessen, B., Neef, R., & Kürschner, H. (2015). When the desert was green: Grassland expansion during the early Holocene in northwestern Arabia. *Quaternary International*, 382, 293–302. <https://doi.org/10.1016/j.quaint.2015.03.007>
- Djohy, G., Edja, A. H., Akponikpè, P. B. I., Olokesusi, F., Belem, M., & Bellwood-Howard, I. (2014). Cattle pastoralists' strategies to cope with water scarcity in climate change context in Northern Benin, West Africa. *Journal of Livestock Extension*. 14. 21-30.
- D'Odorico, P., & Bhattachan, A. (2014). Hydrologic variability in dryland regions: Impacts on ecosystem dynamics and food security. *Philosophical Transactions of the Royal Society B: Biological Sciences*, 367(1606), 3145–3157. <https://doi.org/10.1098/rstb.2012.0016>
- D'Odorico, P., Bhattachan, A., Davis, K. F., Ravi, S., & Runyan, C. W. (2013). Global desertification: Drivers and feedbacks. *Advances in Water Resources*, 51, 326–344. <https://doi.org/10.1016/j.advwatres.2012.01.013>

- Drechsler, P. (2007). The Neolithic dispersal into Arabia. *Proceedings of the Seminar for Arabian Studies*, 37, 27–29.
- Dyson-Hudson, R., & Dyson-Hudson, N. (1980). Nomadic pastoralism. *Annual review of anthropology*, 9(1), 15-61.
- Eglinton, G., & Hamilton, R. J. (1967). Leaf Epicuticular Waxes. *American Association for the Advancement of Science*, 156(No. 3780), 1322–1335.
- Eglinton, T. I., & Eglinton, G. (2008). Molecular proxies for paleoclimatology. *Earth and Planetary Science Letters*, 275(1-2), 1-16.
- Ehleringer, J. R., Cerling, T. E., & Helliker, B. R. (1997). C 4 photosynthesis, atmospheric CO₂, and climate. *Oecologia*, 112(3), 285–299. <https://doi.org/10.1007/s004420050311>
- El-Mahi, A. T. (2001). The traditional pastoral groups of Dhofar, Oman: a parallel for ancient cultural ecology. *Proceedings of the Seminar for Arabian Studies*, 31, 131–143.
- El-Mahi, A. T. (2011). Old Ways in a Changing Space: The Issue of Camel Pastoralism in Dhofar. *Journal of Agricultural and Marine Sciences [JAMS]*, 16, 51. <https://doi.org/10.24200/jams.vol16iss0pp51-64>
- El-Moslimany, A. P. (1990). Ecological significance of common nonarboreal pollen: Examples from drylands of the Middle East. *Review of Palaeobotany and Palynology*, 64(1–4), 343–350. [https://doi.org/10.1016/0034-6667\(90\)90150-H](https://doi.org/10.1016/0034-6667(90)90150-H)
- El-Sheikh, M. A. (2013). Population structure of woody plants in the arid cloud forests of Dhofar, southern Oman. *Acta Botanica Croatica*, 72(1), 97–111. <https://doi.org/10.2478/v10184-012-0008-6>
- Enzel, Y., Kushnir, Y., & Quade, J. (2015). The middle Holocene climatic records from Arabia: Reassessing lacustrine environments, shift of ITCZ in Arabian Sea, and impacts

- of the southwest Indian and African monsoons. *Global and Planetary Change*, 129, 69–91. <https://doi.org/10.1016/j.gloplacha.2015.03.004>
- Evans, R. D. (2001). Physiological mechanisms influencing plant nitrogen isotope composition. *Trends in Plant Science*, 6(3), 121–126. [https://doi.org/10.1016/S1360-1385\(01\)01889-1](https://doi.org/10.1016/S1360-1385(01)01889-1)
- Farquhar, G. D., Ehleringer, J. R., & Hubick, K. T. (1989). Carbon Isotope Discrimination and Photosynthesis. *Annual Review of Plant Physiology and Plant Molecular Biology*, 40(1), 503–537. <https://doi.org/10.1146/annurev.pp.40.060189.002443>
- Feakins, S. J. (2013). Pollen-corrected leaf wax D/H reconstructions of northeast African hydrological changes during the late Miocene. *Palaeogeography, Palaeoclimatology, Palaeoecology*, 374, 62–71. <https://doi.org/10.1016/j.palaeo.2013.01.004>
- Feakins, S. J., Liddy, H. M., Tauxe, L., Galy, V., Feng, X., Tierney, J. E., Miao, Y., & Warny, S. (2020). Miocene C₄ Grassland Expansion as Recorded by the Indus Fan. *Paleoceanography and Paleoclimatology*, 35(6). <https://doi.org/10.1029/2020PA003856>
- Feakins, S. J., & Sessions, A. L. (2010). Controls on the D/H ratios of plant leaf waxes in an arid ecosystem. *Geochimica et Cosmochimica Acta*, 74(7), 2128–2141. <https://doi.org/10.1016/j.gca.2010.01.016>
- Feakins, S. J., Wu, M. S., Ponton, C., Galy, V., & West, A. J. (2018). Dual isotope evidence for sedimentary integration of plant wax biomarkers across an Andes-Amazon elevation transect. *Geochimica et Cosmochimica Acta*, 242, 64–81. <https://doi.org/10.1016/j.gca.2018.09.007>
- Fleitmann, D., Burns, S. J., Mangini, A., Mudelsee, M., Kramers, J., Villa, I., Neff, U., Al-Subbary, A. A., Buettner, A., Hippler, D., & Matter, A. (2007). Holocene ITCZ and

Indian monsoon dynamics recorded in stalagmites from Oman and Yemen (Socotra).

Quaternary Science Reviews, 26(1–2), 170–188.

<https://doi.org/10.1016/j.quascirev.2006.04.012>

Fleitmann, D., Burns, S. J., Neff, U., Mudelsee, M., Mangini, A., & Matter, A. (2004).

Palaeoclimatic interpretation of high-resolution oxygen isotope profiles derived from annually laminated speleothems from Southern Oman. *Quaternary Science Reviews*,

23(7–8), 935–945. <https://doi.org/10.1016/j.quascirev.2003.06.019>

Fleitmann, D., Burns, S. J., Pekala, M., Mangini, A., Al-Subbary, A., Al-Aowah, M., Kramers,

J., & Matter, A. (2011). Holocene and Pleistocene pluvial periods in Yemen, southern Arabia. *Quaternary Science Reviews*, 30(7–8), 783–787.

<https://doi.org/10.1016/j.quascirev.2011.01.004>

Fratkin, E. (1997). Pastoralism: Governance and Development Issues. *Annual Review of*

Anthropology, 26(1), 235–261. <https://doi.org/10.1146/annurev.anthro.26.1.235>

Fretwell, S.D., Lucas, H.L. (1969). On territorial behavior and other factors influencing habitat distribution in birds. *Acta Biotheor* **19**, 16–36.

Friesen, J., Zink, M., Bawain, A., & Müller, T. (2018). Hydrometeorology of the Dhofar cloud

forest and its implications for groundwater recharge. *Journal of Hydrology: Regional Studies*, 16, 54–66. <https://doi.org/10.1016/j.ejrh.2018.03.002>

Galletti, C. S., Turner, B. L., & Myint, S. W. (2016). Land changes and their drivers in the

cloud forest and coastal zone of Dhofar, Oman, between 1988 and 2013. *Regional*

Environmental Change, 16(7), 2141–2153. <https://doi.org/10.1007/s10113-016-0942-2>

- Garba, R. (2019, May). Triliths, the stone monuments of Southern Arabia: preliminary results and path towards the interpretation. In *Proceedings of the Seminar for Arabian Studies* (Vol. 49, pp. 147-158).
- Gasse, F. (2000). Hydrological changes in the African tropics since the Last Glacial Maximum. *Quaternary Science Reviews*, 19(1–5), 189–211.
[https://doi.org/10.1016/S0277-3791\(99\)00061-X](https://doi.org/10.1016/S0277-3791(99)00061-X)
- Gasse, F., & Van Campo, E. (1994). Abrupt post-glacial climate events in West Asia and North Africa monsoon domains. *Earth and Planetary Science Letters*, 126(4), 435–456.
[https://doi.org/10.1016/0012-821X\(94\)90123-6](https://doi.org/10.1016/0012-821X(94)90123-6)
- Genet, M., Daniau, A.-L., Mouillot, F., Hanquiez, V., Schmidt, S., David, V., Georget, M., Abrantes, F., Anschutz, P., Bassinot, F., Bonnin, J., Dennielou, B., Eynaud, F., Hodell, D. A., Mulder, T., Naughton, F., Rossignol, L., Tzedakis, P., & Sánchez-Goñi, M. F. (2021). Modern relationships between microscopic charcoal in marine sediments and fire regimes on adjacent landmasses to refine the interpretation of marine paleofire records: An Iberian case study. *Quaternary Science Reviews*, 270, 107148.
<https://doi.org/10.1016/j.quascirev.2021.107148>
- Ghazanfar, S. A. (2004). Biology of the Central Desert of Oman. *Turkish Journal of Botany*, 28, 65-71.
- Ghazanfar, S. A. (1998). Status of the flora and plant conservation in the sultanate of Oman. *Biological Conservation*, 85(3), 287–295. [https://doi.org/10.1016/S0006-3207\(97\)00162-6](https://doi.org/10.1016/S0006-3207(97)00162-6)
- Ghazanfar, S. A. (1999). Coastal Vegetation of Oman. *Estuarine, Coastal and Shelf Science*, 49, 21–27. [https://doi.org/10.1016/S0272-7714\(99\)80004-3](https://doi.org/10.1016/S0272-7714(99)80004-3)

- Gillet, F. (2008). Modelling vegetation dynamics in heterogeneous pasture-woodland landscapes. *Ecological Modelling*, 217(1–2), 1–18.
<https://doi.org/10.1016/j.ecolmodel.2008.05.013>
- Gil-Romera, G., Lamb, H. F., Turton, D., Sevilla-Callejo, M., & Umer, M. (2010a). Long-term resilience, bush encroachment patterns and local knowledge in a Northeast African savanna. *Global Environmental Change*, 20(4), 612–626.
<https://doi.org/10.1016/j.gloenvcha.2010.04.008>
- Gil-Romera, G., Lamb, H. F., Turton, D., Sevilla-Callejo, M., & Umer, M. (2010b). Long-term resilience, bush encroachment patterns and local knowledge in a Northeast African savanna. *Global Environmental Change*, 20(4), 612–626.
<https://doi.org/10.1016/j.gloenvcha.2010.04.008>
- Griepentrog, M., De Wispelaere, L., Bauters, M., Bodé, S., Hemp, A., Verschuren, D., & Boeckx, P. (2019). Influence of plant growth form, habitat and season on leaf-wax n-alkane hydrogen-isotopic signatures in equatorial East Africa. *Geochimica et Cosmochimica Acta*, 263, 122–139. <https://doi.org/10.1016/j.gca.2019.08.004>
- Grigson, C., Gowlett, J. A. J., & Zarins, J. (1989). The Camel in Arabia—A direct radiocarbon date, calibrated to about 7000 BC. *Journal of Archaeological Science*, 16(4), 355–362.
[https://doi.org/10.1016/0305-4403\(89\)90011-3](https://doi.org/10.1016/0305-4403(89)90011-3)
- Grimm, E. C. (1987). CONISS: A FORTRAN 77 program for stratigraphically constrained cluster analysis by the method of incremental sum of squares. *Computers & Geosciences*, 13(1), 13–35. [https://doi.org/10.1016/0098-3004\(87\)90022-7](https://doi.org/10.1016/0098-3004(87)90022-7)
- Guinet, Ph., & Vassal, J. (1978). Hypotheses on the Differentiation of the Major Groups in the Genus *Acacia* (Leguminosae). *Kew Bulletin*, 32(3), 509. <https://doi.org/10.2307/4109653>

- Hardin, G. (1968). The tragedy of the commons: the population problem has no technical solution; it requires a fundamental extension in morality. *science*, *162*(3859), 1243-1248.
- Harrower, M. J., Senn, M. J., & McCorrison, J. (2014). Tombs, Triliths and Oases: Spatial Analysis of the Arabian Human Social Dynamics (AHSD) Project, Archaeological Survey 2009-2010. *Archaeological Survey*.
- Helbing, D. (Ed.). (2012). *Social Self-Organization: Agent-Based Simulations and Experiments to Study Emergent Social Behavior*. Springer Berlin Heidelberg.
<https://doi.org/10.1007/978-3-642-24004-1>
- Herrmann, N., Boom, A., Carr, A. S., Chase, B. M., West, A. G., Zabel, M., & Schefuß, E. (2017). Hydrogen isotope fractionation of leaf wax n-alkanes in southern African soils. *Organic Geochemistry*, *109*, 1–13. <https://doi.org/10.1016/j.orggeochem.2017.03.008>
- Hilbert, Y. H., Parton, A., Morley, M. W., Linnenlucke, L. P., Jacobs, Z., Clark-Balzan, L., Roberts, R. G., Galletti, C. S., Schwenninger, J.-L., & Rose, J. I. (2015). Terminal Pleistocene and Early Holocene archaeology and stratigraphy of the southern Nejd, Oman. *Quaternary International*, *382*, 250–263.
<https://doi.org/10.1016/j.quaint.2015.02.053>
- Hilbert, Y. H., Usik, V. I., Galletti, C. S., Morley, M. W., Parton, A., Clark-Balzan, L., Schwenninger, J.-L., Linnenlucke, L. P., Roberts, R. G., Jacobs, Z., & Rose, J. I. (2015). Archaeological evidence for indigenous human occupation of Southern Arabia at the Pleistocene/ Holocene transition: The case of al-Hatab in Dhofar, Southern Oman. *Paléorient*, *41*(2), 31–49. <https://doi.org/10.3406/paleo.2015.5674>

Hildebrandt, A., Al Aufi, M., Amerjeed, M., Shammass, M., & Eltahir, E. A. B. (2007).

Ecohydrology of a seasonal cloud forest in Dhofar: 1. Field experiment: Seasonal cloud forest, 1. *Water Resources Research*, 43(10). <https://doi.org/10.1029/2006WR005261>

Hoorn, C., & Cremaschi, M. (2004). Late Holocene palaeoenvironmental history of Khawr

Rawri and Khawr Al Balid (Dhofar, Sultanate of Oman). *Palaeogeography,*

Palaeoclimatology, Palaeoecology, 213(1–2), 1–36.

<https://doi.org/10.1016/j.palaeo.2004.03.014>

Hoover, D. L., Pfennigwerth, A. A., & Duniway, M. C. (2021). Drought resistance and

resilience: The role of soil moisture–plant interactions and legacies in a dryland

ecosystem. *Journal of Ecology*, 109(9), 3280–3294. <https://doi.org/10.1111/1365->

[2745.13681](https://doi.org/10.1111/1365-2745.13681)

Horisk, K. E., Ivory, S. J., McCorrison, J., McHale, M., Al Mehri, A., Anderson, A., ... & Al

Kathiri, A. A. (2023). Vegetation dynamics in Dhofar, Oman, from the Late Holocene to

present inferred from rock hyrax middens. *Quaternary Research*, 116, 12–29.

IPCC, 2022: *Climate Change 2022: Impacts, Adaptation, and Vulnerability*. Contribution of

Working Group II to the Sixth Assessment Report of the Intergovernmental Panel on

Climate Change [H.-O. Pörtner, D.C. Roberts, M. Tignor, E.S. Poloczanska, K.

Mintenbeck, A. Alegría, M. Craig, S. Langsdorf, S. Löschke, V. Möller, A. Okem, B.

Rama (eds.)]. Cambridge University Press. Cambridge University Press, Cambridge, UK

and New York, NY, USA, 3056 pp., doi:[10.1017/9781009325844](https://doi.org/10.1017/9781009325844).

Ivory, S. J., Cole, K. L., Anderson, R. S., Anderson, A., McCorrison, J., & Williams, J.

(2021). Human landscape modification and expansion of tropical woodland in southern

- Arabia during the mid-Holocene from rock hyrax middens. *Journal of Biogeography*, 48(10), 2588–2603. <https://doi.org/10.1111/jbi.14226>
- Ivory, S. J., & Lézine, A.-M. (2009). Climate and environmental change at the end of the Holocene Humid Period: A pollen record off Pakistan. *Comptes Rendus Geoscience*, 341(8–9), 760–769. <https://doi.org/10.1016/j.crte.2008.12.009>
- Kahmen, A., Hoffmann, B., Schefuß, E., Arndt, S. K., Cernusak, L. A., West, J. B., & Sachse, D. (2013). Leaf water deuterium enrichment shapes leaf wax n-alkane δD values of angiosperm plants II: Observational evidence and global implications. *Geochimica et Cosmochimica Acta*, 111, 50–63. <https://doi.org/10.1016/j.gca.2012.09.004>
- Kahmen, A., Wanek, W., & Buchmann, N. (2008). Foliar $\delta^{15}N$ values characterize soil N cycling and reflect nitrate or ammonium preference of plants along a temperate grassland gradient. *Oecologia*, 156(4), 861–870. <https://doi.org/10.1007/s00442-008-1028-8>
- Keeley, J. E., & Rundel, P. W. (2003). Evolution of CAM and C₄ Carbon-Concentrating Mechanisms. *International Journal of Plant Sciences*, 164(S3), S55–S77. <https://doi.org/10.1086/374192>
- Keeling, C. D. (1979). The Suess effect: ¹³Carbon- ¹⁴Carbon interrelations. *Environment International*, 2(4–6), 229–300. [https://doi.org/10.1016/0160-4120\(79\)90005-9](https://doi.org/10.1016/0160-4120(79)90005-9)
- Killops, S. D., & Killops, V. J. (2013). *Introduction to organic geochemistry*. John Wiley & Sons.
- Kröpelin, S., Verschuren, D., Lézine, A.-M., Eggermont, H., Cocquyt, C., Francus, P., Cazet, J.-P., Fagot, M., Rumes, B., Russell, J. M., Darius, F., Conley, D. J., Schuster, M., von Suchodoletz, H., & Engstrom, D. R. (2008). Climate-Driven Ecosystem Succession in the

Sahara: The Past 6000 Years. *Science*, 320(5877), 765–768.

<https://doi.org/10.1126/science.1154913>

Kwarteng, A. Y., Dorvlo, A. S., & Vijaya Kumar, G. T. (2009). Analysis of a 27-year rainfall data (1977-2003) in the Sultanate of Oman. *International Journal of Climatology*, 29, 605–617. <https://doi.org/DOI: 10.1002/joc.1727>

Laland, K., Matthews, B., & Feldman, M. W. (2016). An introduction to niche construction theory. *Evolutionary Ecology*, 30(2), 191–202. <https://doi.org/10.1007/s10682-016-9821-z>

Laland, K. N., & O'Brien, M. J. (2010). Niche Construction Theory and Archaeology. *Journal of Archaeological Method and Theory*, 17(4), 303–322. <https://doi.org/10.1007/s10816-010-9096-6>

Lézine, A.-M., Bassinot, F., & Peterschmitt, J.-Y. (2014). Orbitally-induced changes of the Atlantic and Indian monsoons over the past 20,000 years: New insights based on the comparison of continental and marine records. *Bulletin de La Société Géologique de France*, 185(1), 3–12. <https://doi.org/10.2113/gssgfbull.185.1.3>

Lézine, A.-M., Ivory, S. J., Braconnot, P., & Marti, O. (2017). Timing of the southward retreat of the ITCZ at the end of the Holocene Humid Period in Southern Arabia: Data-model comparison. *Quaternary Science Reviews*, 164, 68–76. <https://doi.org/10.1016/j.quascirev.2017.03.019>

Lézine, A.-M., Robert, C., Cleuziou, S., Inizan, M.-L., Braemer, F., Saliège, J.-F., Sylvestre, F., Tiercelin, J.-J., Crassard, R., Méry, S., Charpentier, V., & Steimer-Herbet, T. (2010). Climate change and human occupation in the Southern Arabian lowlands during the last

deglaciation and the Holocene. *Global and Planetary Change*, 72(4), 412–428.

<https://doi.org/10.1016/j.gloplacha.2010.01.016>

Lézine, A.-M., Saliège, J.-F., Mathieu, R., Tagliatela, T.-L., Mery, S., Charpentier, V., & Cleuziou, S. (2002). Mangroves of Oman during the late Holocene; climatic implications and impact on human settlements. *Vegetation History and Archaeobotany*, 11(3), 221–232. <https://doi.org/10.1007/s003340200025>

Lézine, A.-M., Saliège, J.-F., Robert, C., Wertz, F., & Inizan, M.-L. (1998). Holocene Lakes from Ramlat as-Sab'atayn (Yemen) Illustrate the Impact of Monsoon Activity in Southern Arabia. *Quaternary Research*, 50(3), 290–299.

<https://doi.org/10.1006/qres.1998.1996>

Lézine, A.-M., Tiercelin, Jean.-J., Robert, C., Saliège, J.-F., Cleuziou, S., Inizan, M.-L., & Braemer, F. (2007). Centennial to millennial-scale variability of the Indian monsoon during the early Holocene from a sediment, pollen and isotope record from the desert of Yemen. *Palaeogeography, Palaeoclimatology, Palaeoecology*, 243(3–4), 235–249.

<https://doi.org/10.1016/j.palaeo.2006.05.019>

Lippi, M. M., Gonnelli, T., & Raffaelli, M. (2007). Pollen morphology of trees, shrubs and woody herbs of the coastal plain and the monsoon slopes of Dhofar (Sultanate of Oman). *Webbia*, 62(2), 245–260. <https://doi.org/10.1080/00837792.2007.10670826>

Liu, J., & An, Z. (2020). Leaf wax *n*-alkane carbon isotope values vary among major terrestrial plant groups: Different responses to precipitation amount and temperature, and implications for paleoenvironmental reconstruction. *Earth-Science Reviews*, 202, 103081.

<https://doi.org/10.1016/j.earscirev.2020.103081>

- Liu, W., & Yang, H. (2008). Multiple controls for the variability of hydrogen isotopic compositions in higher plant *n*-alkanes from modern ecosystems: Variability of hydrogen isotopic compositions. *Global Change Biology*, *14*(9), 2166–2177. <https://doi.org/10.1111/j.1365-2486.2008.01608.x>
- Maestre, F. T., Eldridge, D. J., Soliveres, S., Kéfi, S., Delgado-Baquerizo, M., Bowker, M. A., García-Palacios, P., Gaitán, J., Gallardo, A., Lázaro, R., & Berdugo, M. (2016). Structure and Functioning of Dryland Ecosystems in a Changing World. *Annual Review of Ecology, Evolution, and Systematics*, *47*(1), 215–237. <https://doi.org/10.1146/annurev-ecolsys-121415-032311>
- Maestre, F. T., Salguero-Gómez, R., & Quero, J. L. (2012). It is getting hotter in here: Determining and projecting the impacts of global environmental change on drylands. *Philosophical Transactions of the Royal Society B: Biological Sciences*, *367*(1606), 3062–3075. <https://doi.org/10.1098/rstb.2011.0323>
- Magliano, P. N., Whitworth-Hulse, J. I., Cid, F. D., Leporati, J. L., Van Stan, J. T., & Jobbágy, E. G. (2022). Global rainfall partitioning by dryland vegetation: Developing general empirical models. *Journal of Hydrology*, *607*, 127540. <https://doi.org/10.1016/j.jhydrol.2022.127540>
- Majdi, F., Hosseini, S. A., Karbalaee, A., Kaseri, M., & Marjanian, S. (2022). Future projection of precipitation and temperature changes in the Middle East and North Africa (MENA) region based on CMIP6. *Theoretical and Applied Climatology*, *147*(3–4), 1249–1262. <https://doi.org/10.1007/s00704-021-03916-2>

- Martin, L. (2020). The Kheshiya Cattle Skull Ring. In *Landscape History of Hadramawt, The Roots of Agriculture in Southern Arabia (RASA) Project 1998-2008* (pp. 274–348). UCLA Cotsen Institute of Archaeology Press.
- Martin, L., McCorrison, J., & Crassard, R. (2009, January). Early Arabian pastoralism at Manayzah in Wādī Ṣanā, Ḥaḍramawt. In *Proceedings of the Seminar for Arabian Studies* (pp. 271-282). Archaeopress.
- McClure, H. A. (1976). Radiocarbon chronology of late Quaternary lakes in the Arabian Desert. *Nature*, 263(5580), 755–756. <https://doi.org/10.1038/263755a0>
- McCorrison, J., Buffington, A., Olson, K., Martin, L., Abuazizeh, W., Everhart, T., Al Maashani, A., Al Kathiri, A. A., & Al Mehri, A. (2020). Ancient Pastoral Settlement in The Dhofar Mountains: Archaeological Excavations at Shakil and Halqoot. *Journal of Oman Studies*, 21, 152–171.
- McCorrison, J., & Harrower, M. J. (Eds.). (2020). *Landscape history of Hadramawt: The Roots of Agriculture in Southern Arabia (RASA) Project 1998-2008*. UCLA, Cotsen Institute of Archaeology Press.
- McCorrison, J., Harrower, M., Steimer, T., Williams, K. D., & Senn, M. (2014). *Monuments and Landscape of Mobile Pastoralists in Dhofar: The Arabian Human Social Dynamics (AHSD) Project, 2009-201*.
- McCorrison, J., Moritz, M., Buffington, A., Pustovoytov, K., Ivory, S. J., & Abuazizeh, W. (2018). Constructing the South Arabian Pastoral Landscape. In *From Refugia to Oases. Acts of the 38th Rencontres Internationales d'Archéologie et d'Histoire d'Antibes* (Antibes: Éditions ADPCA, pp. 119–133).

- McCorriston, J., Oches, E. A., Walter, D. E., & Cole, K. L. (2002). Holocene Paleoecology and Prehistory in Highland Southern Arabia. *Paléorient*, 28(1), 61–88.
<https://doi.org/10.3406/paleo.2002.4739>
- Miller, A. G., & Morris, M. (1988). *Plants of Dhofar, The Southern Region of Oman: Traditional, Economic, and Medicinal Uses*. Office of the Adviser for Conservation of the Environment, Diwan of Royal Court, Sultanate of Oman.
- Moritz, M., Hamilton, I. M., Yoak, A. J., Scholte, P., Cronley, J., Maddock, P., & Pi, H. (2015). Simple movement rules result in ideal free distribution of mobile pastoralists. *Ecological Modelling*, 305, 54–63. <https://doi.org/10.1016/j.ecolmodel.2015.03.010>
- Moritz, M., Soma, E., Scholte, P., Xiao, N., Taylor, L., Juran, T., & Kari, S. (2010). An Integrated Approach to Modeling Grazing Pressure in Pastoral Systems: The Case of the Logone Floodplain (Cameroon). *Human Ecology*, 38(6), 775–789.
<https://doi.org/10.1007/s10745-010-9361-z>
- Morrill, C., Overpeck, J. T., & Cole, J. E. (2003). A synthesis of abrupt changes in the Asian summer monsoon since the last deglaciation. *The Holocene*, 13(4), 465–476.
<https://doi.org/10.1191/0959683603hl639ft>
- Nettle, D., Gibson, M. A., Lawson, D. W., & Sear, R. (2013). Human behavioral ecology: Current research and future prospects. *Behavioral Ecology*, 24(5), 1031–1040.
<https://doi.org/10.1093/beheco/ars222>
- Newton, L. S., & Zarins, J. (2010). Preliminary results of the Dhofar archaeological survey. *Proceedings of the Seminar for Arabian Studies*, 40, 247–265.
- Nicholson, S. E. (2011). *Dryland Climatology* (1st ed.). Cambridge University Press.
<https://doi.org/10.1017/CBO9780511973840>

- Nicholson, S. E. (2015). Evolution and current state of our understanding of the role played in the climate system by land surface processes in semi-arid regions. *Global and Planetary Change*, 133, 201–222. <https://doi.org/10.1016/j.gloplacha.2015.08.010>
- Nicholson, S. E. (2018). The ITCZ and the Seasonal Cycle over Equatorial Africa. *Bulletin of the American Meteorological Society*, 99(2), 337-348.
- Oberprieler, C., Meister, J., Schneider, C., & Kilian, N. (2009). Genetic structure of *Anogeissus dhofarica* (Combretaceae) populations endemic to the monsoonal fog oases of the southern Arabian Peninsula: Genetic structure of *A. dhofarica* (Combretaceae). *Biological Journal of the Linnean Society*, 97(1), 40–51. <https://doi.org/10.1111/j.1095-8312.2008.01173.x>
- Odling-Smee, J., Erwin, D. H., Palkovacs, E. P., Feldman, M. W., & Laland, K. N. (2013). Niche Construction Theory: A Practical Guide for Ecologists. *The Quarterly Review of Biology*, 88(1), 3–28. <https://doi.org/10.1086/669266>
- Odling-Smee, J., & Laland, K. N. (2011). Ecological Inheritance and Cultural Inheritance: What Are They and How Do They Differ? *Biological Theory*, 6(3), 220–230. <https://doi.org/10.1007/s13752-012-0030-x>
- Odum, E. P. (1969). The Strategy of Ecosystem Development. *American Association for the Advancement of Science*, 164(No. 3877), 262–270.
- Parker, A. G., Goudie, A. S., Stokes, S., White, K., Hodson, M. J., Manning, M., & Kennet, D. (2006). A Record of Holocene Climate Change from Lake Geochemical Analyses in Southeastern Arabia. *Quaternary Research*, 66(3), 465–476. <https://doi.org/10.1016/j.yqres.2006.07.001>

- Parker, A. G., & Rose, J. I. (2008, January). Climate change and human origins in southern Arabia. In *Proceedings of the seminar for Arabian studies* (pp. 25-42). Archaeopress.
- Patzelt, A. (2015). Synopsis of the flora and vegetation of Oman, with special emphasis on patterns of plant endemism. *Abhandlungen der Braunschweigischen Wissenschaftlichen Gesellschaft*, 282, 317.
- Peng, C. (2000). From static biogeographical model to dynamic global vegetation model: A global perspective on modelling vegetation dynamics. *Ecological Modelling*, 135(1), 33–54. [https://doi.org/10.1016/S0304-3800\(00\)00348-3](https://doi.org/10.1016/S0304-3800(00)00348-3)
- Peters, D. P., Havstad, K. M., Archer, S. R., & Sala, O. E. (2015). Beyond desertification: New paradigms for dryland landscapes. *Frontiers in Ecology and the Environment*, 13(1), 4–12. <https://doi.org/10.1890/140276>
- Polissar, P. J., & D'Andrea, W. J. (2014). Uncertainty in paleohydrologic reconstructions from molecular δD values. *Geochimica et Cosmochimica Acta*, 129, 146–156. <https://doi.org/10.1016/j.gca.2013.12.021>
- Polissar, P. J., & Freeman, K. H. (2010). Effects of aridity and vegetation on plant-wax δD in modern lake sediments. *Geochimica et Cosmochimica Acta*, 74(20), 5785–5797. <https://doi.org/10.1016/j.gca.2010.06.018>
- Pour, M. J., Mohadjer, M. R. M., Etemad, V., & Zobeiri, M. (2012). Effects of grazing on natural regeneration of tree and herb species of Kheyroud forest in northern Iran. *Journal of Forestry Research*, 23(2), 299–304. <https://doi.org/10.1007/s11676-012-0256-2>
- Racsko, P., Szeidl, L., & Semenov, M. (1991). A serial approach to local stochastic weather models. *Ecological Modelling*, 57(1–2), 27–41. [https://doi.org/10.1016/0304-3800\(91\)90053-4](https://doi.org/10.1016/0304-3800(91)90053-4)

- Raffaelli, M., & Tardelli, M. (n.d.). *Phytogeographic zones of Dhofar (Southern Oman)*. 7.
- Ramadan, E., Al-Awadhi, T., & Charabi, Y. (2021). Land Cover/ Land Use Change and Climate Change in Dhofar Governorate, Oman. *International Journal of Geoinformatics*, 41–47. <https://doi.org/10.52939/ijg.v17i4.1949>
- Rao, Z., Guo, W., Cao, J., Shi, F., Jiang, H., & Li, C. (2017). Relationship between the stable carbon isotopic composition of modern plants and surface soils and climate: A global review. *Earth-Science Reviews*, 165, 110–119. <https://doi.org/10.1016/j.earscirev.2016.12.007>
- Ravi, S., Breshears, D. D., Huxman, T. E., & D’Odorico, P. (2010). Land degradation in drylands: Interactions among hydrologic–aeolian erosion and vegetation dynamics. *Geomorphology*, 116(3–4), 236–245. <https://doi.org/10.1016/j.geomorph.2009.11.023>
- Rbsamen, K., & Hume, D. (n.d.). *PHYSIOLOGY OF THE ROCK HYRAX*. 7.
- Reimer, P. J., Austin, W. E. N., Bard, E., Bayliss, A., Blackwell, P. G., Bronk Ramsey, C., Butzin, M., Cheng, H., Edwards, R. L., Friedrich, M., Grootes, P. M., Guilderson, T. P., Hajdas, I., Heaton, T. J., Hogg, A. G., Hughen, K. A., Kromer, B., Manning, S. W., Muscheler, R., ... Talamo, S. (2020). The IntCal20 Northern Hemisphere Radiocarbon Age Calibration Curve (0–55 cal kBP). *Radiocarbon*, 62(4), 725–757. <https://doi.org/10.1017/RDC.2020.41>
- Renssen, H., Brovkin, V., Fichefet, T., & Goosse, H. (2003). Holocene climate instability during the termination of the African Humid Period. *Geophysical Research Letters*, 30(4), 2002GL016636. <https://doi.org/10.1029/2002GL016636>
- Reynolds, J. F., Smith, D. M. S., Lambin, E. F., Turner, B. L., Mortimore, M., Batterbury, S. P. J., Downing, T. E., Dowlatabadi, H., Fernández, R. J., Herrick, J. E., Huber-Sannwald,

- E., Jiang, H., Leemans, R., Lynam, T., Maestre, F. T., Ayarza, M., & Walker, B. (2007). Global Desertification: Building a Science for Dryland Development. *Science*, 316(5826), 847–851. <https://doi.org/10.1126/science.1131634>
- Rodriguez-Lopez, J. M., Schickhoff, M., Sengupta, S., & Scheffran, J. (2021). Technological and social networks of a pastoralist artificial society: Agent-based modeling of mobility patterns. *Journal of Computational Social Science*, 4(2), 681–707. <https://doi.org/10.1007/s42001-020-00100-w>
- Romanowska, I., Wren, C. D., & Crabtree, S. A. (2021). *Agent-based modeling for archaeology: Simulating the complexity of societies*. SFI Press.
- Rozanski, K., Araguás-Araguás, L., & Gonfiantini, R. (2013). Isotopic Patterns in Modern Global Precipitation. In P. K. Swart, K. C. Lohmann, J. Mckenzie, & S. Savin (Eds.), *Geophysical Monograph Series* (pp. 1–36). American Geophysical Union. <https://doi.org/10.1029/GM078p0001>
- Rübsamen, K., & Hume, D. (1981). Physiology of the Rock Hyax. *Comp. Biochem. Physiol.*, 72A, 271–277.
- Runge, J., Gosling, W. D., Lézine, A.-M., & Scott, L. (2021). *Quaternary Vegetation Dynamics – The African Pollen Database: The African Pollen Database* (1st ed.). CRC Press. <https://doi.org/10.1201/9781003162766>
- Sachse, D., Billault, I., Bowen, G. J., Chikaraishi, Y., Dawson, T. E., Feakins, S. J., Freeman, K. H., Magill, C. R., McInerney, F. A., van der Meer, M. T. J., Polissar, P., Robins, R. J., Sachs, J. P., Schmidt, H.-L., Sessions, A. L., White, J. W. C., West, J. B., & Kahmen, A. (2012). Molecular Paleohydrology: Interpreting the Hydrogen-Isotopic Composition of Lipid Biomarkers from Photosynthesizing Organisms. *Annual Review of Earth and*

- Planetary Sciences*, 40(1), 221–249. <https://doi.org/10.1146/annurev-earth-042711-105535>
- Sage, R. F. (2004). The evolution of C₄ photosynthesis. *New Phytologist*, 161(2), 341–370. <https://doi.org/10.1111/j.1469-8137.2004.00974.x>
- Sale, J. B. (1965). THE FEEDING BEHAVIOUR OF BOCK HYRACES (genera PROCAVIA and HETEROHYRAX) IN KENYA. *African Journal of Ecology*, 3(1), 1–18. <https://doi.org/10.1111/j.1365-2028.1965.tb00733.x>
- Sayre, N. F., deBuys, W., Bestelmeyer, B. T., & Havstad, K. M. (2012). “The Range Problem” After a Century of Rangeland Science: New Research Themes for Altered Landscapes. *Rangeland Ecology & Management*, 65(6), 545–552. <https://doi.org/10.2111/REM-D-11-00113.1>
- Schulz', E., & Whitney', J. W. (n.d.). *Upper Pleistocene and Holocene lakes in the An Nafud, Saudi Arabia*. 16.
- Scott, L. (1996). Palynology of hyrax middens: 2000 years of palaeoenvironmental history in Namibia. *Quaternary International*, 33, 73–79. [https://doi.org/10.1016/1040-6182\(95\)00093-3](https://doi.org/10.1016/1040-6182(95)00093-3)
- Scott, L., & Cooremans, B. (1992). Pollen in Recent Procavia (Hyrax), Petromus (Dassie Rat) and Bird Dung in South Africa. *Journal of Biogeography*, 19(2), 205. <https://doi.org/10.2307/2845506>
- Scott, L., & Woodborne, S. (2007). Vegetation history inferred from pollen in Late Quaternary faecal deposits (hyraceum) in the Cape winter-rain region and its bearing on past climates in South Africa. *Quaternary Science Reviews*, 26(7-8), 941-953.

- Sessions, A. L., & Hayes, J. M. (2005). Calculation of hydrogen isotopic fractionations in biogeochemical systems. *Geochimica et Cosmochimica Acta*, 69(3), 593–597. <https://doi.org/10.1016/j.gca.2004.08.005>
- Shipley, L. A. (1999). Grazers and browsers: how digestive morphology affects diet selection. *Grazing behavior of livestock and wildlife*, 70, 20-27.
- Smith, F. A., & Freeman, K. H. (2006). Influence of physiology and climate on δD of leaf wax n-alkanes from C3 and C4 grasses. *Geochimica et Cosmochimica Acta*, 70(5), 1172–1187. <https://doi.org/10.1016/j.gca.2005.11.006>
- Smith, F., Wing, S., & Freeman, K. (2007). Magnitude of the carbon isotope excursion at the Paleocene–Eocene thermal maximum: The role of plant community change. *Earth and Planetary Science Letters*, 262(1–2), 50–65. <https://doi.org/10.1016/j.epsl.2007.07.021>
- Staubwasser, M., Sirocko, F., Grootes, P. M., & Erlenkeuser, H. (2002). South Asian monsoon climate change and radiocarbon in the Arabian Sea during early and middle Holocene. *Paleoceanography*, 17(4). <https://doi.org/10.1029/2000PA000608>
- Stavi, I., Roque de Pinho, J., Paschalidou, A. K., Adamo, S. B., Galvin, K., de Sherbinin, A., Even, T., Heaviside, C., & van der Geest, K. (2022). Food security among dryland pastoralists and agropastoralists: The climate, land-use change, and population dynamics nexus. *The Anthropocene Review*, 9(3), 299–323. <https://doi.org/10.1177/20530196211007512>
- Steimer-Herbet, T. (2022). Megalithism in the Middle East. In *Megaliths in the World* (pp. 921–934). Archaeopress.
- Strauch, G., Al-Mashaikhi, K. S., Bawain, A., Knöller, K., Friesen, J., & Müller, T. (2014). Stable H and O isotope variations reveal sources of recharge in Dhofar, Sultanate of

Oman. *Isotopes in Environmental and Health Studies*, 50(4), 475–490.

<https://doi.org/10.1080/10256016.2014.961451>

Strengers, B. J., Müller, C., Schaeffer, M., Haarsma, R. J., Severijns, C., Gerten, D., Schaphoff, S., van den Houdt, R., & Oostenrijk, R. (2010). Assessing 20th century climate-vegetation feedbacks of land-use change and natural vegetation dynamics in a fully coupled vegetation-climate model. *International Journal of Climatology*, 30(13), 2055–2065. <https://doi.org/10.1002/joc.2132>

ter Braak, C. J. F. (1985). Correspondence Analysis of Incidence and Abundance Data: Properties in Terms of a Unimodal Response Model. *Biometrics*, 41(4), 859.

<https://doi.org/10.2307/2530959>

Tipple, B. J., Berke, M. A., Doman, C. E., Khachatryan, S., & Ehleringer, J. R. (2013). Leaf-wax *n*-alkanes record the plant–water environment at leaf flush. *Proceedings of the National Academy of Sciences*, 110(7), 2659–2664.

<https://doi.org/10.1073/pnas.1213875110>

van Dam, K. H., Nikolic, I., & Lukszo, Z. (Eds.). (2013). *Agent-Based Modelling of Socio-Technical Systems*. Springer Netherlands. <https://doi.org/10.1007/978-94-007-4933-7>

Vincens, A., Lézine, A.-M., Buchet, G., Lewden, D., & Le Thomas, A. (2007). African pollen database inventory of tree and shrub pollen types. *Review of Palaeobotany and Palynology*, 145(1–2), 135–141. <https://doi.org/10.1016/j.revpalbo.2006.09.004>

Vuorio, V., Muchiru, A., Reid, R. S., & Ogutu, J. O. (2014). How pastoralism changes savanna vegetation: Impact of old pastoral settlements on plant diversity and abundance in south-western Kenya. *Biodiversity and conservation*, 23, 3219–3240.

- Walker, B. H., & Janssen, M. A. (2002). Rangelands, pastoralists and governments: Interlinked systems of people and nature. *Philosophical Transactions of the Royal Society of London. Series B: Biological Sciences*, 357(1421), 719–725.
<https://doi.org/10.1098/rstb.2001.0984>
- Wang, C., Wang, X., Liu, D., Wu, H., Lü, X., Fang, Y., Cheng, W., Luo, W., Jiang, P., Shi, J., Yin, H., Zhou, J., Han, X., & Bai, E. (2014). Aridity threshold in controlling ecosystem nitrogen cycling in arid and semi-arid grasslands. *Nature Communications*, 5(1), 4799.
<https://doi.org/10.1038/ncomms5799>
- Wang, X.-P., Wang, Z.-N., Berndtsson, R., Zhang, Y.-F., & Pan, Y.-X. (2010). *Stemflow of desert shrub and its significance in soil moisture replenishment* [Preprint].
 Ecohydrology/Instruments and observation techniques. <https://doi.org/10.5194/hessd-7-5213-2010>
- Warren, A. (1995). Changing Understandings of African Pastoralism and the Nature of Environmental Paradigms. *Transactions of the Institute of British Geographers*, 20(2), 193. <https://doi.org/10.2307/622431>
- Weyhenmeyer, C. E., Burns, S. J., Waber, H. N., Macumber, P. G., & Matter, A. (2002). Isotope study of moisture sources, recharge areas, and groundwater flow paths within the eastern Batinah coastal plain, Sultanate of Oman: ISOTOPE STUDY OF GROUNDWATER MOVEMENT IN OMAN. *Water Resources Research*, 38(10), 2-1-2-22. <https://doi.org/10.1029/2000WR000149>
- Williams, C. A., & Albertson, J. D. (2006). Dynamical effects of the statistical structure of annual rainfall on dryland vegetation: Dryland system response to rainfall structure.

Global Change Biology, 12(5), 777–792. [https://doi.org/10.1111/j.1365-](https://doi.org/10.1111/j.1365-2486.2006.01111.x)

[2486.2006.01111.x](https://doi.org/10.1111/j.1365-2486.2006.01111.x)

Williams, J. W., & Jackson, S. T. (2007). Novel climates, no-analog communities, and ecological surprises. *Frontiers in Ecology and the Environment*, 5(9), 475–482.

<https://doi.org/10.1890/070037>

Yule, P. (2004). Proceedings of the Seminar for Arabian Studies. *Journal of the American Oriental Society*, 124(2), 408. <https://doi.org/10.2307/4132263>

Zarins, J. (2009). The Latest on the Archaeology of Southern Oman. *American Oriental Society*, 129, 665–674.

Zarins, J. (2013). Hailat Araka and the South Arabian Neolithic. *Arabian Archaeology and Epigraphy*, 24(1), 109–117. <https://doi.org/10.1111/aae.12009>

Zerboni, A., Perego, A., Mariani, G. S., Brandolini, F., Al Kindi, M., Regattieri, E., Zanchetta, G., Borgi, F., Charpentier, V., & Cremaschi, M. (2020). Geomorphology of the Jebel Qara and coastal plain of Salalah (Dhofar, southern Sultanate of Oman). *Journal of Maps*, 16(2), 187–198. <https://doi.org/10.1080/17445647.2019.1708488>

Zhou, S., Williams, A. P., Lintner, B. R., Berg, A. M., Zhang, Y., Keenan, T. F., Cook, B. I., Hagemann, S., Seneviratne, S. I., & Gentine, P. (2021). Soil moisture–atmosphere feedbacks mitigate declining water availability in drylands. *Nature Climate Change*, 11(1), 38–44. <https://doi.org/10.1038/s41558-020-00945-z>

Appendix A
Hyrax Midden Pollen Count Data

Modern Hyrax Midden Pollen

Sample ID	region	veg region	lat	lon
WP19	base escarpment	coastal plain/escarpment	17°12.804'	55°03.446'
WP18	base escarpment	coastal plain/escarpment	17°12.854'	55°03.761'
C1 Camel	escarpment	escarpment	17°4.655	54°27.068'E
C2 Camel	escarpment	escarpment	17°4.655	54°27.068'E
136-1	Wadi Ayoon	distal plateau	17°14.612'N	53°53.365'E
135-2	Wadi Ayoon	distal plateau	17°14.618'N	53°53.380'E
135-1	Wadi Ayoon	distal plateau	17°14.618'N	53°53.380'E
135-3	Wadi Ayoon	distal plateau	17°14.618'N	53°53.380'E
WP79-2c	Wadi Ghadun	Nejd - west	17°20.987'	53°42.938'

WP83-1	Wadi Ghadun	Nejd - west	17°24.138'	53°41.690'
WP61-1	Wadi Dhahabun	Nejd - east	17°24.865'	54°20.822'
WP61-2	Wadi Dhahabun	Nejd - east	17°24.865'	54°20.822'
WP48-1B	Wadi Dhahabun	Nejd - east	17°25.431'	54°29.385'
108-1b	Wadi Dhahabun	Nejd - east	17°23.123'N	54°29.767'E
WP57-4	Wadi Dhahabun	Nejd - east	17°23.210'	54°20.848'
107-2b	Wadi Dhahabun	Nejd - east	17°23.110'N	54°29.755'E
WP45-2	Wadi Dhahabun	Nejd - east	17°25.454'	54°29.296'

Pollen Habit	A	A	A	N
Date	<i>Terminalia dhofarica</i>	<i>Olea europaea</i> - type ssp <i>africana</i>	Cyperaceae undiff.	<i>Flacourtia</i>
modern (no date)	0	0	3	0
modern (no date)	2	0	15	0
none	38	0	1	0
none	6	0	5	0
modern (no date)	2	1	4	0
modern (no date)	0	0	10	0
modern (no date)	0	1	5	0
modern (no date)	3	0	8	1
modern	2	0	18	0
modern	0	0	29	0
modern	0	0	19	0
modern	5	0	3	0
modern	0	0	12	0
110	0	1	3	0
130	4	0	3	0
140	0	1	3	0
160	18	0	3	0

A	I	A	I	A
Poaceae undiff.	<i>Ziziphus</i> -type	<i>Euphorbia</i> -type	<i>Salvadora persica</i>	<i>Artemisia</i>
50	0	0	3	5
56	2	2	0	2
220	1	0	0	0
143	0	0	0	0
14	10	2	43	3
34	6	1	41	2
11	4	2	79	1
54	3	0	53	0
54	41	1	34	8
5	10	0	81	3
26	9	0	0	2
7	12	0	6	1
47	2	0	7	5
32	7	1	14	3
49	2	0	22	6
7	0	0	2	0

I	A	AL	AL	A
<i>Pinus</i>	<i>Senegalia</i> Group I	<i>Senegalia</i> Group III	<i>Commiphora</i>	<i>Ficus</i>
8	5	19	5	3
0	2	22	5	27
0	0	1	0	7
0	0	0	0	2
1	3	37	0	13
0	2	15	1	7
0	0	20	0	7
0	2	17	0	9
0	0	31	0	1
1	1	25	0	86
0	7	21	0	2
0	0	9	0	3
0	7	37	9	0
0	0	24	2	66
0	1	17	2	1
2	0	10	0	6
0	8	20	3	0

A	N	A	Ap	I
<i>Tribulus terrestris</i> -type	<i>Dodonaea viscosa</i> -type	<i>Tapinanthus</i> -type	<i>Dracaena?</i>	<i>Fagonia</i>
3	0	0	180	0
0	2	0	10	0
0	0	0	0	0
0	1	0	1	0
2	21	18	0	0
2	29	10	0	0
0	28	8	0	0
3	23	12	0	0
4	3	0	0	0
0	0	5	0	0
0	0	0	0	0
0	1	0	0	1
5	0	0	0	0
0	1	0	0	1
0	3	6	0	0
0	0	0	0	0
2	0	0	0	3

I	N	N	N	A
<i>Suaeda</i>	<i>Kohautia</i>	<i>Cornulaca/Aerva</i>	<i>Celtis africana</i> -type	<i>Solanum</i> -type
0	0	3	0	0
0	2	0	0	2
15	0	1	0	0
17	0	0	0	1
3	1	3	0	0
1	2	0	0	0
4	5	6	0	1
12	0	13	4	0
4	12	16	0	0
3	10	2	0	0
21	118	5	0	0
14	0	1	0	0
5	2	16	0	0
1	2	14	0	0
12	15	14	0	0
0	0	1	0	0
13	3	26	0	0

I	I	N	I	I
<i>Zygophyllum</i>	<i>Justicia</i> -type	<i>Cassia</i> -type	Asteraceae undiff.	<i>Vernonia perrottetii</i> -type
0	3	0	3	3
0	0	0	27	7
0	4	0	3	2
0	0	0	7	2
1	0	1	8	5
7	0	0	6	5
4	0	0	7	2
1	0	0	8	1
5	0	1	6	2
4	0	2	4	0
0	0	0	5	7
7	0	1	0	1
0	0	19	12	2
1	0	0	6	0
4	0	5	10	3
0	0	2	2	0
2	0	0	5	2

N	I	A	A	N
<i>Pavonia</i>	<i>Tamarix</i>	<i>Maerua-type crassifolia</i>	<i>Celosia-type</i>	<i>Boswellia sacra</i>
0	0	0	5	0
0	5	0	7	2
0	0	0	0	0
1	0	0	2	4
0	2	0	0	15
0	0	7	1	49
0	6	3	0	6
0	0	2	1	14
0	5	10	7	0
0	2	16	6	0
0	0	0	0	0
0	1	1	11	0
0	5	0	2	0
0	5	5	0	6
0	1	2	4	1
0	1	1	0	3
0	3	0	0	2

A	I	N	I	I
Fabaceae undiff.	<i>Corchorus</i> -type	<i>Hypoestes</i> -type	<i>Abutilon</i>	<i>Indigofera</i>
0	0	0	0	0
0	0	0	0	0
0	1	0	4	0
0	5	0	0	0
6	2	0	0	1
0	0	0	0	4
6	0	0	0	13
1	0	0	0	0
1	0	0	0	2
0	0	0	0	0
0	0	0	0	0
0	0	0	0	0
0	0	0	0	0
0	0	0	0	0
3	0	0	0	1
0	0	0	0	1
1	0	0	0	0
0	0	0	0	0

I	N	N	NL	A
<i>Polycarpon</i> -type (<i>Reseda</i>)	<i>Boerhavia</i> -type	<i>Merremia/Convolvulus</i>	<i>Maytenus</i>	<i>Cleome</i> -type
3	0	0	0	0
17	0	0	2	2
0	0	3	0	2
0	1	8	0	2
0	0	2	1	3
0	0	1	2	13
3	0	2	1	8
0	0	2	0	17
0	0	1	0	2
1	0	1	0	9
67	0	0	0	0
225	0	1	0	0
77	0	2	0	0
0	0	0	7	1
80	0	2	1	1
0	0	0	0	3
65	0	1	0	2

N	A	AL	I	I
<i>Cadaba</i> -type	<i>Ephedra</i>	<i>Acalypha</i>	<i>Heliotropium</i>	<i>Blepharis</i> -type
0	0	0	3	0
0	0	2	5	0
0	0	0	0	0
0	0	0	0	0
1	1	0	11	0
0	0	0	12	0
4	0	0	6	0
1	0	0	8	0
0	0	0	2	0
1	0	0	2	0
0	0	0	0	0
1	0	0	2	1
0	0	0	28	0
5	0	1	8	1
0	0	0	3	0
0	0	0	1	0
2	3	0	37	0

N	I	I	NG	L
<i>Mimosa</i>	<i>Polygala</i> -type	<i>Ricinus communis</i>	<i>Cocculus pendulus</i> -type	<i>Capparis</i>
0	0	0	0	0
0	0	0	0	2
0	0	0	0	1
0	0	0	1	0
0	0	2	48	0
0	0	1	2	5
0	0	1	26	0
0	0	2	21	1
0	0	0	0	6
0	0	0	0	0
0	0	0	0	0
0	0	0	0	2
0	0	0	0	2
0	1	0	17	15
0	0	0	0	5
0	0	0	3	0
0	0	0	0	3

AL	N	N	N	N
<i>Pupalia</i> -type	<i>Striga</i> -type	<i>Scoparia</i> -type dulcis	<i>Salsola</i>	Amaranthaceae undiff.
0	0	0	0	0
0	0	0	0	0
0	2	2	4	0
0	0	0	0	0
0	0	0	0	0
0	0	0	0	0
0	0	0	0	0
0	0	0	0	0
0	0	0	0	0
0	0	0	1	0
0	0	0	0	0
0	0	0	0	0
0	0	0	0	0
0	0	0	0	0
0	0	0	0	0
1	0	0	0	0
0	0	0	0	0
0	0	0	0	0

I	A	A	A	Nq
<i>Mallotus</i> -type	<i>Boscia</i> -type <i>arabica</i>	<i>Ixora</i> -type	<i>Typha</i>	<i>Limonium</i> -type
0	0	0	0	0
0	7	0	53	0
0	0	0	0	0
0	0	0	0	0
0	0	0	1	0
0	0	0	1	0
0	0	0	0	0
0	0	0	0	0
0	0	0	1	0
0	0	0	0	0
0	0	0	0	0
0	0	0	0	0
0	0	0	0	0
0	0	0	0	0
0	0	0	0	0
0	0	0	0	1
0	0	0	0	0
0	0	0	0	0
0	0	0	2	0

I	A	A	A	I
<i>Alchornea</i>	<i>Tetrorchidium</i>	<i>Ormocarpum-</i> type	<i>Barleria</i>	<i>Tamarindus</i>
0	0	0	0	0
0	0	0	0	0
0	0	0	0	0
0	1	0	0	0
0	3	0	0	1
0	12	0	1	1
0	8	0	0	0
0	3	1	0	0
0	0	0	0	0
0	0	0	0	0
0	0	0	0	0
0	0	0	0	0
0	0	0	0	0
0	0	0	0	0
0	3	0	0	1
0	0	0	0	0
0	1	0	0	0
0	0	0	0	0

N	N	I	N	A
<i>Basilicum</i> -type	<i>Tephrosia</i>	<i>Commelina</i> -type	<i>Trilepisium</i> -type <i>madagascariensis</i>	Apocynaceae undiff.
0	0	0	0	0
0	0	0	0	0
0	0	0	0	0
0	0	0	0	0
0	0	0	0	2
0	0	0	0	0
0	0	0	0	0
0	0	0	0	0
0	1	0	0	0
0	0	0	0	0
0	0	0	0	0
0	0	0	0	0
0	0	0	0	0
0	0	0	42	0
0	0	0	0	0
1	0	1	0	0
0	0	0	0	0

I	N	AL	NL	I
<i>Impatiens</i>	Rutaceae undiff.	Cucurbitaceae undiff.	<i>Ipomoea</i> -type	<i>Palmae</i>
0	0	0	0	0
0	0	0	0	0
0	0	0	0	0
0	0	5	0	0
0	0	0	0	0
0	0	0	0	0
0	0	0	0	0
0	0	0	0	0
0	0	0	0	0
0	0	0	0	0
0	0	0	0	0
0	0	0	0	0
0	0	0	0	0
0	1	0	0	0
0	0	0	0	0
0	0	0	0	0
0	0	0	0	0

PI	I	S	Sp	
Asclepiadaceae undiff.	Moss	Trilete Fern	Broken	Unknown
0	0	0	0	0
0	0	5	2	0
0	0	0	3	0
0	0	0	0	3
0	0	0	3	4
0	0	0	2	11
0	0	0	3	5
0	0	0	3	5
0	0	1	0	1
0	0	0	0	1
0	0	0	0	2
0	0	0	1	0
0	0	2	0	0
7	0	0	1	0
0	0	0	2	0
0	0	0	1	0
0	0	1	1	1

Total	Spike	Type 3 AS (clusters)	<i>Sporormiella</i> (single cell)	Charcoal
307	795	5708	0	13
296	738	2655	0	2
315	43	225	1	0
219	14	1	0	1
306	123	0	3	4
307	109	0	0	5
301	59	0	6	3
309	121	1	0	14
283	1035	0	1	13
311	328	916	0	0
311	702	4212	0	2
318	384	0	0	5
305	719	3925	0	0
311	73	0	0	2
283	2244	0	1	14
53	125	0	1	2
328	961	0	0	19

Type 2 AS	Simple 1 AS	All other AS	insect egg	Bosquia-like NAP	volume	total spike
11	3	116	137	0	25	13911
22	5	363	194	0	25	13911
64	11	15	0	0	25	13911
1	21	7	0	0	25	13911
0	57	2	3	0	25	13911
0	0	0	2	0	25	13911
0	21	3	0	0	25	13911
1	5	13	0	0	25	13911
0	6	5	152	0	25	13911
13	0	8	59	0	25	13911
28	0	260	190	0	25	13911
2	301	1	15	0	25	13911
12	2	21	14	0	25	13911
0	1	5	0	0	25	13911
2	335	64	25	0	25	13911
0	12	1	30	0	25	13911
0	18	24	0	0	25	13911

Fossil Midden Pollen Counts

Pollen Habit		A	A	A	A	A
Sample ID	Age (cal yr BP)	<i>Abies</i>	<i>Allophylus</i>	<i>Balanites</i>	<i>Boswellia sacra</i>	<i>Boscia/Cadaba</i> -type
WP48-1 B	0	0	0	0	0	0
WP 135-2	0	0	0	0	49	0
WP 135-1	0	0	0	0	6	4
WP 135-3	0	0	0	0	14	1
WP144-4	107	0	0	0	2	4
WP 108-1b	109	0	0	0	6	5
WP 107-2b	114	0	0	0	3	0
WP142-B	115	0	0	13	0	4
WP45-2	177	0	0	0	2	0
WP153-2	384	0	0	3	0	18
WP155-2B	529	0	0	3	0	10
38-3a 4-6	665	0	0	0	3	83
WP146	706	0	0	10	15	5
WP50-2 0.5-2	853	0	0	0	6	0
WP155-2C	1403	0	0	0	2	4
WP38-2 B	1461	0	0	0	0	0
WP147-1	1466	0	0	16	9	9
WP50-3a 7-9	1522	0	0	0	35	0
WP138	1566	0	0	0	7	11
WP151	1574	0	0	0	42	12
WP145-4	1638	0	1	6	58	10
WP111-2E	1651	0	0	1	3	7
WP155-D	2920	0	0	0	2	4
WP103-2c	3103	0	0	0	8	19
WP149-2	3233	0	0	0	34	2
155-F	4038	0	0	0	10	28

Pollen Habit	A	A	A	A	A	A
Sample ID	<i>Catha</i>	<i>Celtis</i>	<i>ombretaceae</i>	<i>ommiphora</i>	<i>Delonix</i>	<i>Dodonaea</i>
WP48-1 B	0	0	2	10	0	0
WP 135-2	0	0	0	1	0	29
WP 135-1	0	0	0	0	0	28
WP 135-3	0	4	3	0	0	23
WP144-4	0	0	0	0	0	0
WP 108-1b	0	0	0	2	0	1
WP 107-2b	0	0	0	0	0	0
WP142-B	0	0	23	5	0	0
WP45-2	0	0	18	3	0	0
WP153-2	0	0	2	2	0	1
WP155-2B	0	0	11	0	0	0
38-3a 4-6	0	0	7	1	0	4
WP146	0	0	3	0	0	0
WP50-2 0.5-2	0	0	2	8	0	0
WP155-2C	0	0	14	1	0	0
WP38-2 B	0	0	3	36	0	3
WP147-1	4	0	8	0	0	0
WP50-3a 7-9	0	0	3	21	0	2
WP138	5	0	11	2	0	0
WP151	3	0	9	3	0	0
WP145-4	1	0	6	2	0	0
WP111-2E	0	0	7	0	0	0
WP155-D	0	0	9	1	0	0
WP103-2c	0	0	139	7	0	1
WP149-2	2	0	2	0	0	0
155-F	0	0	9	0	0	1

Pollen Habit	A	A	A	A	A	A
Sample ID	Ericaceae undiff.	<i>Ficus</i>	<i>Flacourtia</i>	<i>Juniperus</i>	<i>Clainanthuslaineanthus</i> -typ	
WP48-1 B	2	0	0	5	0	0
WP 135-2	0	7	0	0	0	0
WP 135-1	0	7	0	0	0	0
WP 135-3	0	9	1	0	0	0
WP144-4	0	1	0	0	0	0
WP 108-1b	0	66	0	0	0	0
WP 107-2b	0	6	0	0	0	0
WP142-B	0	3	0	0	0	1
WP45-2	0	0	0	0	0	0
WP153-2	0	5	2	0	0	0
WP155-2B	0	3	2	0	0	2
38-3a 4-6	2	1	0	0	2	0
WP146	0	1	2	0	0	1
WP50-2 0.5-2	0	0	0	1	0	0
WP155-2C	0	11	1	0	0	0
WP38-2 B	0	0	0	0	0	0
WP147-1	0	68	0	0	0	0
WP50-3a 7-9	0	9	0	0	0	0
WP138	0	10	0	0	0	1
WP151	0	44	0	0	0	0
WP145-4	0	7	0	0	0	0
WP111-2E	1	66	0	0	0	0
WP155-D	0	13	4	0	0	0
WP103-2c	0	9	0	0	0	0
WP149-2	0	58	0	0	0	1
155-F	0	14	1	0	0	0

Pollen Habit	A	A	A	A	A	A
Sample ID	<i>Macaranga</i>	<i>Maerua</i>	<i>Mallotus</i>	<i>Maytenus</i>	<i>Musanga</i>	<i>Olea capensis</i>
WP48-1 B	0	0	0	0	0	0
WP 135-2	0	7	0	2	0	0
WP 135-1	0	3	0	1	0	0
WP 135-3	0	2	0	0	0	0
WP144-4	0	10	0	7	0	0
WP 108-1b	0	5	0	7	0	0
WP 107-2b	0	1	0	0	0	0
WP142-B	0	0	0	0	0	0
WP45-2	0	0	0	0	0	0
WP153-2	0	3	0	0	0	0
WP155-2B	3	7	0	2	0	0
38-3a 4-6	0	8	0	3	0	0
WP146	0	14	0	0	0	0
WP50-2 0.5-2	0	6	0	0	0	0
WP155-2C	0	8	0	0	0	0
WP38-2 B	0	3	0	0	0	0
WP147-1	0	1	0	0	0	0
WP50-3a 7-9	0	19	0	5	0	1
WP138	0	0	0	9	0	0
WP151	0	1	0	5	0	0
WP145-4	0	12	0	5	0	0
WP111-2E	0	1	0	11	0	0
WP155-D	0	5	0	0	0	0
WP103-2c	0	0	0	3	0	0
WP149-2	0	2	0	0	0	0
155-F	0	3	0	3	0	0

Pollen Habit	A	A	A	A	A	A
Sample ID	<i>Olea africana</i>	<i>Ormocarpum</i>	<i>Pinus</i>	<i>Podocarpus</i>	<i>Prunus</i>	<i>Rhus</i>
WP48-1 B	0	0	0	0	0	0
WP 135-2	0	0	0	0	0	0
WP 135-1	1	0	0	0	0	0
WP 135-3	0	1	0	0	0	0
WP144-4	0	0	0	0	2	0
WP 108-1b	1	0	0	0	0	0
WP 107-2b	1	0	2	0	0	0
WP142-B	0	0	0	0	0	0
WP45-2	0	0	0	0	0	0
WP153-2	4	0	0	0	2	0
WP155-2B	0	0	0	0	0	1
38-3a 4-6	0	0	1	0	0	0
WP146	0	0	0	0	3	0
WP50-2 0.5-2	0	0	0	0	0	0
WP155-2C	2	0	0	0	0	0
WP38-2 B	0	0	0	0	0	0
WP147-1	0	0	0	0	8	0
WP50-3a 7-9	4	0	0	1	0	0
WP138	0	0	0	0	0	0
WP151	0	0	1	0	0	0
WP145-4	7	0	0	0	0	0
WP111-2E	0	0	0	0	0	0
WP155-D	0	0	0	0	1	0
WP103-2c	0	0	0	0	0	0
WP149-2	1	0	0	0	0	0
155-F	1	0	0	0	0	0

Pollen Habit	A	A	A	A	A	A
Sample ID	<i>Salvadora persica</i>	<i>Tamarindus</i>	<i>Tamarix</i>	<i>Tetrorchidium</i>	<i>Trema</i>	<i>Ziziphus</i>
WP48-1 B	7	0	5	0	0	2
WP 135-2	41	1	0	12	0	6
WP 135-1	79	0	6	8	0	4
WP 135-3	53	0	0	3	0	3
WP144-4	0	0	0	0	0	2
WP 108-1b	14	1	5	3	0	7
WP 107-2b	2	0	1	1	0	0
WP142-B	4	0	0	0	0	2
WP45-2	10	0	3	0	0	0
WP153-2	5	0	0	0	3	6
WP155-2B	26	0	0	0	0	2
38-3a 4-6	5	0	0	0	0	4
WP146	1	0	0	0	0	8
WP50-2 0.5-2	2	0	2	0	0	0
WP155-2C	24	0	0	0	0	4
WP38-2 B	5	0	0	0	0	3
WP147-1	6	0	0	0	0	7
WP50-3a 7-9	20	0	0	0	0	0
WP138	1	0	0	0	0	14
WP151	4	0	0	0	0	7
WP145-4	0	0	0	0	0	3
WP111-2E	1	0	0	0	0	10
WP155-D	9	0	0	0	1	2
WP103-2c	4	0	0	0	0	0
WP149-2	3	0	0	0	0	1
155-F	5	0	0	0	0	7

Pollen Habit	AL	AL	AL	AL	AL	AL
Sample ID	<i>Senegalia I</i>	<i>Senegalia II</i>	<i>Senegalia III</i>	<i>Capparis</i>	<i>Ephedra</i>	<i>Maesa</i>
WP48-1 B	24	0	7	2	0	0
WP 135-2	10	0	1	5	0	0
WP 135-1	12	0	0	0	0	0
WP 135-3	8	0	1	1	0	0
WP144-4	17	0	0	51	1	0
WP 108-1b	13	0	0	15	0	0
WP 107-2b	1	0	0	0	0	0
WP142-B	37	0	0	56	0	0
WP45-2	4	0	3	3	0	0
WP153-2	0	0	1	39	4	0
WP155-2B	0	0	4	4	0	0
38-3a 4-6	47	0	0	1	0	0
WP146	3	0	0	35	0	0
WP50-2 0.5-2	13	0	2	15	0	0
WP155-2C	0	0	6	7	0	0
WP38-2 B	15	0	5	5	0	0
WP147-1	7	0	0	6	0	0
WP50-3a 7-9	15	0	6	4	0	1
WP138	6	0	2	4	0	0
WP151	20	0	0	13	0	0
WP145-4	9	0	0	22	1	0
WP111-2E	12	0	5	0	1	0
WP155-D	5	0	3	8	0	0
WP103-2c	1	0	3	0	0	0
WP149-2	2	0	2	1	0	0
155-F	6	2	6	16	0	0

Pollen Habit	Ap	I	I	I	I	I
Sample ID	<i>Tapinanthus</i>	<i>Acalypha</i>	Acanthaceae-type	<i>Aeschynomene</i>	Aizoaceae- small	<i>Alchemilla</i>
WP48-1 B	0	0	0	0	0	0
WP 135-2	10	0	0	0	0	0
WP 135-1	8	0	0	1	0	0
WP 135-3	12	0	0	0	0	0
WP144-4	0	0	2	0	3	0
WP 108-1b	0	1	0	0	0	0
WP 107-2b	0	0	0	0	0	0
WP142-B	0	0	1	0	26	0
WP45-2	0	0	0	0	0	0
WP153-2	0	0	0	0	12	3
WP155-2B	0	0	1	0	1	1
38-3a 4-6	1	0	0	0	0	0
WP146	0	0	1	0	8	0
WP50-2 0.5-2	2	0	0	0	0	0
WP155-2C	0	1	0	0	0	2
WP38-2 B	0	0	0	0	0	0
WP147-1	0	2	0	0	0	4
WP50-3a 7-9	2	0	0	0	0	0
WP138	3	0	2	0	8	0
WP151	2	0	1	0	0	0
WP145-4	0	0	7	0	1	0
WP111-2E	1	0	4	0	0	0
WP155-D	0	0	0	0	0	0
WP103-2c	4	0	0	0	0	0
WP149-2	0	0	0	0	0	0
155-F	1	0	0	0	0	3

Pollen Habit	I	I	I	I	I	I
Sample ID	<i>Aloe</i>	Amaranthaceae	Apiaceae	Apocynaceae	Asclepiadaceae	Asteraceae
WP48-1 B	0	22	0	0	0	19
WP 135-2	0	1	0	0	0	13
WP 135-1	0	10	0	0	0	10
WP 135-3	0	25	0	0	0	9
WP144-4	0	31	2	0	0	5
WP 108-1b	0	15	0	0	7	9
WP 107-2b	0	1	0	0	0	2
WP142-B	0	41	0	0	0	8
WP45-2	0	39	1	0	0	28
WP153-2	2	58	0	0	0	6
WP155-2B	0	34	0	0	0	2
38-3a 4-6	0	20	0	0	0	8
WP146	0	33	0	0	0	18
WP50-2 0.5-2	0	97	0	0	0	14
WP155-2C	0	38	0	0	0	0
WP38-2 B	0	6	0	0	0	0
WP147-1	0	29	3	1	0	10
WP50-3a 7-9	0	24	0	0	0	12
WP138	0	52	1	0	0	15
WP151	0	28	0	0	0	12
WP145-4	0	46	1	0	0	10
WP111-2E	0	21	0	0	0	8
WP155-D	0	35	0	0	0	3
WP103-2c	0	56	0	1	0	4
WP149-2	0	7	0	0	0	2
155-F	0	26	0	0	0	10

Pollen Habit	I	I	I	I	I	I
Sample ID	<i>Barleria</i>	<i>Bosquia</i> (3P)	Brassicaceae	Capparaceae undiff	<i>Cassia</i>	<i>Cissus</i>
WP48-1 B	0	0	2	0	20	0
WP 135-2	1	0	0	0	0	0
WP 135-1	0	0	0	0	0	0
WP 135-3	0	0	0	0	0	0
WP144-4	1	0	4	0	0	0
WP 108-1b	0	42	0	0	0	0
WP 107-2b	0	0	0	0	2	0
WP142-B	0	0	0	0	0	0
WP45-2	0	0	2	0	0	0
WP153-2	0	0	1	0	0	0
WP155-2B	0	0	1	4	0	0
38-3a 4-6	0	0	0	0	11	0
WP146	1	0	12	0	0	0
WP50-2 0.5-2	0	0	6	0	1	0
WP155-2C	0	0	1	7	0	0
WP38-2 B	0	0	19	0	3	0
WP147-1	0	0	1	0	0	0
WP50-3a 7-9	0	0	8	0	3	3
WP138	0	0	0	0	0	0
WP151	0	0	0	0	0	0
WP145-4	1	0	1	0	0	0
WP111-2E	0	0	0	0	0	0
WP155-D	0	0	0	1	0	0
WP103-2c	0	0	0	0	0	0
WP149-2	0	0	1	0	0	0
155-F	0	0	0	0	2	0

Pollen Habit	I	I	I	I	I	I
Sample ID	<i>Crotolaria</i>	<i>Desmodium</i> -type	<i>Euphorbia</i>	Fabaceae undiff.	<i>Fagonia</i>	<i>Indigofera</i>
WP48-1 B	0	0	0	0	0	0
WP 135-2	1	0	1	0	0	4
WP 135-1	1	0	2	6	0	13
WP 135-3	0	0	0	1	0	0
WP144-4	0	0	6	0	0	0
WP 108-1b	0	0	1	3	0	1
WP 107-2b	0	0	0	1	0	0
WP142-B	0	0	3	0	0	1
WP45-2	0	0	0	0	3	0
WP153-2	0	0	6	0	0	3
WP155-2B	0	0	3	0	0	2
38-3a 4-6	0	0	2	0	0	0
WP146	0	1	3	0	0	7
WP50-2 0.5-2	0	0	0	0	0	0
WP155-2C	0	0	5	0	0	0
WP38-2 B	0	0	0	0	3	0
WP147-1	0	0	0	0	0	47
WP50-3a 7-9	0	0	1	0	1	0
WP138	0	0	8	0	0	10
WP151	0	0	9	0	0	20
WP145-4	0	0	1	0	0	2
WP111-2E	0	1	8	0	0	2
WP155-D	0	0	1	0	0	0
WP103-2c	0	0	48	0	0	0
WP149-2	0	0	0	0	0	35
155-F	0	0	11	0	0	3

Pollen Habit	I	I	I	I	I	I
Sample ID	Lamiaceae (3c)	Lamiaceae (6c)	<i>Limonium</i>	<i>Kickxia/Acridocarpus</i>	<i>Merremia</i>	<i>Polygala</i>
WP48-1 B	0	0	0	0	0	0
WP 135-2	0	0	0	0	0	0
WP 135-1	0	0	0	1	0	0
WP 135-3	0	0	0	0	0	0
WP144-4	0	0	3	0	0	0
WP 108-1b	0	0	1	0	0	1
WP 107-2b	1	0	0	0	0	0
WP142-B	0	0	3	0	0	0
WP45-2	1	0	0	0	0	0
WP153-2	0	0	2	0	0	0
WP155-2B	0	0	0	0	0	0
38-3a 4-6	2	0	0	1	0	0
WP146	0	2	0	0	1	1
WP50-2 0.5-2	1	0	0	2	0	0
WP155-2C	0	0	0	0	1	0
WP38-2 B	0	0	0	5	0	0
WP147-1	0	0	0	0	0	0
WP50-3a 7-9	0	0	0	2	0	0
WP138	0	0	3	0	3	0
WP151	0	0	0	0	0	0
WP145-4	0	2	0	0	1	1
WP111-2E	0	0	2	0	1	0
WP155-D	0	0	0	0	0	0
WP103-2c	0	0	0	0	3	0
WP149-2	0	0	0	0	0	0
155-F	0	1	0	0	1	0

Pollen Habit	I	I	I	I	I	I
Sample ID	<i>Polygonum</i>	<i>Reseda</i>	Rutaceae	Sapindaceae-type	<i>Solanum</i>	<i>Tephrosia</i>
WP48-1 B	2	0	0	0	0	0
WP 135-2	0	0	0	0	0	0
WP 135-1	0	0	0	0	1	0
WP 135-3	0	0	0	0	0	0
WP144-4	0	0	0	0	0	0
WP 108-1b	0	0	1	0	0	0
WP 107-2b	0	0	0	0	0	0
WP142-B	0	0	0	0	0	0
WP45-2	0	0	0	0	0	0
WP153-2	0	0	0	0	2	0
WP155-2B	0	0	0	0	0	0
38-3a 4-6	1	0	0	0	0	0
WP146	0	0	0	0	0	0
WP50-2 0.5-2	0	0	0	0	0	0
WP155-2C	0	3	0	0	0	0
WP38-2 B	0	0	0	0	0	0
WP147-1	0	0	0	0	0	0
WP50-3a 7-9	0	0	0	0	0	0
WP138	0	0	0	4	0	0
WP151	0	0	0	0	0	0
WP145-4	0	0	0	0	2	0
WP111-2E	0	0	0	0	0	1
WP155-D	0	1	0	0	0	0
WP103-2c	0	0	0	0	0	0
WP149-2	0	0	0	0	0	0
155-F	0	0	0	0	3	0

Pollen Habit	I	L	N	N	N	N
Sample ID	<i>Zygophyllum</i>	<i>Cocculus pendulus</i>	<i>Blepharis</i>	<i>Boerhavia erecta</i>	<i>Celosia</i>	<i>Centaurea</i>
WP48-1 B	0	77	0	0	2	0
WP 135-2	7	2	0	0	1	0
WP 135-1	4	26	0	0	0	0
WP 135-3	1	21	0	0	1	0
WP144-4	0	67	1	0	0	0
WP 108-1b	1	17	1	0	0	0
WP 107-2b	0	3	0	0	0	0
WP142-B	0	34	0	0	0	0
WP45-2	2	61	0	0	0	0
WP153-2	0	70	0	0	0	0
WP155-2B	0	52	0	0	0	0
38-3a 4-6	0	29	2	0	0	0
WP146	0	8	0	0	0	0
WP50-2 0.5-2	1	29	0	0	3	1
WP155-2C	0	108	0	0	0	0
WP38-2 B	8	81	0	0	3	0
WP147-1	0	19	0	0	0	0
WP50-3a 7-9	2	11	0	0	3	0
WP138	0	75	0	0	0	0
WP151	0	24	0	0	0	0
WP145-4	0	13	0	0	0	0
WP111-2E	0	89	0	0	0	0
WP155-D	0	81	0	0	0	0
WP103-2c	0	6	0	1	0	0
WP149-2	0	9	0	0	0	0
155-F	0	50	0	0	0	0

Pollen Habit	N	N	N	N	N	N
Sample ID	<i>Cleome</i>	<i>Commelina</i>	<i>Corchorus</i>	Poaceae	<i>Heliotropium</i>	<i>Impatiens</i>
WP48-1 B	0	0	0	49	29	0
WP 135-2	13	0	0	34	12	0
WP 135-1	8	0	0	11	6	0
WP 135-3	17	0	0	54	8	0
WP144-4	0	0	0	19	5	1
WP 108-1b	1	0	0	32	8	0
WP 107-2b	3	1	0	7	1	0
WP142-B	0	0	0	34	23	0
WP45-2	2	0	0	66	37	0
WP153-2	4	0	1	26	1	0
WP155-2B	2	0	0	15	10	0
38-3a 4-6	18	0	0	48	14	0
WP146	4	0	0	46	6	0
WP50-2 0.5-2	5	0	0	22	7	0
WP155-2C	0	0	2	18	6	0
WP38-2 B	0	0	0	11	0	0
WP147-1	5	0	0	25	6	0
WP50-3a 7-9	9	0	0	23	2	0
WP138	4	0	0	26	7	0
WP151	6	0	0	31	3	0
WP145-4	0	0	0	39	6	0
WP111-2E	1	0	0	35	6	0
WP155-D	1	0	0	22	6	0
WP103-2c	10	0	0	39	0	0
WP149-2	0	0	0	0	0	0
155-F	0	0	0	18	9	0

Pollen Habit	N	N	N	N	N	N
Sample ID	<i>Kohautia</i>	<i>Linaria</i>	<i>Lotus</i>	<i>Phyllanthus materspatensis</i>	<i>Plantago</i>	<i>Polycarpon</i> -type (<i>Reseda</i>)
WP48-1 B	2	0	0	0	0	5
WP 135-2	2	0	0	0	0	0
WP 135-1	5	0	0	0	1	3
WP 135-3	0	0	0	0	0	0
WP144-4	68	0	0	0	0	0
WP 108-1b	1	0	0	2	0	0
WP 107-2b	0	0	0	0	0	0
WP142-B	10	0	0	0	0	0
WP45-2	3	0	1	0	0	2
WP153-2	5	0	0	0	0	0
WP155-2B	12	0	0	0	0	0
38-3a 4-6	30	0	0	0	0	4
WP146	17	0	0	0	0	0
WP50-2 0.5-2	100	1	0	0	0	0
WP155-2C	14	0	0	0	0	0
WP38-2 B	16	0	0	0	0	5
WP147-1	85	0	0	0	0	0
WP50-3a 7-9	118	0	0	0	0	0
WP138	45	0	0	0	0	0
WP151	4	0	0	0	0	0
WP145-4	42	0	0	0	0	0
WP111-2E	4	2	0	0	0	0
WP155-D	12	0	0	0	0	0
WP103-2c	7	0	0	0	0	0
WP149-2	0	0	0	0	0	0
155-F	10	3	0	0	0	0

Pollen Habit	N	NG	NL	NL	NL	NL
Sample ID	<i>Tribulus</i>	<i>Ricinus</i>	<i>Commicarpus</i>	<i>Convolvulus</i>	Cucurbitaceae	Cyperaceae
WP48-1 B	5	0	0	2	0	12
WP 135-2	2	1	0	1	0	10
WP 135-1	0	1	1	2	0	5
WP 135-3	3	2	0	2	0	8
WP144-4	1	0	0	0	0	27
WP 108-1b	0	0	0	0	0	3
WP 107-2b	0	0	0	0	0	3
WP142-B	0	0	0	0	0	14
WP45-2	2	0	0	1	0	3
WP153-2	0	0	0	0	0	13
WP155-2B	0	0	0	0	0	12
38-3a 4-6	0	0	0	1	0	5
WP146	3	0	0	0	0	25
WP50-2 0.5-2	2	0	0	3	0	14
WP155-2C	0	0	0	0	0	8
WP38-2 B	0	0	0	3	0	71
WP147-1	0	0	0	0	0	14
WP50-3a 7-9	2	0	0	1	1	15
WP138	0	0	0	0	0	10
WP151	1	0	0	0	0	9
WP145-4	0	0	0	0	0	15
WP111-2E	1	0	0	0	0	6
WP155-D	0	0	0	0	0	9
WP103-2c	1	0	0	0	0	5
WP149-2	0	0	0	0	0	3
155-F	0	0	0	0	0	27

Pollen Habit	PA	PA	F	F	X	X
Sample ID	<i>Hyphaene</i>	<i>Phoenix</i>	Monoletes	Triletes	Broken	Unknown
WP48-1 B	0	0	0	2	0	0
WP 135-2	0	0	0	0	2	11
WP 135-1	0	0	0	0	3	5
WP 135-3	0	0	0	0	3	5
WP144-4	0	0	0	0	16	0
WP 108-1b	0	0	0	0	1	0
WP 107-2b	0	0	0	0	1	0
WP142-B	0	0	0	1	23	0
WP45-2	0	0	0	1	1	1
WP153-2	0	0	1	1	43	0
WP155-2B	0	0	0	0	29	1
38-3a 4-6	0	0	0	0	0	0
WP146	0	0	0	0	36	0
WP50-2 0.5-2	0	0	0	0	0	0
WP155-2C	0	0	0	0	26	4
WP38-2 B	0	0	0	0	3	3
WP147-1	0	4	0	0	18	0
WP50-3a 7-9	0	0	0	0	0	0
WP138	0	0	0	0	20	2
WP151	0	0	0	3	12	0
WP145-4	0	0	0	0	23	0
WP111-2E	0	0	3	6	24	0
WP155-D	0	0	0	2	23	0
WP103-2c	0	0	0	0	32	4
WP149-2	0	0	0	2	16	0
155-F	0	0	0	0	10	0

Pollen Habit	X	X	Nq	X	X	X
Sample ID	Unidentifiable	All Total	<i>Typha</i>	Contaminant	Charcoal	total spike
WP48-1 B	0	316	0	4119	12	9666
WP 135-2	0	300	1	109	5	9666
WP 135-1	0	293	0	59	3	9666
WP 135-3	0	299	0	121	14	9666
WP144-4	0	359	0	162	324	9666
WP 108-1b	0	300	0	73	2	9666
WP 107-2b	0	44	0	125	2	9666
WP142-B	0	370	0	205	118	9666
WP45-2	0	303	2	961	19	9666
WP153-2	0	360	0	556	1167	9666
WP155-2B	0	262	0	857	2857	9666
38-3a 4-6	0	369	0	1019	26	9666
WP146	0	334	0	351	2600	9666
WP50-2 0.5-2	0	368	0	132	9	9666
WP155-2C	0	328	0	1200	3200	9666
WP38-2 B	0	318	0	9354	74	9666
WP147-1	0	422	0	202	304	9666
WP50-3a 7-9	0	389	0	783	200	9666
WP138	0	381	0	145	172	9666
WP151	10	339	0	280	1037	9666
WP145-4	0	364	0	419	1746	9666
WP111-2E	0	352	0	498	940	9666
WP155-D	0	264	0	722	969	9666
WP103-2c	31	446	0	28	700	9666
WP149-2	0	186	0	438	368	9666
155-F	0	300	0	150	208	9666

Pollen Habit	X	X	X	X	X	X	X	X	X
Sample ID	volume (mL)	1as	2as	3as	4as	5as	6as	8as	Large 1as
WP48-1 B	45	27	2	0	0	0	0	0	5
WP 135-2	45	0	0	0	0	0	0	0	0
WP 135-1	45	21	0	0	0	0	0	0	0
WP 135-3	45	5	1	1	0	0	0	0	0
WP144-4	45	210	5	7	2	1	0	0	23
WP 108-1b	45	1	0	0	0	0	0	0	0
WP 107-2b	45	12	0	0	0	0	0	0	0
WP142-B	45	98	9	3	2	0	0	0	50
WP45-2	45	40	0	0	0	0	0	0	2
WP153-2	45	125	0	1	0	0	0	0	9
WP155-2B	45	78	0	0	0	0	0	0	8
38-3a 4-6	45	4	0	0	0	0	0	0	6
WP146	45	116	0	1	0	0	0	0	16
WP50-2 0.5-2	45	40	0	0	0	0	0	0	7
WP155-2C	45	106	1	0	0	0	0	0	7
WP38-2 B	45	11	0	0	0	0	0	0	0
WP147-1	45	32	0	1	1	0	0	0	14
WP50-3a 7-9	45	4	0	0	0	0	0	0	0
WP138	45	27	1	1	1	0	0	1	2
WP151	45	119	1	0	1	0	0	0	3
WP145-4	45	84	2	2	2	0	0	0	24
WP111-2E	45	95	5	0	0	0	0	0	0
WP155-D	45	92	1	0	0	0	0	0	6
WP103-2c	45	3	0	0	0	0	0	0	0
WP149-2	45	30	0	1	0	0	0	0	1
155-F	45	12	0	0	0	0	0	0	0

Pollen Habit	X	X	X	X	X	X	X
Sample ID	Large 3as	poly	echinate	large echinate	polyechinate	parasite egg	<i>Sporormiella</i>
WP48-1 B	0	0	0	0	0	5	0
WP 135-2	0	0	0	0	0	2	0
WP 135-1	0	3	0	0	0	0	6
WP 135-3	0	13	0	0	0	0	0
WP144-4	0	0	10	0	1	17	0
WP 108-1b	0	5	0	0	0	0	0
WP 107-2b	0	1	0	0	0	30	1
WP142-B	0	0	7	0	0	11	0
WP45-2	0	0	0	0	0	0	0
WP153-2	0	0	4	0	1	0	7
WP155-2B	0	0	2	0	2	0	0
38-3a 4-6	0	0	0	0	0	3	2
WP146	0	1	11	2	9	3	0
WP50-2 0.5-2	0	0	0	0	0	10	1
WP155-2C	0	0	4	0	0	0	1
WP38-2 B	0	0	0	0	0	8	0
WP147-1	0	5	11	0	0	1	0
WP50-3a 7-9	0	0	0	0	0	4	1
WP138	0	3	1	0	0	0	0
WP151	0	0	1	0	0	0	0
WP145-4	1	2	19	1	0	17	0
WP111-2E	0	0	5	0	0	0	0
WP155-D	0	0	2	0	0	1	2
WP103-2c	0	0	0	0	0	1	0
WP149-2	0	0	1	0	0	8	0
155-F	0	0	0	0	0	0	1

Appendix B

Hyrax Midden Sampling and Processing Methods

Rock hyraxes are distributed throughout Africa and the Arabian Peninsula (Sale, 1965; Chase et al., 2012). These herbivorous creatures live in colonies and are indiscriminate, resourceful foragers. Because of these qualities, their range is mostly limited by the availability of rocky shelters, often small caves in the sides of cliffs (Sale, 1965; Chase et al., 2012). Hyraxes separate living spaces in a colony from latrines, and through subsequent use of a latrine over time, fine layers of hyraceum (urinary product) and fecal pellets accumulate, trapping paleoenvironmental indicators. These latrines, or middens, then crystallize and preserve in arid drylands, preserving this information for thousands of years.

Through this understanding of modern rock hyrax distributions, their preferred habitats, midden preservation, and knowledge of living colonies, one could assess potential areas to survey for fossil middens. In Dhofar, this involves identifying wadi drainage systems with carbonate cliffsides, which small caves and crevices have been eroded out of over time through dissolution, aeolian activity, and overland flow. Many modern hyrax communities inhabit similar areas, and you may come across some of these elusive and shy critters if you are lucky. While middens can be found at the base of the cliffs, under boulders on the scree slopes by the wadi beds, these are often affected by storm flooding. Moreover, hyraxes prefer being up and out of the channel for protection from predators. Thus, it is less likely to find fossil middens preserved in these areas. Surveying efforts should focus on areas above this flooding zone. A cave that was used as a hyrax latrine will have small (~1-1.5cm), oblong fecal pellets are usually visible at the opening and cascading downhill. Once this has been discovered, a midden can be identified as an indurated mass inside the cave, and sizes of these middens can range between a few centimeters in thickness to a meter or more.

To excavate a midden, sledgehammers, chisels, and rock hammers are useful tools to have on hand. One may need to break off part of an overhang to gain room to access the midden. It is wise to also use one of these tools to bang around the midden in the dust, to ensure there are no snakes or other potentially dangerous inhabitants. Then, using a rock hammer and chisel, you can extract the midden from the side of the cliff or up off of the cave floor. In doing so, be careful to try and preserve the vertical stratigraphy/thickness and remove the midden in the orientation it was deposited. Once retrieved, wrap the midden in plastic wrap to prevent as much contamination as possible, and secure with electrical tape, writing in sharpie the coordinates and marking the orientation (top and bottom). These can be packed into suitcases and cushioned with bubble wrap, blankets, etc. to be shipped back to the lab.

Depending on the thickness of the midden, one could choose to treat it as a thin, time-averaged, single sample, or subsample it into individual layers. For the former (which was the only strategy used in this dissertation), ~10 fecal pellets can be selected to obtain an average radiocarbon age throughout the midden. For the latter, the midden can be split using a circular saw or dry tile saw, polished, and organic material can be drilled out of subsequent layers. This study focused on thin middens, and so we will discuss the processing protocol for these types of samples. About 100g of midden material should be disaggregated and rehydrated in ~1L of deionized water. Large particles can be sieved out to retain the <500 μ m fraction. Smaller volumes of this fine fraction can then be processed for pollen or other geochemical indicators following the protocols described in the previous chapters.

A few additional considerations should be taken into account when using midden samples for palynology or organic geochemistry. For palynology, we found that use of the traditional pollen extraction methods using hydrofluoric acid (HF) resulted in a vigorous exothermic reaction. Although the reason is not completely clear, the limestone bedrock from which the middens were sampled introduces a large amount detrital carbonate into midden extracts. As HF

reacts strongly with carbonate to form fluorosilicates, which is a dangerous process as well as making the samples more challenging to observe, this should be avoided. Therefore, we suggest extra digestion in concentrated HCl until reaction has fully stopped before adding HF.

For organic geochemistry, we recommend sub-sampling the solid midden for analysis and using Accelerated Solvent Extraction (ASE) to extract the samples and separate out the hexane fraction. This process is simpler. However, if you decide to look at these compounds after the middens have been processed for pollen analysis, we have the following advice: when freeze drying the liquid sample, use as large a beaker as possible and weigh the beaker prior to freeze drying. The middens will bubble up and overflow in the freeze drier in smaller containers. Moreover, you may notice the frozen puck at the bottom of the beaker begin to rise due to the difference in pressure beneath the frozen matter and the vacuum being created above. You should remove the samples from the freeze drier at this point and break up the frozen sample with a clean (solvent rinsed) metal lab spatula or another similar instrument. Then weigh the mass of the residue after freeze drying to standardize the alkane concentrations to a mass of organic material rather than volume. Better yet, get %TOC data for the samples! Most importantly, do not get discouraged. It is a tedious process, and some middens will yield more than others, but you will make it through!

VITA

Kaitlyn Eileen Horisk

Education:

- Doctor of Philosophy, Geosciences, The Pennsylvania State University, May 2024; Advisor: Dr. Sarah J. Ivory
- Bachelor of Science, Geological Sciences, Binghamton University, May 2019
- Bachelor of Arts, Anthropological Perspectives, Binghamton University, May 2019

Publications:

Horisk, K., Ivory, S., McCorriston, J., McHale, M., Mehri, A., Anderson, A., and Anderson, R. S., A., Kathiri. (2023). *Vegetation Dynamics in Dhofar, Oman from the late Holocene to present inferred from rock hyrax middens*. *Quaternary Research*, 1-18.

Selected Presentations:

- **Horisk, K.**, Lau, K., Ivory, S., Snider, J., Finkle, P. Assessing an interpretive exhibit through undergraduate lab assignments in Geosciences. The Society for the Preservation of Natural History Collections, June 2023.
- **Horisk, K.**, Ivory, S., Freeman, K., Baczynski, A., McCorriston, J., Kathiri, A., Mahri, A. Understanding drivers of vegetation change in Dhofar, Oman: a biodiverse dryland ecosystem. Geological Society of America, Oct 2022.
- **Horisk, K.**, Ivory, S. and McCorriston, J. Complex interactions between plants, precipitation, and people in Dhofar, Oman from the mid-Holocene to present. Geological Society of America, Oct 2021.

Selected Awards:

- Teaching Assistant Award, Penn State, EMS Department of Geosciences
- Marilyn L. Fogel Student Research Fund in Biogeosciences, Penn State, Earth and Environmental Systems Institute
- Elsevier Organic Geochemistry Research Scholarship
- Cleveland Museum of Natural History John H. Hoskins Grant-in-Aid Program
- Honorable Mention NSF Graduate Research Fellowship

Related Experience:

- Project Manager, Cretaceous Oceans and Climate Exhibit, Earth and Mineral Sciences (EMS) Museum & Art Gallery, Penn State (2023)
- Volunteer, Wildlife Ambassador and Educator, Shaver's Creek Environmental Center, Penn State (2022)
- Fall 2020, Fall 2022, Spring 2024: Teaching Assistant, Geobiology (GEOSC 204), Department of Geosciences, Penn State
- Summer 2022: Instructor of Record, Geology of the National Parks (GEOSC 010), Penn State Department of Geosciences.